Quantification of Quantum Features in an Electro-Optomechanical System with an Optical Parametric Amplifier, Coherent Feedback and Two-Level Atoms

Habtamu Dagnaw Mekonnen

A Dissertation Submitted to the Department of Applied Physics

College of Applied Natural Science

Presented in Partial Fulfillment of the Requirement for the Degree of Doctor of Philosophy in Applied Physics
(Quantum Optics and Information)

Office of Graduate Studies

Adama Science and Technology University

December, 2024
Adama, Ethiopia

Quantification of Quantum Features in an Electro-Optomechanical System with an Optical Parametric Amplifier, Coherent Feedback and Two-Level Atoms

Habtamu Dagnaw Mekonnen

Major supervisor: Tesfay Gebremariam (Ph.D.)

Co-supervisor: Tewodros Yirgashewa (Ph.D.)

A Dissertation Submitted to the Department of Applied Physics

College of Applied Natural Science

Presented in Partial Fulfillment of the Requirement for the Degree of Doctor of Philosophy in Applied Physics
(Quantum Optics and Information)

Office of Graduate Studies

Adama Science and Technology University

December, 2024
Adama, Ethiopia

Declaration

I declare that this dissertation entitled **Quantification of quantum features in an electro-optomechanical system with an optical parametric amplifier, coherent feedback, and two-level atoms** is my own work and has not been submitted to any university for a similar purpose. The references used in this dissertation are duly recognized by proper citations.

Habtamu Dagnaw Mekonnen	____________	____________
Name of student	Signature	Date

Recommendation of Supervisors

We, the supervisors of this dissertation, hereby certify that we have closely supervised the student while developing this dissertation and read the draft dissertation entitled **Quantification of quantum features in an electro-optomechanical system with an optical parametric amplifier, coherent feedback, and two-level atoms** prepared under my guidance by **Habtamu Dagnaw Mekonnen**. Therefore, we recommend the submission of the dissertation to the department for further review and defense.

Tesfay Gebremariam (Ph.D.)	__________	__________
Major Supervisor	Signature	Date
Tewodros Yirgashewa (Ph.D.)	__________	__________
Co-supervisor	Signature	Date

Approval Page

We hereby certify that the recommendation and suggestion given by the dissertation review committee is appropriately incorporated into the dissertation entitled **Quantification of quantum features in an electro-optomechanical system with an optical parametric amplifier, coherent feedback, and two-level atoms** by **Habtamu Dagnaw Mekonnen**.

Tesfay Gebremariam (Ph.D.) Major supervisor	________ Signature	________ Date
Tewodros Yirgashewa (Ph.D.) Co-supervisor	________ Signature	________ Date

Approval of Board of Reviewers

We, the undersigned, members of the Board of Reviewers of the dissertation open defense by **Habtamu Dagnaw Mekonnen** have read and evaluated the dissertation entitled **Quantification of quantum features in an electro-optomechanical system with an optical parametric amplifier, coherent feedback, and two-level atoms** and assessed the candidate's understanding of the dissertation research. This is therefore to certify that the dissertation is accepted, and we recommend the implementation of the dissertation.

Chairperson	Signature	Date
Internal Examiner-1	Signature	Date
Internal Examiner-2	Signature	Date
External Examiner-1	Signature	Date
External Examiner-2	Signature	Date

Finally, approval and acceptance of the dissertation is contingent upon the submission of its final copy to the Office of Postgraduate Studies (OPGS) through the Department Graduate Council (DGC) and College Graduate Committee (CGC).

Department Head	Signature	Date
College Dean	Signature	Date
Office of Postgraduate Studies, Dean	Signature	Date

Contents

List of Figures

List of Tables

Acknowledgment

First and foremost, I would like to express my heartfelt gratitude to Almighty God for providing me with the strength to reach this milestone, as well as for bestowing good health, wisdom and perseverance on me throughout my research journey. I would like to sincerely thank my supervisor, **Dr. Tesfay Gebremariam**, for his unwavering support, attentive guidance, and prompt responses throughout my PhD journey. His keen intuition in physics and analytical thinking has consistently inspired me, while his enthusiasm for my success and confidence in my abilities have motivated me to strive for excellence. I am especially grateful for his insightful and constructive feedback on my proposal, dissertation work, and final report. I also express my deep gratitude and deep respect to my course teacher and my co-supervisor, **Dr. Tewodros Yirgashew**, for his valuable contribution to my research. His insights, suggestions, and feedback have significantly improved the quality and depth of my work. This endeavor would not have been possible without his steadfast support and assistance.

I would like to express my gratitude to all the staff members in the Applied Physics Departments at ASTU and Injibara University for their unwavering support and encouragement. I want to express my heartfelt thanks to **Dr. Fikadu Tolesa**, the head of the Applied Physics Department at ASTU, for inspiring me during this challenging time. I am also grateful to **Dr. Alemayehu Getahun** and my fellow Ph.D. candidates in the Physics Departments at ASTU. Our mutual respect and engaging discussions have greatly enriched my experience and made my journey enjoyable.

Last but not least, I want to express my heartfelt gratitude to my family, such as:- my father, mother, brothers, sisters, and my son, **Nolawi** for their love, support, and encouragement throughout this journey. I am especially grateful to my wife, **Nitsuh Bekele**, for her unwavering commitment and for managing our family responsibilities during my studies.

Abstract

In this Ph.D. dissertation, we have studied quantum features in an electro-optomechanical system with an optical parametric amplifier, coherent feedback and two-level atoms. We investigated the quantum correlation in an electro-optomechanical system enhanced by an optical parametric amplifier (OPA) and Coulomb-type interaction. Logarithmic negativity, steerability, and quantum discord were used to quantify quantum correlations between mechanical modes. The results show that increasing the nonlinear gain values of the OPA, the phase of the OPA, Coulomb coupling strength, and driven laser power increased the quantum correlations between mechanical modes. However, quantum correlations decrease rapidly with increasing temperature as a result of decoherence. We examined quantum entanglement between mechanical modes assisted by an optical parametric amplifier and a coherent feedback loop. We used logarithmic negativity to quantify steady-state entanglement. The findings reveal that the presence of OPA, coherent feedback, robust Coulomb strength, and increased driving laser power improved quantum entanglement between mechanical modes. Finally, we examined quantum coherence in a hybrid electro-optomechanical system. We quantified Gaussian quantum coherence, using a covariance matrix and steady-state mean value. The results suggest that the presence of coherent feedback, the OPA, atomic ensembles, and strong laser power enhanced quantum coherence. In contrast, increasing atomic decay rates and environmental temperature diminish quantum coherence. These hybrid electro-optomechanical systems provide promising platforms for the realization of continuous variable quantum information processing.

***Keywords**: Quantum features, Quantum coherence, Coherent feedback loop, Optical parametric amplifier, Atomic ensembles, Electro-optomechanical system.*

1

INTRODUCTION

1.1 Background of the Study

In recent years, significant progress has been made in formalizing quantum mechanics based on quantum correlations. These quantum correlations between quantum systems are fundamental to quantum mechanics and applications in quantum information processing, including communication, computing, and metrology (Krenn et al., 2016; Hirvensalo, 2013; Giovannetti et al., 2011). In the realm of quantum mechanics, there exist various quantum correlations with distinct characteristics such as Bell non-locality (Poderini et al., 2022), quantum steering (Kogias et al., 2015), quantum entanglement (Duan et al., 2000), and quantum discord (Adesso and Datta, 2010). Following this, quantum correlations in composite systems lie at the heart of the experimentally verified violation of Bell inequalities (Poderini et al., 2022). A nonlocal state, characterized by its violation of the Bell inequality as demonstrated in Bell-type experiments, is a quantum state that exhibits correlations that cannot be explained by classical theories. In the specific case of pure states, entanglement is a necessary and sufficient condition for nonlocality. So far, the general notion of quantum correlations in mixed states boasts novel features that have played a central role in quantum information processing and communication, such as entanglement (inseparable state), one of the non-local correlations (Horodecki et al., 2009). Specifically, quantum entanglement is a crucial element of quantum information processing, incorporating the non-classical features of multipartite quantum systems (Amazioug et al., 2023). It has been used as an indispensable resource in various tasks of quantum information processing, including quantum teleportation (Vaidman, 1994), dense coding (Mattle et al., 1996), cryptography (Gisin et al., 2002), repeaters (Briegel et al., 1998), and memories (Liu et al., 2001).

In modern quantum information theory, it is generally understood that there exists an asymmetric form of nonclassical correlation that occupies an intermediate position between Bell non-locality and entanglement, known as quantum steering (Horodecki et al., 2009). This quantum phenomenon allows one party to remotely influence the state of another party by exploiting shared entanglement (Kogias et al., 2015). This intriguing concept was notably discussed by Schrödinger (Schrödinger, 1935) and previously acknowledged by Einstein, Podolsky, and Rosen (EPR) in their renowned 1935 paper (Einstein et al., 1935), forming a crucial part of the well-known EPR paradox (Reid et al., 2009). Both theoretical and experimental research has revealed that quantum steering observation serves as a crucial resource in different basic applications, such as the one-sided device-independent quantum key distribution (QKD) (Gisin et al., 2002), randomness generation (Law et al., 2014), quantum teleportation (Reid, 2013), and subchannel discrimination (SCD) (Piani and Watrous, 2015).

On the other hand, separable states which are not entangled can still exhibit nonzero quantum correlations. To quantify these quantum correlations beyond entanglement, Oliver and Zurek introduced the concept of quantum discord (Ollivier and Zurek, 2001). Quantum discord measures the amount of quantum correlations between two subsystems of a quantum system, providing a more comprehensive understanding of quantum correlations. As a result, this type of quantum discord aims to capture all the quantum correlations in a bipartite state. Specifically, quantum discord can be applied to a wide variety of states, including squeezed thermal states (Adesso and Datta, 2010), and is more resistant to decoherence than entanglement, making it suitable for quantifying quantumness in multiparty systems (Galve et al., 2011).

Quantum coherence arising from quantum superposition plays a central role in quantum mechanics. It is a common and necessary condition for both entanglement and other types of quantum correlations, and it is also an important physical resource in quantum computation and quantum information processing, metrology, and biological systems (Xi et al., 2015; Ghobadi et al., 2014; Ma et al., 2016; Reed et al., 2017; Tesfahannes et al., 2024; Uola et al., 2020; Demkowicz-Dobrzański and Maccone, 2014; Lostaglio et al., 2015; Collini et al., 2010). In recent years, there has been an increasing demand for the quantification and examination of quantum coherence in scientific research (Girolami, 2014; Baek et al., 2020; Cimini et al., 2019; Yu et al., 2020; Baumgratz et al., 2014; Napoli et al., 2016). In particular, (Baumgratz et al., 2014) introduced a comprehensive framework for quantifying quantum coherence, while (Napoli et al., 2016) highlighted the resilience and practical utility of coherence as an observable metric.

Cavity optomechanics has emerged as an important multidisciplinary area at the interface of quantum optics and nanophysics (Kippenberg and Vahala, 2008, 2007), attracting considerable attention for its implementation in various systems, including representative whispering gallery microcavities (Zhu et al., 2023), Fabry-Pérot cavities (Arcizet et al., 2006) and optical microwave cavities (Kippenberg et al., 2005). In optomechanical systems, light fields interact with mechanical resonators through radiation pressure (Aspelmeyer et al., 2010). In these systems, the quantum information stored in the optical and mechanical modes is often defined by employing continuous variable (CV) states, usually known as Gaussian states (Vitali et al., 2007a; Amazioug et al., 2018a). This system provides a promising platform for generating quantum states of macroscopic objects and several interesting applications in quantum information and processing, such as quantum entangled states (Teklu et al., 2018), cooling the mechanical mode to their quantum ground states (Chan et al., 2011), photon blockade (Amazioug et al., 2022), generating mechanical quantum superposition states (Liao and Tian, 2016), enhancing precision measurements (Xiong et al., 2017), gravitational wave detectors (Braginsky and Vyatchanin, 2002) and optomechanically induced transparency (Weis et al., 2010; Tesfahannes, 2021) have been studied.

In addition, the quantification of quantum correlations in continuous-variable state optomechanical systems plays a crucial role in applications of quantum information processing (Vitali et al., 2007a). Several researchers have studied the quantum correlation between optical and mechanical modes in optomechanical systems (Amazioug et al., 2018b; Aoune and Habiballah, 2022; Bougouffa et al., 2022; Singh and Ooi, 2014; Eshete, 2022). Particularly,(Amazioug et al., 2020a) have been investigated the transfer of quantum correlations from Einstein–Podolsky–Rosen (EPR) entangled squeezed light to movable mirrors. (Amazioug et al., 2018a) have studied quantum entanglement, EPR steering, and Gaussian geometric discord in a double-cavity optomechanical system. The generation of entanglement in macroscopic systems has garnered more attention (Tesfahannes, 2020). In line with this, mechanical resonators at mesoscopic sizes are emerging as viable tools for studying quantum properties (Zhang et al., 2016; Yang et al., 2017; Pinard et al., 2005). As a result, various methods for creating entanglement in macroscopic systems through radiation pressure coupling in optomechanical systems have been extensively investigated (Tesfahannes and Getahune, 2020; Zhou et al., 2011; Ge et al., 2013; Joshi et al., 2012). In addition, numerous researchers have presented schemes that emphasize the creation of mechanical-mechanical entanglements (Bai et al., 2021; Sohail et al., 2020; Zhang et al., 2003).

Some interesting phenomena occur when an optical parametric amplifier (OPA) is introduced into an optomechanical cavity, such as the generation of entangled and squeezed states of light (He and Li, 2007; Eckstein et al., 2011; Zhai et al., 2023; Wu et al., 1986), improve mechanical cooling (Huang and Agarwal, 2009), generate strong mechanical squeezing (Agarwal and Huang, 2016), and enhance the degree of precision of optomechanical position detection (Peano et al., 2015). Notably, the OPA serves as a non-linear device for laser frequency conversion, amplifying the intensity of the signal light through a nonlinear crystal. The ground-state cooling of a macroscopic mechanical oscillator for quantum manipulation of the mirror by a degenerate optical parametric amplifier has been examined by (Huang and Chen, 2018). In addition, (Hu et al., 2018) examined the two-fold mechanical squeeze in a cavity optomechanical system that involves an OPA driven by a periodically modulated laser field. Later, when an optical parametric amplifier is introduced into electro-optomechanical systems, several fascinating phenomena occur (Bai et al., 2017; Pan et al., 2022; Wang et al., 2018). Specifically,(Pan et al., 2022) investigated entanglement assisted by a distant electro-optomechanical system with two optical parametric amplifiers. Recently, Pan investigated entanglement using an electro-optical hybrid system with an optical parametric amplifier and Coulomb force interactions (Pan et al., 2023). They proposed that the presence of two charged oscillators enhances both entanglement and output squeezing within the electro-optical hybrid system.

Furthermore, the incorporation of an atomic ensemble into an optomechanical cavity has the potential to generate intriguing phenomena (Zhai and Guo, 2022; Singh et al., 2021; Liu et al., 2022). For example, cooling the ground state of a micromechanical system through a two-level atomic system (Liu et al., 2022) and two-level atoms effectively enhancing the radiation pressure of the optical cavity field (Ma and Zhou, 2012) has been extensively studied on the basis of atom-assisted hybrid optomechanical systems. Quantum coherence in a hybrid Laguerre-Gaussian rotating cavity optomechanical system with a two-level atom was investigated by (Singh et al., 2021). Furthermore, (Zhai and Guo, 2022) examined quantum coherence in a hybrid system with an atomic ensemble trapped in a cavity coupled with a typical cavity optomechanical system.

Coherent feedback has received a lot of interest in quantum information processing and quantum optics. Coherent feedback, a highly regarded feedback mechanism (Lloyd, 2000), enables a system to be controlled by coherently feeding its output back into its input via another controlling system while avoiding the impact of measurements. This concept was first introduced by Lloyd (Lloyd, 2000), followed by the systematic exploration of coherent feedback by Wiseman and colleagues in the context of optical systems, using a more comprehensive and generalized model (Wiseman and Milburn, 1994a). It has attracted much attention due to its wide applications in quantum information processing, such as ground state cooling (Huang and Chen, 2019), enhancement of normal mode splitting (Li et al., 2023), quantum state transfer (Harwood et al., 2021), quantum steering (Asjad et al., 2016), enhancement of entanglement (Li et al., 2017), and correction of quantum errors (Kerckhoff et al., 2010). Despite this broad spectrum of possibilities, there have been surprisingly few experiments exploring coherent feedback in optomechanics (Schmid et al., 2022; Kerckhoff et al., 2013). Therefore, the integration of coherent feedback, an optical parametric amplifier, and an ensemble of two-level atoms within an electro-optomechanical system remains a topic of active research. In this research, we consider a hybrid system that consists of an optical cavity, a coherent feedback loop, two charged mechanical oscillators, an optical parametric amplifier (OPA), and an ensemble of two-level atoms inside the cavity.

1.2 Statement of the Problem

Cavity optomechanical systems have emerged as powerful platforms for studying quantum phenomena at the mesoscopic scale. In the past decade, significant theoretical and experimental attention has been devoted to optomechanical systems. It offers a platform for achieving coherent quantum control over massive objects, creating non-classical states, reducing quantum noise, maintaining coherence, and exploring the boundary between classical and quantum realms. Furthermore, the interaction between light fields and mechanical resonators through radiation pressure in optomechanical systems gives rise to a rich variety of quantum effects, including quantum entanglement, quantum steering, quantum discord, and quantum coherence. Several researchers have studied the quantum correlation between optical and mechanical modes in optomechanical systems. In addition, many schemes have been proposed to improve entanglement in electro-optomechanical systems via optical parametric amplifier and transfer quantum states between subsystems. However, to the best of our knowledge, the measurement of quantum correlations in a hybrid electro-optomechanical system has not been addressed. Furthermore, coherent feedback control has emerged as a powerful tool for manipulating and optimizing the behavior of optomechanical systems. Currently, some research has focused on the impact of coherent feedback control in the area of optomechanical systems. In addition, the influence of coherent feedback on quantum entanglement in optomechanical systems has been explored. Nevertheless, the enhancement of quantum entanglement between the two mechanical modes in an electro-optomechanical system through coherent feedback and optical parametric amplifier has not been explored. Furthermore, the inclusion of an atomic ensemble into an optomechanical cavity could lead to the emergence of fascinating quantum phenomena, including quantum entanglement, quantum steering, quantum discord, and quantum coherence. Moreover, various schemes have recently been proposed to quantify macroscopic quantum coherence in optomechanical systems. However, the quantification of quantum coherence in an electro-optomechanical system with coherent feedback, an optical parametric amplifier, and an atomic ensemble has not been investigated.

1.3 Objectives of the Study

1.3.1 General Objective

The general objective of this dissertation is to investigate quantum features in an electro-optomechanical system with an optical parametric amplifier, coherent feedback and two-level atoms.

1.3.2 Specific Objectives

The specific objectives of this dissertation are to:-

- analyze quantum correlation in an electro-optomechanical system enhanced by an optical parametric amplifier and Columb interaction type
- examine macroscopic entanglement in an electro-optomechanical system through a coherent feedback loop
- determine quantum coherence in a hybrid electro-optomechanical system via coherent feedback loop

1.4 Significance of the Study

This study investigates the enhancement of quantum features in a hybrid electro-optomechanical system, exploring the effects of parameters such as the nonlinear gain of the OPA, Coulomb coupling strength, phase of the optical field phase, reflection coefficient, atomic collective coupling strengths, and environmental temperature on quantum entanglement, quantum steering, quantum discord, and quantum coherence. The findings provide valuable insights into how these various factors affect quantum properties. This research contributes to advancement in quantum technologies such as quantum metrology, cryptography, teleportation, and computation. It plays a crucial role in bridging the gap between theoretical concepts and practical applications in quantum information processing. Consequently, the results will provide valuable guidance to researchers and establish a foundation for future studies, with broad potential applications in quantum information processing, sensing, and metrology.

1.5 Scope of the Study

This study focuses on quantifying various quantum features within a hybrid electro-optomechanic al system. We employ many approaches to quantify quantum properties, such as entanglement, quantum steering, quantum discord, and quantum coherence. In particular, logarithmic negativity is employed to quantify quantum entanglement, while quantum discord serves as a measure of quantum correlation between the two mechanical oscillators. Furthermore, quantum steering is assessed to determine the steerability between mechanical oscillators. Lastly, Gaussian quantum coherence is evaluated using the covariance matrix and steady-state mean values.

The research presented in this dissertation is structured as follows: In chapter one, the background, the statement of the problem, the objectives, the significance of the study, and the scope of the study are discussed. In chapter two, the interaction between radiation and atoms, the dynamics of the quantum system, the development of an optomechanics system, recent advances in electro-optomechanical systems, the principle of optical parametric amplifier, basic concepts of the coherent feedback mechanisms, the radiation-pressure and optomechanical coupling, and basic optomechanics tools and approaches. Finally, the quantification of quantum features including entanglement, quantum steering, quantum discord, and quantum coherence were discussed in detail.

In chapter three, materials and procedures are described. In the first part, various optical components and software are widely utilized in research. In the second part, the methodologies employed in this study are briefly discussed. The third section of chapter three explores quantum correlations, including entanglement, steering, and discord between two mechanical modes. The fourth section of chapter three delves deeply into mechanical entanglement in an electro-optomechanical system. Finally, the last section of chapter three addresses quantum coherence in hybrid electro-optomechanical systems.

In chapter four, we present the results and discussion of the dissertation. The first and second sections of chapter four explore the impact of the non-linear gain of the optical parametric amplifier, the phase of the optical field driving the OPA, Coulomb coupling strength, environmental temperature, and driven laser power on the quantum correlations and entanglement between mechanical oscillators, as demonstrated by simulation results, respectively. Finally, the last section examines how various parameters, including the nonlinear gain of the OPA, reflection coefficient, atomic decay rate, atomic coupling, driving laser power, and ambient temperature, affect quantum coherence utilizing numerical simulation results.

Finally, chapter five presents the conclusions drawn from the investigation, offers recommendations based on the findings, and provides directions for future work.

2

LITERATURE REVIEW

In this chapter, the interaction between radiation and atom, the dynamics of the quantum system, the development of an optomechanical system, radiation pressure and optomechanical coupling, recent advances in electro-optomechanical systems, the principles of optical parametric amplifier, coherent feedback mechanisms, and basic optomechanics tools and approaches are discussed. Finally, quantification of quantum features that include entanglement, quantum steering, quantum discord, and quantum coherence is also widely discussed.

2.1 Atom-field interaction

The interaction between radiation and atoms is one of the central problems in the field of quantum optics. The coupling of a single two-level atom to a single-mode optical field is the basic model that shows the essential component of this interaction (Priyesh and Ramesh, 2014). This model has become very important and widely used in condensed matter physics and quantum optics, helping researchers to understand the complex nature of atom-photon interactions and providing crucial insights into the basic concepts of these systems. There are three main approaches to describe how atoms interact with electromagnetic fields: classical, semiclassical, and quantum mechanical. In the classical approach, both the electromagnetic field and atoms are treated classically. In the semi-classical approach, the field is treated classically while atoms are treated quantum mechanically. In quantum mechanics, both atoms and light are quantized (Scully and Zubairy, 1997). In quantum mechanical treatment, the interaction between an atom and a field is explained by the idea of photons, which are discrete energy units of electromagnetic radiation.

The Jaynes-Cummings model (JCM) is a key principle in quantum optics. It describes the interaction between a single two-level atom and a single mode of the quantized electromagnetic field confined within an optical cavity (Priyesh and Ramesh, 2014). A single-mode electric field in free space is given by (Gerry and Knight, 2023)

$$\hat{E}(r,t) = i\sqrt{\frac{\hbar\omega_c}{2\epsilon_o V}}\left[\hat{a}e^{i(k.r-\omega t)} - \hat{a}^\dagger e^{-i(k.r-\omega t)}\right]\hat{u}, \tag{2.1}$$

where k is the wave vector of the radiation, ϵ_o is the permittivity of free space, ω_c is the cavity frequency, V indicates the volume of the cavity, $\hat{a}(\hat{a}^\dagger)$is the annihilation(creation) cavity operator and $\hat{u}$ is the unit vector. The spatial variation of the field is negligible in the atomic extension. Considering that r has typical atomic dimensions (few angstroms), the size of the atom is much smaller than the wavelength of the laser field ($k.r \ll 1$). Therefore, the electric field is spatially uniform across the atom and can be expressed as $\hat{E}(r,t) = \hat{E}(t)$. This approximation is commonly referred to as the dipole approximation, which is a widely recognized concept in the field. On account of this condition, Eq.(2.1) can be written in this manner

$$\hat{E}(t) = i\sqrt{\frac{\hbar\omega_c}{2\epsilon_o V}}\left[\hat{a}e^{-i\omega t} - \hat{a}^\dagger e^{i\omega t}\right]\hat{u}. \tag{2.2}$$

Consider a two-level atom with the upper- and lower-energy eigenstates denoted by $|a\rangle$ and $|b\rangle$, respectively. Assume that the only possible allowable transition from $|a\rangle$ to $|b\rangle$. We assume that these eigenstates form a complete set so that, $I = \sum_\alpha |\alpha\rangle\langle\alpha|$, where $\alpha = a, b$. In standard notation, we denote the raising and lowering atomic, and energy operators are

$$\hat{\sigma}_+ = |a\rangle\langle b|,\ \hat{\sigma}_- = |b\rangle\langle a|, \tag{2.3}$$

and

$$\hat{\sigma}_z = |a\rangle\langle a| - |b\rangle\langle b|. \tag{2.4}$$

It is worth mentioning that the atomic operators satisfy the commutation relations

$$[\hat{\sigma}_z, \hat{\sigma}_\pm] = \pm 2\hat{\sigma}_\pm, \tag{2.5}$$

and

$$[\hat{\sigma}_+, \hat{\sigma}_-] = \hat{\sigma}_z. \tag{2.6}$$

Upon taking the atomic states to be complete and orthonormal, the free Hamiltonian of the atom is given by (Tesfa, 2021)

$$\hat{H}_A = \frac{1}{2}\hbar\omega_o\hat{\sigma}_z, \tag{2.7}$$

where ω_o is atomic transition frequency.

The free Hamiltonian of the cavity field is (Tesfa, 2021)

$$\hat{H}_F = \hbar\omega_c \hat{a}^\dagger \hat{a}. \tag{2.8}$$

Employing Eq.(2.2), the interaction Hamiltonian is defined as

$$\hat{H}_I = -e\hat{r}(t).\hat{E}(t). \tag{2.9}$$

Eq.(2.9), if the electric dipole interacts with the electric field. Substituting Eq.(2.2) into Eq.(2.9), finally expressed as

$$\hat{H}_I = ie\sqrt{\frac{\hbar\omega_c}{2\epsilon_o V}}\left[\hat{a}e^{-i\omega t} - \hat{a}^\dagger e^{i\omega t}\right]\hat{r}.\hat{u}. \tag{2.10}$$

Furthermore, applying twice the identity operator, the position operator $\hat{r}$ can be written as

$$\hat{r}(t) = \sum_\alpha \sum_\beta r_{\alpha\beta}(t)|\alpha\rangle\langle\beta|, \tag{2.11}$$

where $r_{\alpha\beta}(t) = \langle\alpha|\hat{r}(t)|\beta\rangle$. Eq.(2.11) can be put in this form

$$\hat{r}(t) = r_{aa}\hat{\sigma}_{aa} + r_{bb}\hat{\sigma}_{bb} + r_{ab}\hat{\sigma}_+ + r_{ba}\hat{\sigma}_-. \tag{2.12}$$

The position operator $\hat{r}(t)$ for the atomic electron in the absence of interaction. The equation of evolution of the position operator can be written as

$$i\hbar\frac{d\hat{r}}{dt} = [\hat{r}, \hat{H}_A], \tag{2.13}$$

Inserting Eq.(2.7) into Eq.(2.13), we easily get the solution of the position operator as

$$\hat{r}(t) = r_{aa}\hat{\sigma}_{aa} + r_{bb}\hat{\sigma}_{bb} + r_{ab}\hat{\sigma}_+ e^{i\omega_o t} + r_{ba}\hat{\sigma}_- e^{-i\omega_o t}, \tag{2.14}$$

suppose $r_{aa} = r_{bb} = 0$, and $r_{ab} = r_{ba}$. Thus, Eq.(2.14) can be written as

$$\hat{r}(t) = r_{ab}(\hat{\sigma}_+ e^{i\omega_o t} + \hat{\sigma}_- e^{-i\omega_o t}). \tag{2.15}$$

Inserting Eq.(2.15) into Eq.(2.10), then the interaction Hamiltonian contains the exponentials $e^{\pm(\omega+\omega_o)t}$ are rapidly varying functions of time. By neglecting rapid terms comparison with the slowly $e^{\pm(\omega-\omega_o)t}$ varying functions time using the rotating wave approximation. Finally, the interaction Hamiltonian at resonance can be written as (Kassahun, 2014)

$$\hat{H}_I = i\hbar g_a(\hat{a}\hat{\sigma}_+ - \hat{a}^\dagger\hat{\sigma}_-), \tag{2.16}$$

in which $g_a = \sqrt{\frac{\omega_c}{2\epsilon_o V}} d_{ab}.u$ is the coupling constant between the atom and radiation and $d_{ab} = er_{ab}$ is the electric dipole matrix element.

2.2 Closed and open quantum systems

Quantum systems have been used as the foundation for several novel technologies in quantum information processing, quantum computing, quantum communication, and quantum sensing (Nielsen and Chuang, 2010). Thus, quantum systems are classified into two parts: closed and open quantum systems. A closed quantum system is a fundamental concept in quantum mechanics that has attracted a lot of attention in the physics community. The study of closed quantum systems examines the behavior of isolated quantum systems (Breuer and Petruccione, 2002). In this context, the evolution of the system is assumed to be unitary and hence is described by the Schrödinger equation. Moreover, quantum mechanics provides a theoretical framework for understanding the behavior of microscopic particles in closed systems, such as atoms and photons.

In contrast, open quantum systems (OQS) interact with their environment, leading to decoherence and dissipation. The Markov approximation simplifies this interaction by assuming an environment that quickly returns to equilibrium, resulting in a continuous information flow from the system to the environment. However, this approximation is limited by the requirement of distinct system and environment timescales. To overcome these limitations, Vega and Alonso outlined advanced methods for a more detailed analysis of OQS dynamics (De Vega and Alonso, 2017). In particular, the specific approach to studying an OQS varies considerably between different fields. For example, quantum optics (Cohen and Tannoudji, 1992) utilizes distinct methodologies compared to condensed matter physics or open systems related to chemical physics (Leggett et al., 1987).

Several mathematical frameworks have been devised to represent these systems. Specifically, for atomic, molecular, and optical (AMO) systems, these frameworks offer a precise portrayal of the open quantum system at the microscopic level. In recent times, the use of AMO systems, encompassing cold atomic and molecular gases as well as trapped ions, has gained significant traction in the field of many-body physics (Daley, 2014; Nielsen and Chuang, 2010). There has been significant renewed interest in the study of open many-body systems, mostly encouraged by advances in quantum information science (Nielsen and Chuang, 2010). Furthermore, the idea of open systems is especially important for studying quantum phenomena such as quantum discord, squeezing, quantum coherence, entanglement, and quantum steering in cavity optomechanics and magnon mechanics (Aolita et al., 2015).

2.3 Development of cavity optomechanics

Cavity optomechanics is a field of physics that studies the interaction of light with mechanical systems at small energy scales. It has emerged as a field that combines quantum optics and nanophysics. An example of cavity optomechanics is a Fabry-Pérot cavity, which consists of one mirror that is fixed and the other is a movable mirror, as illustrated in Fig. (2.1). In this setup, the displacement of the moving mirror alters the resonance frequency of the cavity, resulting in a radiation pressure force on the moving mirror created by the light within the cavity. The frequency of the cavity mode is determined by the mechanical displacement $\hat{x}$ and can be represented as $\omega_c(\hat{x})$. It is a recently developed field that explores and exploits the radiation-pressure coupling between the cavity mode and the mechanical degrees of freedom (Aspelmeyer et al., 2010; Marquardt and Girvin, 2009).

Several of the techniques employed in cavity optomechanics are already in use in gravitational wave detectors, which require the measurement of mirror displacements (Caves, 1980; Braginsky et al., 1977). Although these detectors do not specifically target quantum effects, they face analogous challenges and employ similar techniques to enhance precision. The objective of this field is to observe the quantum mechanical behavior of macroscopic systems through the advanced fabrication of high-quality mechanical resonators (Meystre, 2013). The basic concepts that are important when measuring mechanical systems with high accuracy and/or at very low temperatures, such as thermal and quantum noise, linear response theory, and back action, are explained. The quantum limit on linear position detection is obtained and the sensitivities that have been achieved in recent opto- and electromechanical experiments are compared to this limit (Midolo et al., 2018). The following may contribute to strong coupling in the quantum regime, with applications in metrology, sensing, quantum information processing, and testing fundamental physics laws (DiVincenzo, 2000). Although these studies have focused mainly on the interaction between electromagnetic radiation and individual mechanical resonators, there is a growing interest in the theoretical and practical study of multi-element optomechanical systems (Dantan et al., 2008; Karuza et al., 2013).

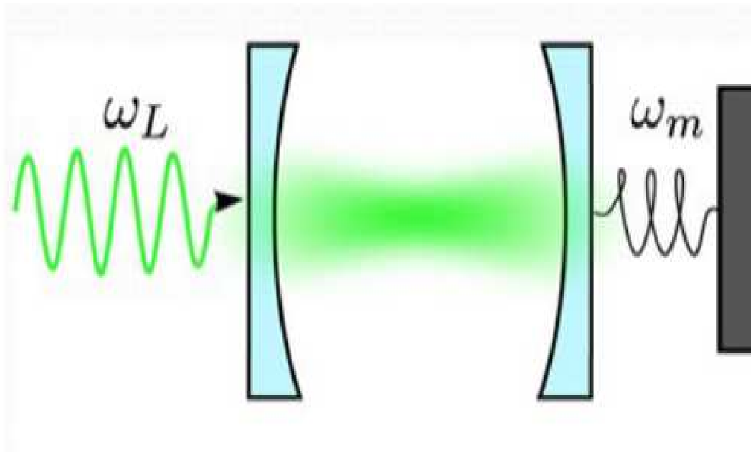

Figure 2.1: Sketch of Fabry Perot cavity. A laser-driven optical cavity connects to a mechanical mirror via radiation pressure (Aspelmeyer et al., 2010).

2.4 Radiation pressure and optomechanical coupling

Radiation pressure forces between light and matter occur due to momentum transfers between photons and the movable mirror, in which the momentum alter indicates that light creates a force on the mirror (Aspelmeyer et al., 2014). The effect of radiation pressure was first seen in comet dust tails centuries before scientists could directly quantify it. Johannes Kepler first observed this phenomenon in the 17th century, and it has since grown to be a fundamental aspect of our understanding of how light interacts with matter (Kepler, 1963). Maxwell predicted that electromagnetic fields could apply force on objects. In the twentieth century, this prediction was tested by experiments conducted that same year by (Nichols and Hull, 1901) and (Lebedev, 1901). Later, Einstein determined the statistics of the fluctuations in radiation pressure acting on a moving mirror (Einstein, 1909). This analysis included the frictional effects of the radiation force, and it allowed him to reveal the dual wave-particle nature of black-body radiation. Afterward,(Frisch, 1933) and (Beth, 1936) proved the linear and angular momentum transfer of photons to atoms and macroscopic objects, respectively.

Later, in the 1960s and 1970s, Braginsky and co-workers examined radiation pressure phenomena in gravitation using gravitational wave antennas. Braginsky considered the dynamical influence of the radiation pressure on a harmonically suspended end mirror of a cavity. His analysis revealed that the retarded nature of the force, due to the finite lifetime of the cavity, provides damping or anti-damping of mechanical motion, two effects that he was able to demonstrate in pioneering experiments using a microwave cavity (Braginsky, 1967; Braginskiǐ et al., 1970). Furthermore, Braginsky discussed the basic effect of radiation pressure force and quantum fluctuations to precisely estimate the location of an oscillating mirror (Braginsky et al., 1978). In addition, (Caves, 1980) addressed the quantum noise effect and its significance. These works acknowledge the basic quantum limit for continuous position detection, which is crucial in gravitational wave detectors such as the well-known Laser Interferometer Gravitational-wave Observatory.

The simplest form of radiation pressure coupling is momentum transfer due to reflection that occurs in a Fabry-Perot cavity, as shown in Fig.(2.2). Consider the momentum arriving at the surface of a mechanical oscillator. Its impact on the mechanical oscillator will cause a momentum kick and start its oscillation. Therefore, the momentum change of the mirror would be twice the momentum of a single photon, such as $\Delta P = 2\hbar k$, where $k = 2\pi/\lambda$ is the wave number of the light. The radiation pressure force is given by (Aspelmeyer et al., 2014)

$$\langle \hat{F} \rangle = 2\hbar k \frac{\langle \hat{a}^\dagger \hat{a} \rangle}{\tau_c} = \frac{\hbar \omega_c}{L} \langle \hat{a}^\dagger \hat{a} \rangle = g_o \langle \hat{a}^\dagger \hat{a} \rangle, \tag{2.17}$$

where $\tau_c = 2L/c$ denotes the cavity round trip time. The parameter g_o is the optomechanical coupling or describes the change in the resonance frequency of the cavity with position.

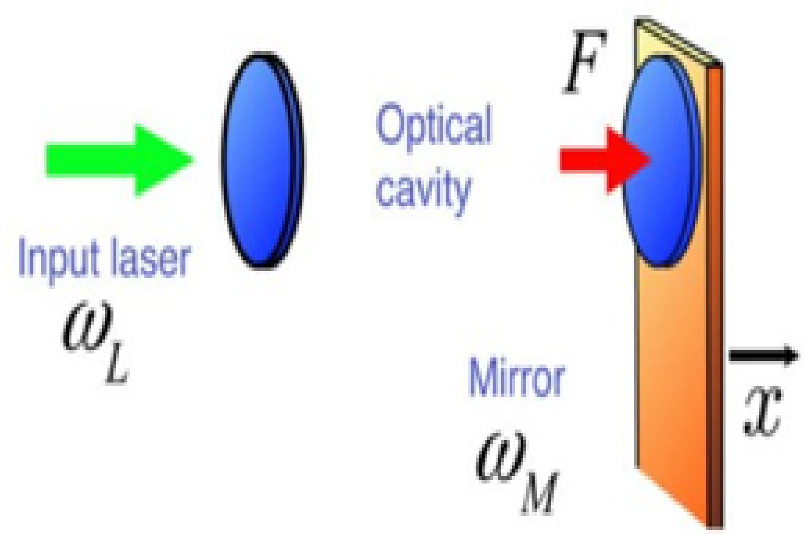

Figure 2.2: Fabry-Perot cavity driven by ω_L and with one movable mirror and one fixed end adopted from (Marquardt and Girvin, 2009).

Numerous quantum features of optomechanical systems have been explored both theoretically and experimentally. These include the squeeze of light (Mancini and Tombesi, 1994), the quantum nondemolition (QND) measurements of intense light (Jacobs et al., 1994), entangled photon pairs creation (Giovannetti et al., 2001), entanglement between mechanical mode and light (Vitali et al., 2007a), the quantum-state transfer from the light field to the mechanical oscillator (Zhang et al., 2003), feedback cooling of the mechanical motion (Mancini et al., 1998) (which was experimentally realized (Cohadon et al., 1999) and superposition of states (Marshall et al., 2003).

2.5 Recent advances in electro-optomechanical system

Recent advances in micro and nanotechnology, as well as quantum information technology (O'brien et al., 2009; Slussarenko and Pryde, 2019), have enabled researchers to manipulate photons (Sato et al., 2012), electrons (Sazonova et al., 2004), and even phonons at the single quantum level (Mathew et al., 2020). In recent decades, micro/nanotechnology has also promoted the rapid development of microelectromechanical systems (MEMS), where the interaction between mechanical and electrical degrees of freedom has been widely studied (Xu et al., 2021). The MEMS area has increasingly been transferred into the realm of nano-electromechanical systems (NOEMS) as device sizes continue to reduce. A nano-electromechanical system is defined as systems with dimensions in the nanometer range. With these concepts and technologies inherent to NOEMS, researchers can develop advanced functionalities such as high-speed, low-power consumption switches, and high-efficiency microwave-to-optical conversion devices.

In recent years, amazing breakthroughs have been made in the field of nanophotonics, with nanoelectro-optomechanical systems emerging as novel platforms for exploring optical, mechanical and electrical degrees of freedom (Ma et al., 2024). These systems integrate mechanical, electrical, and optical aspects, opening novel possibilities for manipulating information in the quantum domain. Furthermore, the electro-optomechanical system holds promise for the development of hybrid quantum systems. By combining the principles of quantum optics and nano-electromechanical systems, researchers aim to create systems where both optical and mechanical degrees of freedom can exhibit quantum behavior (Schleich et al., 2016). This has the potential to revolutionize quantum computing, quantum communication, and quantum sensing (Aspelmeyer et al., 2014).

Many researchers have attempted to study electro-optomechanical systems using a variety of approaches, leading to a deep and diversified understanding of their features and potential applications (Wang et al., 2018; Bai et al., 2017; Pan et al., 2022, 2023; Zhang et al., 2012; Ma et al., 2014). Specifically, (Bai et al., 2017) proposed a scheme to show that a system consisting of two separated macroscopic oscillators in space that are coupled through the Coulomb interaction displays classical-to-quantum transition behavior under the action of the optomechanical coupling interaction. The optical parametric amplifier plays a very significant role in the interaction of cavity optomechanics, and the possibility to enhance the radiation pressure in the sum sideband in an optomechanical system containing an OPA has been developed to perform quantum applications (Li and Huang, 2019). Most recently, (Pan et al., 2023) investigated the entanglement phenomena, assisted through an electro-optical hybrid system with an optical parametric amplifier and a Coulomb force interaction, and suggested that the two charged oscillators improved entanglement and output squeezing in an electro-optical hybrid system.

2.6 Principle of optical parametric amplifier

Optical parametric amplifier (OPA) use second-order nonlinearity to efficiently transfer energy from a pump frequency to both a signal and an idler frequency (see Fig. 2.3). It has attracted a lot of attention in the domains of optics and photonics, with different research studying its theoretical basis and practical applications (Hansryd et al., 2002; Marhic et al., 2015). It also plays a crucial role in generating squeezed light states, which are fundamental for quantum information processing, quantum metrology, and various other applications in quantum technologies (Manzoni and Cerullo, 2016). Recently, the optical parametric amplifier plays a very important role in the optomechanical system, and some interesting phenomena have been reported (Hu et al., 2018; Bai et al., 2017; Pan et al., 2022). As is well known, the non-linearity of OPA results in many interesting phenomena, such as the generation of entangled and squeezed states of light (He and Li, 2007), enhances mechanical cooling (Huang and Chen, 2018), generates strong mechanical squeezing (Agarwal and Huang, 2016), and improve the degree of precision of optomechanical position detection (Peano et al., 2015).

Figure 2.3: Schematic diagram of an optical parametric amplifier.

2.7 Basic ideas of coherent feedback

Coherent feedback is a type of feedback in which a system can be controlled by feeding its output into its input coherently through another controlling system without being disturbed by measurements. It is a useful approach in quantum control, especially in regulating quantum systems without adding unwanted noise (Zhang et al., 2017). Unlike typical measurement-based feedback systems, coherent feedback dramatically improves a quantum system's coherence by modifying the optical field. The concept of coherent feedback was developed by (Lloyd, 2000) and is a more comprehensive method than the all-optical feedback previously proposed in 1994 by (Wiseman and Milburn, 1994b) within the realm of quantum optical systems.

Quantum feedback control is becoming important in applications including quantum information processing, metrology, communication, and simulation (Nielsen and Chuang, 2010). Furthermore, coherent feedback techniques have been used to facilitate a wide range of tasks, including noise cancellation (Mabuchi, 2008), pure state preparation (Jacobs et al., 2014), optical squeezing (Gough and Wildfeuer, 2009), sympathetic cooling (Rohde et al., 2001), swaps of arbitrary states (Nelson et al., 2000), qubit state manipulation (Hirose and Cappellaro, 2016), and the generation of significant optical nonlinearities at the single-photon level (Wang and Safavi-Naeini, 2017). Additionally, feedback techniques can be employed to cool various degrees of freedom, facilitating their transition into the quantum regime. In the past decade, numerous quantum optical demonstrations of these feedback techniques have been realized, culminating in the remarkable stabilization of photon number states within a cavity quantum electrodynamics setup, as well as improved optical phase estimation (Serafini, 2012).

There has been significant research focus on the impact of coherent feedback control within the area of optomechanical systems (Zhou et al., 2015; Huang and Chen, 2019; Mabuchi, 2008; Li et al., 2023; Mansouri et al., 2022). Consequently, numerous researchers have addressed the impact of coherent feedback on quantum entanglement (Amazioug et al., 2020b; Wang et al., 2015a; Lü et al., 2022; Li et al., 2017; Mekonnen et al., 2024). In particular, (Lü et al., 2022) have examined the impact of feedback control on quantum entanglement in an optomechanical system. In addition, (Li et al., 2017) have explored the enhancement of the scheme to generate entanglement of the mechanical resonators using a coherent feedback loop.

2.8 Basic tools and approaches of optomechanics

2.8.1 Hamiltonian formulation

The Hamiltonian of a Fabry-Perot cavity has been extensively examined and analyzed in numerous studies (Vitali et al., 2007a; Meystre, 2013; Vitali et al., 2007b). Especially, (Meystre, 2013) has considered the Fabry-Pérot cavity, which consists of a partially fixed mirror on one side and a reflective mirror on the other side, as shown in Fig.(2.1). The interaction between light and the mirrors is characterized by the coupling of the cavity mode with the displacement or position of the mirrors. The total Hamiltonian of the Fabry-Perot cavity can be defined as

$$\hat{H} = \hat{H}_{free} + \hat{H}_{in} + \hat{H}_{d}, \tag{2.18}$$

where $\hat{H}_{free}$ is the free Hamiltonian of the cavity and mechanical modes, $\hat{H}_{in}$ denotes the interaction Hamiltonian between the cavity and mechanical modes, and $\hat{H}_d$ refers to the Hamiltonian of the driven laser. The Hamiltonian of the free is defined as

$$\hat{H}_{free} = \hbar\omega_c \hat{c}^\dagger \hat{c} + \hbar\omega_m \hat{b}^\dagger \hat{b}, \tag{2.19}$$

where, $\hat{c}(\hat{c}^\dagger)$ is the annihilation (creation) operator of the optical cavity mode and $\hat{b}(\hat{b}^\dagger)$ is the annihilation (creation) operator of the mechanical mode. The commutation relations satisfy $[\hat{c}, \hat{c}^\dagger] = [\hat{b}, \hat{b}^\dagger] = 1$. The optical field couples to the movable mirror, it exerts radiation pressure on the mirror, and displaces it from its equilibrium position. The cavity resonance frequency is modulated by the mechanical position ($\hat{x}$) and using Taylor expansion as (Aspelmeyer et al., 2010), $\omega_c(\hat{x}) = \omega_c - \hat{x}\frac{\partial}{\partial x}\omega_c(\hat{x}) + \vartheta(x)$, where $\hat{x} = x_{zpf}(\hat{b}^\dagger + \hat{b})$, $x_{zpf} = \sqrt{\frac{\hbar}{2m_{eff}\omega_m}}$ is the zero-point fluctuation, with m_{eff} being the effective mass of the mechanical oscillator. The total Hamiltonian system as

$$\hat{H} = \hbar\omega_c \hat{c}^\dagger \hat{c} + \hbar\omega_m \hat{b}^\dagger \hat{b} - \hbar g \hat{c}^\dagger \hat{c}(\hat{b} + \hat{b}^\dagger) + i\hbar\Omega\left(\hat{c}^\dagger e^{-i\omega_l t} - \hat{c} e^{i\omega_l t}\right), \tag{2.20}$$

where $g = \frac{\partial}{\partial x}\omega_c(\hat{x})x_{zpf}$ is a single photon optomechanical coupling interaction and Ω is amplitude of the driven field.

2.8.2 Quantum Langevin equation

The quantum Langevin approach is used to investigate the dynamics of the quantum system interacting with its environment. In quantum Langevin equation is well-suited tool for modeling open quantum system. The general formulation of the quantum Langevin equation for a system that interacts with the environment can also be called a heat bath. The total Hamiltonian can be expressed as follows (Zhang et al., 2017):

$$\hat{H} = \hat{H}_S + \hat{H}_I + \hat{H}_B, \tag{2.21}$$

$$\hat{H}_B = \hbar \int_{-\infty}^{\infty} d\omega \hat{b}^\dagger(\omega)\hat{b}(\omega), \tag{2.22}$$

$$\hat{H}_I = i\hbar \int_{-\infty}^{\infty} d\omega \kappa(\omega)[\hat{c}^\dagger \hat{b}(\omega) - \hat{b}^\dagger(\omega)\hat{c}], \tag{2.23}$$

where $\kappa(\omega)$ is the coupling constant between the modes, $\hat{H}_S$ is the Hamiltonian of the system, $\hat{b}(\omega)(\hat{b}^\dagger(\omega))$ is annihilation (creation) operator for the bath and $\hat{c}$ is the annihilation operator of the system. The commutation relation

$$[\hat{b}(\omega), \hat{b}^\dagger(\omega')] = \delta(\omega - \omega^{'}). \tag{2.24}$$

The Heisenberg equation of motion for any arbitrary operator $\hat{O}$ and the associated bath $\hat{b}(\omega)$ can be defined as (Walls et al., 1994)

$$\dot{\hat{O}} = \frac{-i}{\hbar}[\hat{O}, \hat{H}_s] + \int d\omega \kappa(\omega) \left[\hat{O}, \left(\hat{c}^\dagger \hat{b}(\omega) - \hat{b}^\dagger(\omega)\hat{c}\right)\right] - \int d\omega [\hat{O}, \hat{b}^\dagger(\omega)\hat{b}(\omega)]. \tag{2.25}$$

The Heisenberg equation of motion for an arbitrary system operator $\hat{b}(\omega)$ is given by

$$\dot{\hat{b}}(\omega) = -i\omega \hat{b}(\omega) - \kappa(\omega)\hat{c}, \tag{2.26}$$

using the initial condition time $t_o < t$, then the final condition time $t < t_1$, and we have

$$\hat{b}(\omega, t) = e^{-i\omega(t-t_0)}\hat{b}_o(\omega, t_0) - \kappa(\omega)e^{-i\omega(t-t_0)} \int_{t_0}^{t_1} dt^{'} e^{-i\omega(t^{'})} c(t^{'}). \tag{2.27}$$

Substituting Eq. (2.27) into Eq. (2.25), we easily obtain

$$\begin{aligned} \dot{\hat{O}} = \frac{-i}{\hbar}[O, H_s] + \int d\omega \kappa(\omega) e^{-i\omega(t-t_o)}\hat{b}_o(\omega)[\hat{O}, \hat{c}^\dagger] - [\hat{O}, \hat{c}]e^{-i\omega(t-t_o)}\hat{b}_o(\omega) \\ - \int d\omega [\kappa(\omega)]^2 e^{-i\omega(t-t_o)} \int_{t_0}^{t} dt' e^{-i\omega(t')}\hat{c}(t^{'})[\hat{O}, \hat{c}] - [\hat{O}, \hat{c}^\dagger]e^{i\omega(t^{'})}\hat{c}(t^{'}). \end{aligned} \tag{2.28}$$

Assume that $\kappa(\omega)$ is independent of frequency and then substitute $\kappa(\omega) = \sqrt{\frac{\kappa}{\pi}}$ is known as the first Markov approximation process. This approximation can be used to put Eq. (2.28) into the form of a damping equation. Applying the properties

$$\int_{-\infty}^{\infty} d(\omega)e^{-i\omega(t-t_0)} = 2\pi\delta(t - t_0), \tag{2.29}$$

and

$$\int_{t_0}^{t} c(t^{'})\delta(t - t^{'})dt^{'} = c(t). \tag{2.30}$$

Therefore, the formulation operator for the input and output fields (Tesfa, 2021)

$$\hat{c}_{in}(t) = \frac{1}{\sqrt{2\pi}} \int_{-\infty}^{\infty} d\omega e^{-i\omega(t-t_o)} b_o(\omega), \tag{2.31}$$

$$\hat{c}_{out}(t) = -\frac{1}{\sqrt{2\pi}} \int_{-\infty}^{\infty} d\omega e^{-i\omega(t-t_o)} b_f(\omega). \tag{2.32}$$

The quantum Langevin equation for the system operator $\hat{O}$ as follows:

$$\dot{\hat{O}} = -i[\hat{O}, H_s] - \kappa\hat{O} + \sqrt{2\kappa}\hat{O}_{in}(t), \tag{2.33}$$

The cavity mode can be expressed in terms of the output variables as

$$\dot{\hat{O}} = -i[\hat{O}, H_s] + \kappa\hat{O} - \sqrt{2\kappa}\hat{O}_{out}(t), \tag{2.34}$$

where $\hat{O}$ is an arbitrary operator, and also κ is the arbitrary decay rate, and $\hat{O}_{in}(\hat{O}_{out})$ is the arbitrary input (output) quantum noise. Furthermore, the relationship between the input and output cavity mode operator. Replace $\hat{O}$ by $\hat{c}$, then subtract Eq. (2.33) and Eq. (2.34), the input-output relation of the cavity mode operator is defined as

$$\hat{c}_{out} = \sqrt{2\kappa}\hat{c} - \hat{c}_{in}. \tag{2.35}$$

2.8.3 Linearization

In cavity optomechanics, nonlinear interaction between optical and mechanical modes occurs due to the nonlinear nature of the radiation pressure (Burgwal et al., 2020). In order to investigate the quantum dynamics of the system, we apply the linearization technique discussed in Ref. (Hilico et al., 1992) to simplify the analysis. Under strong laser power driving the cavity, the nonlinear quantum Langevin equations can be linearized by expressing each Heisenberg operator as the sum of its steady-state mean value and a small fluctuation with a zero mean value (Tesfahannes, 2020). The linearization technique for any operator $\hat{O}$ can be expressed as follows:

$$\hat{O} = O_s + \delta\hat{O}, \tag{2.36}$$

where O_s is expectation value of the operator and $\delta\hat{O}$ is fluctuation operator from expectation value.

2.9 Fundamental concepts of quantum features and their measurement

Quantum correlation is a vital field of research. Especially important in the context of upcoming quantum technologies is the redefinition of the concept of correlations, drawing a clear distinction between classical phenomena and their quantum counterparts. By understanding the unique characteristics of quantum correlations, researchers can harness their potential to develop novel applications and advance our understanding of the quantum world (De Chiara and Sanpera, 2018). Pure states can be either uncorrelated or just entangled. For mixed states, several layers of quantum correlations have been identified, going significantly beyond the seminal paradigm of (Werner, 1989). Referring to (Adesso et al., 2016), explain the conceptual frameworks of several shades of quantum correlations, such as non-locality and steering, and observe how it connected to quantum entanglement as depicted in Fig. (2.4). In order of decreasing strength, these can be classified as: non-locality $\Rightarrow$ steering $\Rightarrow$ entanglement $\Rightarrow$ general quantum correlations. Non-classical correlations, such as entanglement and coherence, can be used to perform tasks beyond the scope of classical physics. Quantum discord, a more general measure of quantum correlation, provides a wider framework for understanding and using quantum resources. In general, quantum correlations satisfy the following conditions: quantum discord $\supseteq$ quantum entanglement $\supseteq$ quantum steering $\supseteq$ Bell nonlocality. This indicates that steerable states form a strict subset of entangled states while simultaneously being a strict superset of states that can demonstrate Bell nonlocality.

Recently, the investigation of quantum correlations has significantly advanced the field of quantum information and various foundational aspects of quantum theory. From an application perspective, quantum correlations have played a key role in the development of numerous quantum information and quantum computing protocols (Maquedano and Costa, 2024; Nielsen and Chuang, 2001). To this end, this quantum correlation transfer provides a potential tool for

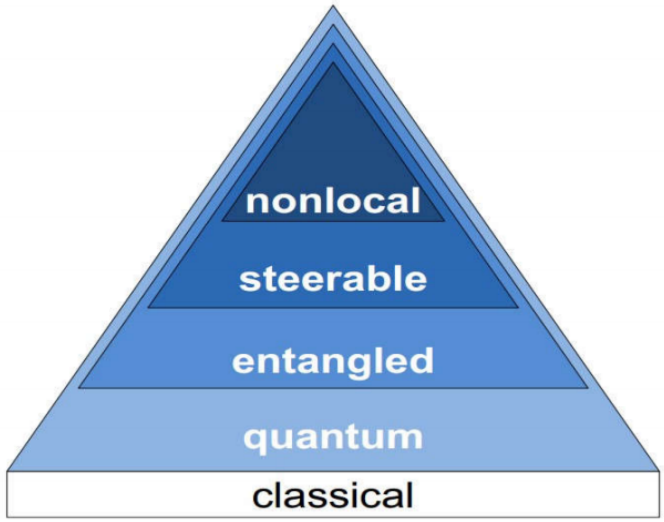

Figure 2.4: Hierarchy of correlations in states of composite quantum systems (Adesso et al., 2016).

exploiting quantum information encoded in mechanical modes that can be more resilient against decoherence effects (Mekonnen et al., 2023). Therefore, we apply different quantum correlation quantifiers, including quantum entanglement, Gaussian quantum steering, and Gaussian quantum discord between subsystems.

2.9.1 Quantum entanglement

Quantum entanglement is an important feature of quantum physics that explains physical phenomena in which two or more quantum systems become permanently connected, regardless of the distance between them. It is a key ingredient of quantum information processing that characterizes the non-classical property of multipartite quantum systems (Amazioug et al., 2023). It is a fascinating feature of quantum mechanics that is believed to serve as a valuable resource for quantum information, for example, quantum computing (Pellizzari et al., 1995), quantum teleportation (Bennett et al., 1993), quantum cryptography (Jennewein et al., 2000), and quantum dense coding (Wang et al., 2015b). Accordingly, numerous researchers have shown that nonzero entanglement assures the existence of quantum correlations but the zero entanglement does not assure the absence of quantum correlations in a bipartite quantum state. Besides, entanglement has been realized in microscopic systems such as atom- atom (Çakir et al., 2005), atom-photon (Fedorov et al., 2005), ion-ion (Cory and Havel, 2004), and ion-photon (Stute et al., 2012).

Recently, much progress has been made, and several interesting quantum optomechanic systems have been widely demonstrated to generate entanglement between optical and mechanical modes (Barzanjeh et al., 2022). Besides, the generation of entanglement in macroscopic systems has garnered more attention. In line with this, mechanical resonators at mesoscopic sizes are emerging as viable tools for studying quantum properties (Zhang et al., 2016; Yang et al., 2017; Pinard et al., 2005). As a result, various methods for creating entanglement in macroscopic systems through radiation-pressure coupling in optomechanical systems have been extensively investigated (Tesfahannes and Getahune, 2020; Zhou et al., 2011; Ge et al., 2013; Joshi et al., 2012). In recent years, numerous researchers have focused on quantifying bipartite entanglement between subsystems (Vidal and Werner, 2002; Vitali et al., 2007b; Teklu et al., 2018). The preparation and manipulation of these entangled states that have non-classical and non-local properties lead to a better understanding of the basic quantum principles. To this aim, many inseparability criteria have been developed to measure, detect, and manipulate the entanglement generated by various quantum optical devices. Some of the criteria include logarithmic negativity, Duan-Giedke-Cirac-Zoller (DGCZ), Hillary Zubairy criteria, and violation of the Cauchy-Schwarz inequality (Abebe et al., 2020). In this dissertation, we utilize logarithmic negativity to quantify the quantum entanglement of bipartite systems. In line with this, logarithmic negativity E_N is the most popular tool to measure the degree of entanglement between the bipartite subsystems in a continuous variable system. It is defined by (Vitali et al., 2007a)

$$E_N = \max[0, -\log 2\nu_s], \tag{2.37}$$

which ν_s is the smallest partial transposed symplectic eigenvalue

$$\nu_s = \left[\frac{\Lambda - \sqrt{\Lambda^2 - 4\det\sigma}}{2}\right]^{\frac{1}{2}}, \tag{2.38}$$

and

$$\Lambda = \det A + \det B - 2\det C, \tag{2.39}$$

with covariance matrix σ, which can be written in the form of a 2×2 block matrix as

$$\sigma = \begin{pmatrix} A & C \\ C^T & B \end{pmatrix}, \tag{2.40}$$

where A and B are the variance of subsystems such as mechanical modes and cavity mode, respectively, while C is the correlations between subsystems. Furthermore, the Gaussian state is said to be entangled if and only if $E_N > 0$ or $\nu_s < 0.5$, which is entirely identical to Simon's criterion, which states that the necessary and sufficient condition for entanglement of the non-positive partial transpose condition for the Gaussian state (Simon, 2000).

2.9.2 Gaussian quantum steering

Quantum steering is a type of quantum correlation that exhibits fundamental asymmetry in the properties of quantum systems. An intermediate form of quantum correlation known as quantum steering (Schrödinger, 1935) lies between the well-established concepts of entanglement (Horodecki et al., 2009) and Bell nonlocality (Brunner et al., 2014). Steering is a quantum mechanical phenomenon that enables one party, Alice, to change (steer) the state of a distant party, Bob, by leveraging their shared entanglement. This intriguing concept was notably discussed by Schrödinger (Schrödinger, 1935) and was previously acknowledged by Einstein, Podolsky, and Rosen (EPR) in their renowned 1935 paper (Einstein et al., 1935), which formed a crucial part of the well-known EPR paradox (Reid et al., 2009). From a quantum information perspective, steering represents the process of verifiable entanglement distribution by an untrusted party. If Alice and Bob share a state that can be specifically steered in one direction from Alice to Bob, then Alice can convince Bob, who does not entirely trust her, of the entanglement of their shared state through local measurements and classical communication (Jones et al., 2007; Kogias and Adesso, 2015). The concept of quantum steering was further studied by Wiseman, Jones, and Doherty (Jones et al., 2007) define the steering to a given task and relate it to quantum information processing. It has recently been shown to be a useful resource for many applications, such as quantum key distribution, secure quantum teleportation, generation of one-way EPR steering, and quantification of entanglement (Kogias and Adesso, 2015).

It has been explored both theoretically and experimentally using continuous-variable (CV) quantum systems (Cavalcanti and Skrzypczyk, 2016; Wittmann et al., 2012; Händchen et al., 2012). In particular, the proposed by (Wittmann et al., 2012) quantification and measurement of Gaussian steering for CV systems. As noted by (Bennett et al., 2011), a steering quantify the amount of correlation present in a given state. In this context, the degree of steerability is determined by assessing the maximum violation of a chosen steering criterion, as revealed through optimal measurements. This violation serves as a manifestation of the correlations, indicating the presence of EPR steering according to the specified criteria. Recently, the proposed steering measure has been easily computed for bipartite Gaussian states of an arbitrary number of modes. His proposal quantifies the steerability of a bipartite Gaussian state characterized by a covariance matrix σ from Eq. (2.40), utilizing Gaussian measurements performed on Alice's side, through the following quantity (Kogias and Adesso, 2015):

$$S^{A\to B} = \max\left[0, -\ln(\bar{v}^B)\right]. \tag{2.41}$$

The symplectic eigenvalue of the matrix M^B is defined by $\bar{v}^B = \sqrt{\det M^B}$ and $M^B = B -$

$C^T A^{-1} C$, where A, B, and C are the 2×2 matrices. Using Eq.(2.40), the measure of Gaussian steering $S^{A\to B}$ is given by

$$S^{A\to B} = \max\left[0, \frac{1}{2}\ln\left(\frac{\det A}{4\det\sigma}\right)\right]. \tag{2.42}$$

The corresponding measure of Gaussian steerability $B \to A$ can be found by

$$S^{B\to A} = \max\left[0, \frac{1}{2}\ln\left(\frac{\det B}{4\det\sigma}\right)\right]. \tag{2.43}$$

From the above, there are three possibilities for quantum steering between A and B: if $S^{A\to B} = S^{B\to A} = 0$, there is no-way steering, which means that Alice cannot steer Bob and vice versa even if they are not separable, two-way steering if $S^{A\to B} = S^{B\to A} > 0$, and one-way steering if $S^{A\to B} = 0$ or $S^{B\to A} > 0$ and vice versa. In reality, a non-separable state is not always a steerable state, while a steerable state is always not separable.

2.9.3 Gaussian quantum discord

In contrast to quantum entanglement, disentangled (separable) quantum systems may exhibit another type of quantum correlation known as quantum discord (Henderson and Vedral, 2001) which was first reported by Ollivier and Zurek (Ollivier and Zurek, 2001). Beyond the quantum entanglement phenomenon, quantum discord describes the measurement of the total correlation in a quantum state, which is the difference between the equivalent expressions of two classical mutual information. Therefore, such a quantum discord strives to capture all the quantum correlations in a bipartite state. The CV of Gaussian quantum discord has received significant attention in recent years due to its potential implications in quantum information technology (Amazioug et al., 2018b; Aoune and Habiballah, 2022; Bougouffa et al., 2022; Singh and Ooi, 2014; Eshete, 2022; Adesso and Datta, 2010; Giorda and Paris, 2010). (Adesso and Datta, 2010) and (Giorda and Paris, 2010) developed Gaussian quantum discord as an approximation for quantum discord in continuous variable systems. Fortunately, under constrained Gaussian measurements, a closed analytical relationship can be established to quantify the quantum discord for two-mode Gaussian states. Furthermore, quantum discord is applicable to almost all squeezed-thermal states with non-zero Gaussian discord (Adesso and Datta, 2010). It is used mainly to assess quantumness in multiparty systems because of its resilience to decoherence compared to entanglement (Galve et al., 2011).

A continuous variable Gaussian state optimization approach was employed to quantify the degree of quantumness in Gaussian states using quantum discord. Notably, prior research has demonstrated that the first- and second-order moments of the quadrature operators within the covariance matrix can effectively determine the continuous-variable Gaussian state. In this research, the focus is on the CV Gaussian states, and we present the Gaussian quantum discord. The Gaussian quantum discord may be measured with extended Gaussian measurements on a bipartite system. In an optomechanical system, the Gaussian quantum discord signifies the non-classical correlations of the mechanical mode and the optical mode is separable or not. Employing Eq.(2.40), the quantum discord for the Gaussian quantum discord between the optical mode and the mechanical mode is as follows (Adesso and Datta, 2010).

$$D_A = f(\sqrt{\det B}) - f(\eta_+) - f(\eta_-) + f(\epsilon), \tag{2.44}$$

where $\eta_\pm$ is the symplectic eigenvalues given by

$$\eta_\pm = \left[\frac{\Lambda \pm \sqrt{\Lambda^2 - 4\det\sigma}}{2}\right]^{\frac{1}{2}}, \tag{2.45}$$

with $\Lambda = \det A + \det B + 2\det C$ and ϵ is defined by

$$\epsilon = \frac{\sqrt{\det A} + 2\sqrt{\det A \det B} + 2\det C}{1 + 2\sqrt{\det B}}. \tag{2.46}$$

Similarly, the quantum discord between the mechanical mode and optical modes can be expressed as

$$D_B = f(\sqrt{\det A}) - f(\eta_+) - f(\eta_-) + f(\epsilon'), \tag{2.47}$$

where

$$\epsilon' = \frac{\sqrt{\det B} + 2\sqrt{\det A \det B} + 2\det C}{1 + 2\sqrt{\det A}}, \tag{2.48}$$

where the function $f(x)$ is defined by

$$f(x) = \left(x + \frac{1}{2}\right) ln\left(x + \frac{1}{2}\right) - \left(x - \frac{1}{2}\right) ln\left(x - \frac{1}{2}\right). \tag{2.49}$$

The quantum state of the optical and mechanical modes is inseparable if $D_A > 1 : D_B > 1$ is satisfied, and the quantum state can be either separable or inseparable when the measurement follows the condition $0 \leq D_A \leq 1 : 0 \leq D_B \leq 1$ is satisfied (Adesso and Datta, 2010; Giorda and Paris, 2010).

2.9.4 Gaussian quantum coherence

Quantum coherence (QC) refers to the property of a quantum system that enables the existence of superposition states, where a system can be in multiple states. It is an indispensable prerequisite for recognizing and exploiting the distinctive traits of quantum systems, which allows advancements in quantum technologies and information processing. It offers a starting point for the development of quantum algorithms and protocols. The exploration of quantum coherence not only reveals the boundary between classical and quantum physics, but also uncovers unique paths to exploring the fundamental laws of nature at the quantum level (Hou et al., 2017). Therefore, it is a crucial issue with quantum correlations, encompassing quantum entanglement, quantum discord, and quantum steering (Ghobadi et al., 2014; Ma et al., 2016; Mekonnen et al., 2023; Tesfahannes and Getahune, 2020). Furthermore, quantum coherence is a vital resource for quantum information processing, quantum metrology, thermodynamics, and biological processes (Uola et al., 2020; Demkowicz-Dobrzański and Maccone, 2014; Lostaglio et al., 2015; Collini et al., 2010).

Several researchers have explored the quantification of Gaussian quantum coherence on a macroscopic scale (Morsch and Oberthaler, 2006; Kundu et al., 2021; O'Connell et al., 2010). In particular, Zheng et al. studied the macroscopic quantum coherence of a driven-cavity optomechanical system with optical and mechanical dissipations (Zheng et al., 2016). Recently investigated quantum coherence in an optomechanical system consisting of two mechanical oscillators and the transfer within the optical cavity and the mechanical modes (Li et al., 2019). Additionally, Jin et al. have been conducted on a spinning optomechanical resonator system encompassing a mechanical mode and two cavity modes moving in opposite directions, with one cavity mode being externally driven by a laser field (Jin et al., 2021). (Zheng et al., 2016) have explored the quantum coherence of the hybrid system by employing steady-state mean values and the covariance matrix. Consider a Gaussian state (ρ), represented by the collective operator $(\hat{x} = (\hat{X}, \hat{Y}))$, which can be completely characterized by its first moment $(\vec{d} = (d_x, d_y) = \mathrm{Tr}(\rho\hat{x}))$. The second moment for different modes can be defined as follows (Zheng et al., 2016)

$$V = \begin{pmatrix} V_j & V_{jk} \\ V_{kj} & V_k \end{pmatrix}, \tag{2.50}$$

in which V_j, V_k represents the 2×2 matrix of local properites of each mode, and $V_{j,k}$ is the 2×2 matrix of the correlations between the respective modes. In the following, the coherence of any given one-mode Gaussian state $\rho(V_j, d)$ can be quantified in terms of the covariance matrix and the displacement vector (Zheng et al., 2016)

$$C(\rho(V_j, \vec{d})) = -F(v_j) + F(2n+1), \tag{2.51}$$

with $F(x) = (\frac{x+1}{2})\log_2(\frac{x+1}{2}) - (\frac{x-1}{2})\log_2(\frac{x-1}{2})$ in which, $n = (Tr(V_j) + d_x^2 + d_y^2 - 2)/4$ and $v_j = \sqrt{\det(V_j)}$ is the symplectic eigen value. In addition, to quantify bipartite quantum coherence, a two-mode Gaussian state $\rho(V, \vec{d})$ can be defined as

$$C_{jk} = C(\rho(V, \vec{d})) = \sum_{i=\pm} F(V_i) + \sum_{\zeta=j,k} F(2n_\zeta + 1), \tag{2.52}$$

where $V_i = \left[\frac{\Lambda_{jk} \pm \sqrt{\Lambda_{jk}^2 - 4\det V}}{2}\right]^{\frac{1}{2}}$ is the minimum symplectic eigenvalue of the partial transposed covariance matrix and $\Lambda_{jk} = \det V_j + \det V_k + 2\det V$. The total quantum coherence of a CV system with N bosonic modes can be defined as (Li et al., 2019)

$$C_T = C(\rho(V, \vec{d})) = \sum_{j=1}^{N} \left(F(w_j) + F(2n_j + 1)\right), \tag{2.53}$$

where, w_j corresponds to the standard eigenspectrum of the matrix $|i\Pi V|$, here Π represents a generic element of the $2N \times 2N$ matrix with a symplectic form, defined as (Adesso et al., 2006): $\Pi = \sum_{k=1}^{N} \bigoplus i\hat{\sigma}_y^k,\ \ \hat{\sigma}_y^k \equiv \begin{pmatrix} 0 & -i \\ i & 0 \end{pmatrix}$.

3

MATERIALS AND METHODS

3.1 Materials

We utilized various optical and mechanical components, such as an optical cavity, the total reflective mirror, a charged mirror, an optical parametric amplifier, two-level atom ensembles, a symmetric beam splitter, and laser light. In addition, we used MATLAB software to plot the analytical results, which facilitates the investigation of quantum features.

3.2 Methods

In this section, we develop models of hybrid systems and formulate a Hamiltonian of the system. Employing the Hamiltonian of the system, we derive the nonlinear quantum Langevin equations. By applying linearization techniques, we calculate the steady-state solutions of motion, as well as the drift matrix. With the aid of the Lyapunov equation, we obtain the steady-state covariance matrix. Using logarithmic negativity, quantum steering, and quantum discord formulas, we measure quantum correlation between the subsystems. Finally, using numerical solutions of the Lyapunov equation and steady-state mean values, we quantify the Gaussian quantum coherence of the system.

3.3 Quantum correlations in electro-optomechanical system

In this section, we examine quantum correlations such as quantum entanglement, quantum steering, and quantum discord between mechanical modes. Our work aims to enhance the quantum correlation in the presence of OPA and strong Coulomb coupling under three quantum correlation quantifiers.

3.3.1 Model and Hamiltonian of the system

The hybrid optomechanical system shown in Figure (3.1) is composed of a fixed partially transmitting mirror, two charged mechanical oscillators and an OPA embedded in the cavity. Thus, we define the mechanical oscillator on the left as the mechanical oscillator (MR_1) and the mechanical oscillator on the right as the mechanical oscillator (MR_2). In this scenario, the mechanical oscillator (MR_1) and the mechanical oscillator (MR_2) are considered quantum mechanical harmonic oscillators characterized by effective masses represented as m_i and frequencies denoted as ω_i (where i = 1, 2). The cavity is coherently driven by an external laser with frequency ω_l and amplitude Ω from the fixed mirror (Mekonnen et al., 2023). The cavity mode couples the first charged mechanical oscillator through the radiation-pressure interaction, and also the first charged mechanical oscillator (MR_1) can be connected to the second spatially separated charged mechanical oscillator (MR_2) by the Coulomb interaction (Ma et al., 2014).

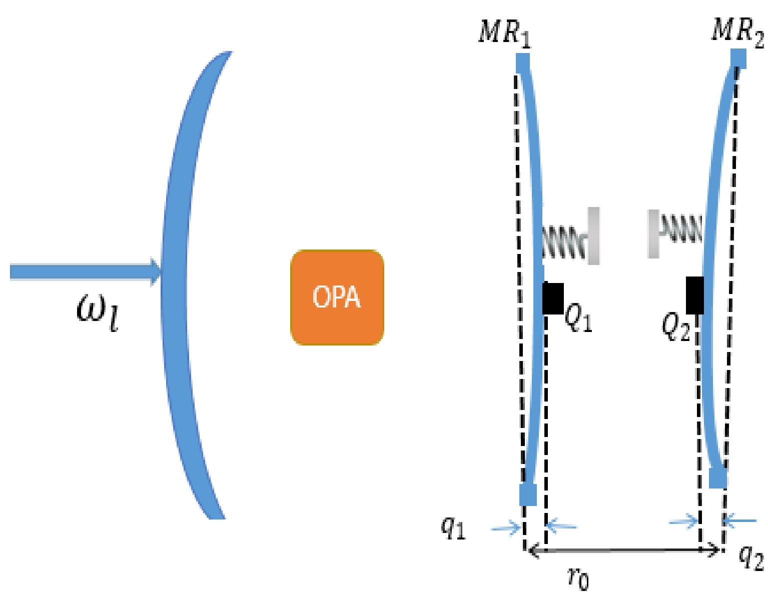

Figure 3.1: Schematic representation of the hybrid system. The hybrid system consists of a fixed mirror, charged mechanical oscillators, and an OPA is placed inside the cavity.

The total Hamiltonian of the system is given by

$$\begin{aligned}\hat{H} &= \hbar\omega_c \hat{c}^\dagger \hat{c} + \sum_{i=1}^{2} \frac{\hbar\omega_i}{2}\left(\hat{p}_i^2 + \hat{q}_i^2\right) - \hbar g q_1 \hat{c}^\dagger \hat{c} + i\hbar\Omega\left(\hat{c}^\dagger e^{-i\omega_l t} - \hat{c} e^{i\omega_l t}\right) \\ &+ i\hbar G_a\left(e^{i\theta}\hat{c}^{\dagger 2} e^{-2i\omega_l t} - e^{-i\theta}\hat{c}^2 e^{2i\omega_l t}\right) + \hat{H}_{coul},\end{aligned} \tag{3.1}$$

where $\hat{c}(\hat{c}^\dagger)$ is the annihilation (creation) operator of the cavity mode with cavity frequency ω_c. The first term describes the free energy of the cavity field. The second term denotes the energy of the mechanical modes with frequency ω_i and momentum (position) $\hat{p}_i(\hat{q}_i)$. The third term is the energy of the photon-phonon interaction between the cavity mode and the mechanical oscillator (MR_1), where $g = \frac{\omega_c}{L}\sqrt{\frac{\hbar}{2m_1\omega_1}}$ represents the optomechanical coupling constant of a single photon and where L is the cavity length. The fourth term describes the cavity field driven by an external laser with frequency ω_l and amplitude $\Omega = \sqrt{\frac{2\kappa P}{\hbar\omega_l}}$, where P and κ are the external laser power and the cavity damping rate, respectively. The fifth term denotes the energy between the OPA and the cavity field, G_a is the nonlinear gain of the OPA, and θ is the phase of the optical field driving the OPA. The last term shows that the Coulomb interaction potential of a charged mechanical oscillator is given as

$$\hat{H}_{coul} = \frac{-C_1V_1C_2V_2}{4\pi\epsilon_0|r_0 + q_1 - q_2|}, \tag{3.2}$$

where $C_1V_1(-C_2V_2)$ is the charges of the two mechanical oscillators with $C_1(C_2)$ denotes the gate capacitance, $V_1(V_2)$ represents the bias gate voltage, ϵ_0 is permittivity in free space , r_0 is the separation of the equilibrium positions of the two mechanical oscillators, and $q_1(q_2)$ is the small oscillations of the charged mechanical oscillators. We suppose that the separation distance between two charged mechanical oscillators is larger than their small oscillations ($q_1, q_2 \ll r_0$). Under this condition, Eq.(3.2) can be expanded to the second order as (Chen et al., 2015)

$$\hat{H}_{coul} = -\frac{C_1V_1C_2V_2}{4\pi\epsilon_0 r_0}\left(1 - \frac{q_1 - q_2}{r_0} + \frac{(q_1 - q_2)^2}{r_0^2}\right), \tag{3.3}$$

where the linear terms are absorbed in equilibrium positions, quadratic terms are incorporated in the renormalization of oscillation frequencies. After omitting the constant term, Eq.(3.3) can be written as

$$\hat{H}_{coul} = \hbar\eta q_1 q_2, \tag{3.4}$$

in which $\eta = \frac{C_1V_1C_2V_2}{4\pi\epsilon_0 m\omega_m r_0^3}$ is Coulomb coupling strength.

The total Hamiltonian of the system in a rotating frame at the frequency ω_l takes the form

$$\hat{H} = \hbar\Delta_o \hat{c}^\dagger \hat{c} + \sum_{i=1}^{2} \frac{\hbar\omega_i}{2}\left(\hat{p}_i^2 + \hat{q}_i^2\right) - \hbar g q_1 \hat{c}^\dagger \hat{c} + i\hbar\Omega\left(\hat{c}^\dagger - \hat{c}\right) + i\hbar G_a\left(e^{i\theta}\hat{c}^{\dagger 2} - e^{-i\theta}\hat{c}^2\right) + \hbar\eta q_1 q_2, \tag{3.5}$$

here $\Delta_o = \omega_c - \omega_l$ is optical cavity detuning.

3.3.2 The time evolution of equation of motion

We now proceed to analyze the time evolution of the system using the quantum Langevin method. The time evolution of a system, including the effect of fluctuation-dissipation on both the cavity and the mechanical modes. By substituting Eq. (3.5) in Eqs.(A.1)-(A.5) and incorporating the commutation relations of the respective operators of Eqs. (A.7)-(A.11), we obtained the nonlinear quantum Langevin equations as follows:

$$\dot{\hat{q}}_1 = \omega_1 \hat{p}_1, \tag{3.6a}$$
$$\dot{\hat{p}}_1 = -\omega_1 \hat{q}_1 + g\hat{c}^\dagger \hat{c} - \eta \hat{q}_2 - \gamma_1 \hat{p}_1 + \xi_1(t), \tag{3.6b}$$
$$\dot{\hat{q}}_2 = \omega_2 \hat{p}_2, \tag{3.6c}$$
$$\dot{\hat{p}}_2 = -\omega_2 \hat{q}_2 - \eta \hat{q}_1 - \gamma_2 \hat{p}_2 + \xi_2(t), \tag{3.6d}$$
$$\dot{\hat{c}} = -(\kappa + i\Delta_o - ig\hat{q}_1)\hat{c} + 2G_a \hat{c}^\dagger e^{i\theta} + \Omega + \sqrt{2\kappa}\hat{c}_{in}, \tag{3.6e}$$

with $\gamma_1(\gamma_2)$ is the damping rate of the two mechanical oscillators, $\xi_1(t)(\ \xi_2(t))$ is quantum Brownian noise operator a rise from the coupling between the two mechanical oscillators with the environment, and $\hat{c}_{in}$ is the input vacuum noise operator.

Next, we seek to estimate the input quantum noise contributions of $\hat{c}_{in}$ and the thermal reservoirs that affect $\xi_1(t)$ and $\xi_2(t)$. The input vacuum noise operators of the cavity mode satisfy the following properties (Genes et al., 2008b; Vitali et al., 2007a)

$$\langle \hat{c}_{in}^\dagger(t)\rangle = \langle \hat{c}_{in}(t)\rangle = 0, \tag{3.7}$$

$$\langle \hat{c}_{in}(t)\hat{c}_{in}^\dagger(t')\rangle = \delta(t - t'). \tag{3.8}$$

Furthermore, the quantum Brownian noise operators have zero mean values and exhibit specific correlation function (Mekonnen et al., 2023)

$$\langle \xi_i(t)\xi_i(t')\rangle = \frac{\gamma_i}{\omega_i}\int \frac{d\omega_i}{2\pi} e^{-i\omega_i(t-t')}\omega_i\left(1 + \coth\left(\frac{\hbar\omega_i}{2K_B T}\right)\right), i = 1, 2., \tag{3.9}$$

where K_B is the Boltzmann constant and T is the temperature of the reservoir related to the mechanical oscillators. However, quantum effects are revealed just for the mechanical oscillators are large quality factor $Q_i = \frac{\omega_i}{\gamma_i} \gg 1$. In this limit, the correlation function of the noise $\xi_i(t)$ can be written as (Sohail et al., 2020)

$$\langle \xi_i(t)\xi_i(t') + \xi_i(t')\xi_i(t)\rangle/2 = \gamma_i(2\bar{n}+1)\delta(t-t'). \tag{3.10}$$

in which, $\bar{n} = (exp(\frac{\hbar\omega_i}{K_B T} - 1))^{-1}$ is the mean thermal phonon number.

3.3.3 Steady-state solution of system

We employ the nonlinear quantum Langevin equations to describe the dynamics of the cavity mode and mechanical modes. Using Eq.(2.36), we can easily expand each operator as the sum of its steady-state mean values and the quantum fluctuation operator as

$$\begin{aligned} \hat{c} &= c^s + \delta\hat{c}, \\ \hat{q}_i &= q_i^s + \delta\hat{q}_i, \\ \hat{p}_i &= p_i^s + \delta\hat{p}_i, \end{aligned} \tag{3.11}$$

with c^s, q_i^s and p_i^s are the steady-state mean values for operators $\hat{c}$, $\hat{q}_i$ and $\hat{p}_i$, and $\delta\hat{c}$, $\delta\hat{q}_i$, $\delta\hat{p}_i$ is the fluctuation operator. Furthermore, by substituting Eq.(3.11) into Eqs.(3.6a)-(3.6e), then the mean value of the fluctuation operators is zero. In addition, mechanical damping $\xi_1(t), \xi_2(t)$ does not affect the steady state of the system. The steady-state mean values of the operator can be calculated by setting all-time derivatives to zero in Eqs. (3.6a)-(3.6e). Finally, we obtain the steady-state mean value for hybrid systems as follows:

$$\begin{aligned} p_1^s &= p_2^s = 0, \\ q_1^s &= \frac{-\omega_2\, g|c^s|^2}{\eta^2 - \omega_1\omega_2}, \\ q_2^s &= \frac{g|c^s|^2\eta}{\eta^2 - \omega_1\omega_2}, \\ c^s &= \frac{\kappa - i\Delta + 2G_a e^{i\theta}}{\kappa^2 + \Delta^2 - 4G_a^2}\Omega, \end{aligned} \tag{3.12}$$

where $\Delta = \Delta_o - gq_1^s$ is the effective cavity detuning from the frequency of the input laser in the presence of the radiation pressure. We choose the phase reference of the cavity field c^s is real.

The cavity is subjected to intense laser driving, resulting in a high-amplitude intra-cavity field at steady state, i.e. $|c^s| \gg 1$ (Gebremariam et al., 2017). In the regime of strong driving, here we have neglected the high-order small terms of the fluctuation part, the linearized quantum Langevin equations can be written as

$$
\begin{aligned}
\delta\dot{\hat{q}}_1 &= \omega_1 \delta\hat{p}_1, \\
\delta\dot{\hat{p}}_1 &= -\omega_1 \delta\hat{q}_1 + g c^s (\delta\hat{c} + \delta\hat{c}^\dagger) - \eta \delta\hat{q}_2 - \gamma_1 \delta\hat{p}_1 + \xi_1(t), \\
\delta\dot{\hat{q}}_2 &= \omega_2 \delta\hat{p}_2, \\
\delta\dot{\hat{p}}_2 &= -\omega_2 \delta\hat{q}_2 - \eta \delta\hat{q}_1 - \gamma_2 \delta\hat{p}_2 + \xi_2(t), \\
\delta\dot{\hat{c}} &= -(\kappa + i\Delta)\delta\hat{c} + i g c^s \delta\hat{q}_1 + 2G_a e^{i\theta} \delta\hat{c}^\dagger + \sqrt{2\kappa}\delta\hat{c}_{in}.
\end{aligned}
\tag{3.13}
$$

3.3.4 Quantum fluctuation and steady-state covariance matrix

We now investigate the quantum correlations between the two mechanical modes in the system. To facilitate this analysis, we have transformed Eq. (3.13) into quadrature operators and Hermitian input noise operators. The dimensionless quadrature operators are introduced for cavity mode as:

$$
\begin{aligned}
\delta\hat{x} &= (\delta\hat{c}^\dagger + \delta\hat{c})/\sqrt{2}, \\
\delta\hat{y} &= i(\delta\hat{c}^\dagger - \delta\hat{c})/\sqrt{2},
\end{aligned}
\tag{3.14}
$$

and the corresponding Hermitian input noise operators are

$$
\begin{aligned}
\delta\hat{x}_{in} &= (\delta\hat{c}_{in}^\dagger + \delta\hat{c}_{in})/\sqrt{2}, \\
\delta\hat{y}_{in} &= i(\delta\hat{c}_{in}^\dagger - \delta\hat{c}_{in})/\sqrt{2}.
\end{aligned}
\tag{3.15}
$$

Using the preceding definitions and Euler's identity, Eq.(3.13) can be written as

$$
\begin{aligned}
\delta\dot{\hat{q}}_1 &= \omega_1 \delta\hat{p}_1, \\
\delta\dot{\hat{p}}_1 &= -\omega_1 \delta\hat{q}_1 - \eta \delta\hat{q}_2 + G_0 \delta\hat{x} - \gamma_1 \delta\hat{p}_1 + \xi_1(t), \\
\delta\dot{\hat{q}}_2 &= \omega_2 \delta\hat{p}_2, \\
\delta\dot{\hat{p}}_2 &= -\omega_2 \delta\hat{q}_2 - \eta \delta\hat{q}_1 - \gamma_2 \delta\hat{p}_2 + \xi_2(t), \\
\delta\dot{\hat{x}} &= -(\kappa - 2G_a \cos\theta)\delta\hat{x} + (\Delta + 2G_a \sin\theta)\delta\hat{y} + \sqrt{2\kappa}\delta\hat{x}_{in}, \\
\delta\dot{\hat{y}} &= G_0 \delta\hat{q}_1 - (\Delta - 2G_a \sin\theta)\delta\hat{x} - (\kappa + 2G_a \cos\theta)\delta\hat{y} + \sqrt{2\kappa}\delta\hat{y}_{in},
\end{aligned}
\tag{3.16}
$$

where $G_0 = \sqrt{2} g c^s$ is the effective optomechanical coupling.

Eq.(3.16) can be written in compact form

$$\dot{u}(t) = Au(t) + n(t), \tag{3.17}$$

where

$$u(t) = (\delta\hat{q}_1, \delta\hat{p}_1, \delta\hat{q}_2, \delta\hat{p}_2, \delta\hat{x}, \delta\hat{y})^T, \tag{3.18}$$

and

$$n(t) = (0, \xi_1(t), 0, \xi_2(t), \sqrt{2\kappa}\delta\hat{x}_{in}, \sqrt{2\kappa}\delta\hat{y}_{in})^T, \tag{3.19}$$

are the column vector of the fluctuation and the column vector of the noise sources, respectively. The drift matrix A can be defined by

$$A = \begin{pmatrix} 0 & \omega_1 & 0 & 0 & 0 & 0 \\ -\omega_1 & -\gamma_1 & -\eta & 0 & G_0 & 0 \\ 0 & 0 & 0 & \omega_2 & 0 & 0 \\ -\eta & 0 & -\omega_2 & -\gamma_2 & 0 & 0 \\ 0 & 0 & 0 & 0 & -\kappa + 2G_a\cos\theta & \Delta + 2G_a\sin\theta \\ G_0 & 0 & 0 & 0 & -\Delta + 2G_a\sin\theta & -\kappa - 2G_a\cos\theta \end{pmatrix}. \tag{3.20}$$

The formal solution of Eq.(3.17), can be written as (Vitali et al., 2007a)

$$u(t) = M(t)u(0) + \int_0^t d\tau M(\tau)n(t-\tau), \tag{3.21}$$

where $M(t) = e^{At}$. The initial condition for the above transformation $M(0) = I$, where I is the identity matrix. According to the Routh-Hurwitz criterion (DeJesus and Kaufman, 1987), the system can achieve a stable steady-state condition when all the real parts of the eigenvalues of the drift matrix A are negative. As $t \to \infty$, so that $M(\infty) = 0$ and Eq. (3.21) can be rewritten as

$$u_i(\infty) = \int_0^\infty d\tau \sum_i M_i(\tau)n_i(t-\tau), \tag{3.22}$$

on account of Eq.(3.22), the steady state of the quantum fluctuations is a continuous-variable Gaussian state. This state is fully characterized by a 6×6 covariance matrix (CM) with corresponding components defined as

$$R_{ij} = \langle u_i(\infty)u_j(\infty) + u_j(\infty)u_i(\infty)\rangle/2. \tag{3.23}$$

Using Eq.(3.22) into Eq.(3.23), we have

$$R_{ij} = \sum_{ij} \int_0^\infty dt \int_0^\infty d\tau M_{ij}(t) M_{ji}(\tau) \chi_{ij}(t-\tau), \tag{3.24}$$

where

$$\chi_{ij}(t-\tau) = \langle n_i(t) n_j(\tau) + n_j(\tau) n_i(t) \rangle / 2. \tag{3.25}$$

Substituting Eq.(3.19) into Eq.(3.25), and on account of Eqs.(3.8),(3.10), finally we obtain

$$\chi_{ij}(t-\tau) = D_{ij} \delta(t-\tau), \tag{3.26}$$

in which D_{ij} is a diagonal matrix that is known as a diffusion matrix. Using Eqs. (3.10) and (3.8), we can easily verify that

$$D = diag(0, \gamma_1(2\bar{n}+1), 0, \gamma_2(2\bar{n}+1), \kappa, \kappa). \tag{3.27}$$

Substituting Eq.(3.26) into Eq.(3.24), we obtain

$$R = \int_0^\infty dt M(t) D M(t)^T. \tag{3.28}$$

The stability conditions of the systems are satisfied, then the steady-state covariance matrix Eq.(3.28), can be derived by considering the Lyapunov equation (Genes et al., 2008a)

$$AR + RA^T = -D. \tag{3.29}$$

The steady-state covariance matrix R can be written in the form of a block matrix (Mekonnen et al., 2023)

$$R = \begin{pmatrix} K_{m_1} & L_{m_1 m_2} & L_{cm_1} \\ L_{m_1 m_2}^T & K_{m_2} & L_{cm_2} \\ L_{cm_1}^T & L_{cm_2}^T & K_c \end{pmatrix}, \tag{3.30}$$

where each block represents a 2×2 matrix. The blocks on the diagonal represent the variance within each subsystem (the mechanical modes (K_{m_1}, K_{m_2}), and the cavity mode (K_c)), while the blocks off the diagonal represent the correlations between the subsystems (mechanical and mechanical ($L_{m_1 m_2}$), mechanical and cavity $L_{cm_j}, j = m_1, m_2$).

3.3.5 Measurement of quantum correlations

We seek to quantify the quantum correlation that exist between subsystems. Several approaches have been established to measure quantum correlations, providing valuable insight into the distinctive properties of quantum systems and their potential applications in quantum information processing, communication, and computation (Head-Marsden et al., 2020). In this sense, the quantum correlation between mechanical modes is measured through three quantum quantifiers such as quantum entanglement, quantum steering, and quantum discord. In continuous variable systems, logarithmic negativity (E_N) can be used to investigate bipartite entanglement between mechanical modes. By suppressing the rows and columns, we formed the relevant mode from Eq. (3.30) in the form of a 2×2 block matrix

$$\chi = \begin{pmatrix} K_{m_1} & L_{m_1 m_2} \\ L^T_{m_1 m_2} & K_{m_2} \end{pmatrix}. \tag{3.31}$$

Using Eq. 2.37, we can easily verify the bipartite entanglement between mechanical modes. Hence, the smallest partial transposed symplectic eigenvalue ν_s is given by

$$\nu_s = \left[\frac{\Lambda - \sqrt{\Lambda^2 - 4 \det \chi}}{2} \right]^{\frac{1}{2}}, \tag{3.32}$$

with

$$\Lambda = \det K_{m_1} + \det K_{m_2} - 2 \det L_{m_1 m_2}. \tag{3.33}$$

Furthermore, the two mechanical modes are said to be entangled if and only if $E_N > 0$ or $\nu_s < 0.5$, which is entirely identical to Simon's criterion, which states that the necessary and sufficient condition for entanglement of nonpositive partial transpose condition for Gaussian state (Simon, 2000). As a result, we present a numerical description of the calculated results through the figures shown in Figs. (4.1-4.4).

Another quantum correlation quantifier is quantum steering, which measures the asymmetry between two entangled observers, specifically between the mechanical oscillator (MR_1) and the mechanical oscillator (MR_2). Furthermore, it allows us to evaluate the degree of steerability of the two separate mechanical oscillators. If we consider the information transfer between the mechanical oscillators due to their correlation and label (A: mechanical oscillator (MR_1)) and (B: mechanical oscillator(MR_2)). Employing Eqs.(3.31), (2.42), and (2.43), we easily quantify the Gaussian quantum steering of the mechanical oscillator (MR_2) by the mechanical oscillator (MR_1) and the corresponding measure of Gaussian steerability $B \to A$, respectively.

The Gaussian quantum discord determines whether the mechanical oscillator (MR_1) and the mechanical oscillator (MR_2) are separable or not. Utilizing Eq.(3.31) and Eq.(2.44-2.49), we can easily quantify Gaussian quantum discord for the mechanical oscillator (MR_1) and (MR_2). We present a numerical illustration of the calculated results in Figs. (4.1)-(4.4).

3.4 Mechanical entanglement in electro-optomechanical system

In this section, we provide a comprehensive overview of the theoretical model underpinning our study and the dynamics of the system. We utilize coherent feedback mechanisms to thoroughly examine input-output relations, clarifying their impact on the overall behavior of the system. Finally, we discuss the quantification of mechanical entanglement through logarithmic negativity.

3.4.1 Model and Hamiltonian of the system

As shown in Fig.(3.2), we consider a hybrid optomechanical system comprised of a fixed mirror, an OPA placed inside the cavity, and a mechanical oscillator (MR_1) coupled with another mechanical oscillator (MR_2) via a Coulomb interaction (Zhang et al., 2012). The cavity mode is coupled with MR_1 through the radiation-pressure interaction. In this case, the mechanical oscillator MR_1 and the mechanical oscillator MR_2 are treated as quantum mechanical harmonic oscillators described by the effective masses denoted as m_i and frequencies indicated as ω_i (where $i = 1, 2$). The external laser that originates from the sources can be split into two parts using an asymmetric beam splitter (BS). The input laser field $\hat{c}_{in}$ enters the cavity across the BS and the transmitted part of the laser drives the cavity. A coherent feedback loop is formed when the output field $\hat{c}_{out}$ is fully reflected by the mirror M and some of it enters the cavity via BS. The beam splitter merges light beams originating from a laser source with those that exit the cavity through the stationary mirror. The asymmetric beam splitter is characterized by the unitary matrix as follows

$$U_{BS} = \begin{pmatrix} t & r \\ -r & t \end{pmatrix}, \tag{3.34}$$

where t is the real amplitude transmission coefficient of the beam splitter and the real amplitude reflectivity coefficient is denoted by r and satisfies $t^2 + r^2 = 1$ (t and r are real and positive) (Mandel and Wolf, 1995). When the input laser enters the cavity without feedback from the output field, $r = 0$ and $t = 1$. Hence, the amplitude of the transmitted input laser field is $t\Omega$, whereas the amplitude of the reflected portion of the input laser field is $-r\Omega$ (Mansouri et al., 2022). Here, $t = \sqrt{\tau}$ and $r = \sqrt{\mu}$ represent in terms of the transmittance τ and reflectance μ of the asymmetric beam splitter, respectively. The optical cavity is coherently driven with a strong input laser field of frequency ω_l and amplitude. In addition, an OPA is pumped by a pump field with frequency $2\omega_l$, and the output frequency of the OPA is ω_l (He et al., 2022).

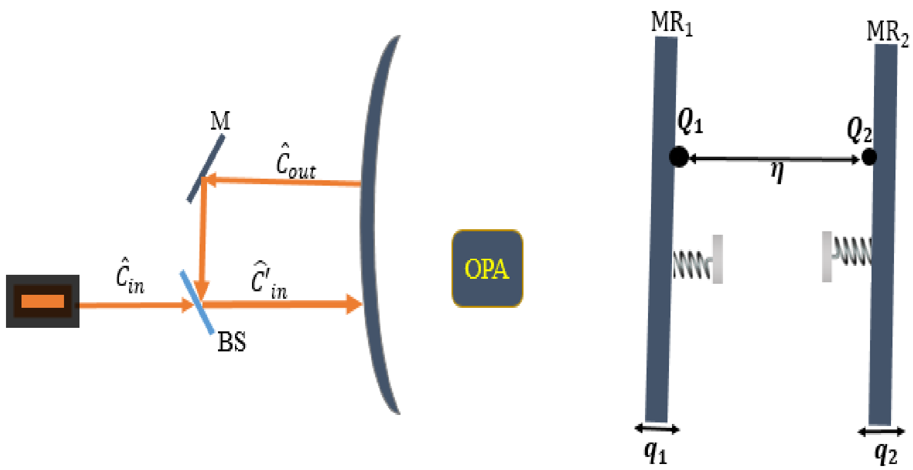

Figure 3.2: Schematic diagram of a hybrid system with a coherent feedback loop. A hybrid system comprised of a fixed mirror, and a charged mechanical oscillator (MR_1) coupled to another charged mechanical oscillator (MR_2) with a Coulomb coupling strength of η. An OPA is placed within the cavity and the pump of the OPA is not shown. An input light field is introduced into the cavity through an asymmetric beam splitter (BS). The output field is reflected off the mirror M, and a portion of the output field is then directed back into the cavity through the BS. The electrode with charge $Q_1(Q_2)$ on both mechanical oscillators. q_1 and q_2 are the small deviations of the two mechanical oscillators from their equilibrium position.

The total Hamiltonian of the hybrid system can be written as (Mekonnen et al., 2024)

$$\begin{aligned}\hat{H} &= \hbar\omega_c\hat{c}^\dagger\hat{c} + \sum_{j=1}^{2}\frac{\hbar\omega_j}{2}\left(\hat{p}_j^2 + \hat{q}_j^2\right) - \hbar g\hat{q}_1\hat{c}^\dagger\hat{c} + i\hbar\Omega\sqrt{\tau}\left(\hat{c}^\dagger e^{-i\omega_l t} - \hat{c}e^{i\omega_l t}\right) \\ &+ i\hbar G_a\left(e^{i\theta}\hat{c}^{\dagger 2}e^{-2i\omega_l t} - e^{-i\theta}\hat{c}^2 e^{2i\omega_l t}\right) + \hat{H}_{coul},\end{aligned} \tag{3.35}$$

where $\hat{c}(\hat{c}^\dagger)$ is the annihilation (creation) operator of the cavity mode with cavity frequency ω_c. The first term describes the free energy of the cavity field. The second term describes the free Hamiltonian of each oscillator with frequency ω_j, momentum operator $\hat{p}_j$, and position operator $\hat{q}_j$. The third term represents the energy of the optomechanical interaction with the coupling strength g. The fourth term specifies the energy of the driven laser field by a portion of the input laser which is transmitted by the beam splitter with the driving field frequency ω_l. The energy interaction between the cavity field and the OPA is represented by the fifth component, where θ denotes the phase of the optical driving field of the OPA and G_a is the nonlinear gain of the OPA. The final term describes the Coulomb interaction potential.

In a rotating frame at the driving frequency ω_l, the total Hamiltonian of the hybrid system is rewritten as

$$\begin{aligned}\hat{H} &= \hbar\Delta_o\hat{c}^\dagger\hat{c} + \sum_{j=1}^{2}\frac{\hbar\omega_j}{2}\left(\hat{p}_j^2+\hat{q}_j^2\right) - \hbar g q_1\hat{c}^\dagger\hat{c} + i\hbar\Omega\sqrt{\tau}\left(\hat{c}^\dagger-\hat{c}\right)\\ &+ i\hbar G_a\left(e^{i\theta}\hat{c}^{\dagger 2}-e^{-i\theta}\hat{c}^2\right)+\hbar\eta q_1 q_2,\end{aligned} \tag{3.36}$$

where $\Delta_o = \omega_c - \omega_l$ is the detuning between the cavity field and the input-driven laser frequency.

3.4.2 Dynamics of the system

The system dynamics are comprehensively characterized by the influence of fluctuation-dissipation processes in the optomechanical system. Dissipation is introduced into the system through the interaction with the external degrees of freedom of the optomechanical system. The optomechanical cavity field is damped by the leakage of photons through the fixed mirror (Ari, 2021). The full dynamics of the system can be described using the quantum Langevin equation. The input cavity field induced via the coherent feedback loop described by the operator

$$\hat{c}'_{in} = \sqrt{\tau}\hat{c}_{in} + \sqrt{\mu}\hat{c}_{out}, \tag{3.37}$$

the reflecting that the beam splitter allows the transmission of $\sqrt{\tau}\hat{c}_{in}$ of the mode and reflects the part $\sqrt{\mu}\hat{c}_{out}$. Using Eq. (2.35),we easily put the output field in this form

$$\hat{c}_{out} = \frac{1}{1+\sqrt{\mu}}\left(\sqrt{2\kappa}\hat{c}-\sqrt{\tau}\hat{c}_{in}\right). \tag{3.38}$$

Inserting Eq.(3.38) into Eq.(3.37), we found

$$\hat{c}'_{in} = \frac{\sqrt{\tau}}{1+\sqrt{\mu}}\hat{c}_{in} + \frac{\sqrt{2\kappa\mu}}{1+\sqrt{\mu}}\hat{c}. \tag{3.39}$$

We now proceed to find the non-linear quantum Langevin equations of the hybrid system. Substituting Eq. (3.36) in Eqs. (A.1-A.5), while simultaneously replacing $\hat{c}_{in}$ by $\hat{c}'_{in}$, then we obtain

$$\begin{aligned}
\dot{\hat{q}}_1 &= \omega_1 \hat{p}_1, \\
\dot{\hat{p}}_1 &= -\omega_1 \hat{q}_1 - \gamma_1 \hat{p}_1 - \eta \hat{q}_2 + g \hat{c}^\dagger \hat{c} + \xi_1(t), \\
\dot{\hat{q}}_2 &= \omega_2 \hat{p}_2, \\
\dot{\hat{p}}_2 &= -\omega_2 \hat{q}_2 - \gamma_2 \hat{p}_2 - \eta \hat{q}_1 + \xi_2(t), \\
\dot{\hat{c}} &= -(\kappa_{eff} + i\Delta_o - ig\hat{q}_1)\hat{c} + 2G_a \hat{c}^\dagger e^{i\theta} + \Omega\sqrt{\tau} + \sqrt{2\kappa}\hat{c}_{fb},
\end{aligned} \tag{3.40}$$

where $\hat{c}_{fb}$ is the effective input noise operator incident on the BS and κ_{eff} is the effective decay rate of the cavity. Thus, the parameters $\hat{c}_{fb}$ and κ_{eff} are expressed as follows, respectively:

$$\hat{c}_{fb}(t) = \left(\frac{\sqrt{\tau}}{1+\sqrt{\mu}}\right)\hat{c}_{in}, \tag{3.41}$$

and

$$\kappa_{eff} = \frac{\kappa\,\left(1-\sqrt{\mu}\right)}{1+\sqrt{\mu}}. \tag{3.42}$$

The cavity damping term, thus $\sqrt{\mu}$ must be less than 1, to ensure that $\kappa_{eff} > 0$. The cavity mode coupled to the vacuum reservoir, thus, the expectation values of $\hat{c}_{fb}$ is given as follows (Mekonnen et al., 2024)

$$\langle \hat{c}_{fb}(t) \rangle = 0, \tag{3.43}$$

$$\langle \hat{c}_{fb}(t)\hat{c}^\dagger_{fb}(t') \rangle = \left(\tau/(1+\sqrt{\mu})^2\right)\delta(t-t'). \tag{3.44}$$

Furthermore, the mechanical oscillators interact with thermal baths, resulting in the creation of quantum Brownian noise operators. The average values of the quantum Brownian noise operators ($\xi_1(t)$ ($\xi_2(t)$)), possess zero mean values and nonzero correlation functions as described in Eq. (3.10).

3.4.3 Linearization of the equation of motions

We employ the linearization approach to obtain a steady-state solution of the equations of motion. To do this, we express each operator as the sum of its expectation value and a quantum fluctuation term, as depicted in Eq.(2.36). Applying Eq. (2.36) in Eq. (3.40), and set all-time derivatives to zero. With the aid of Eqs. (B.1)-(B.7), the steady-state solution of Eq. (3.40) as

$$p_{1s} = p_{2s} = 0. \tag{3.45}$$

$$
\begin{aligned}
q_1^s &= \frac{-\omega_2 g|c^s|^2}{\eta^2 - \omega_1\omega_2}, \\
q_2^s &= \frac{g|c^s|^2\eta}{\eta^2 - \omega_1\omega_2},
\end{aligned} \tag{3.46}
$$

$$
c^s = \frac{\kappa_{eff} - i\Delta + 2G_a e^{i\theta}}{\kappa_{eff}^2 + \Delta^2 - 4G_a^2}\sqrt{\tau}\Omega, \tag{3.47}
$$

where $\Delta = \Delta_o - gq_1^s$ is the effective cavity detuning.

To estimate the steady-state entanglement between the two mechanical modes, we need to set the quadrature fluctuations of each operator. The cavity receives intense laser power, resulting in the amplitude of the intra-cavity field at a steady state ($|c^s| \gg 1$). As a result, we may safely disregard the nonlinear components and estimate the mechanical mode quantum correlation using a strong driving limit. To achieve this purpose, we establish the operators for the quadratures of the cavity field as in Eq. (3.14) and the corresponding Hermitian input noise operators can be defined as

$$
\delta\hat{x}_{in} = (\delta\hat{c}_{fb}^\dagger + \delta\hat{c}_{fb})/\sqrt{2}, \tag{3.48}
$$

$$
\delta\hat{y}_{in} = i(\delta\hat{c}_{fb}^\dagger - \delta\hat{c}_{fb})/\sqrt{2}. \tag{3.49}
$$

On account of Eqs.(3.14),(3.48-3.49), the linearized quantum Langevin equations for the fluctuations read

$$
\begin{aligned}
\delta\dot{\hat{q}}_1 &= \omega_1\delta\hat{p}_1, \\
\delta\dot{\hat{p}}_1 &= -\omega_1\delta\hat{q}_1 - \gamma_1\delta\hat{p}_1 - \eta\delta\hat{q}_2 + G_0\delta\hat{x} + \xi_1(t), \\
\delta\dot{\hat{q}}_2 &= \omega_2\delta\hat{p}_2, \\
\delta\dot{\hat{p}}_2 &= -\omega_2\delta\hat{q}_2 - \gamma_2\delta\hat{p}_2 - \eta\delta\hat{q}_1 + \xi_2(t), \\
\delta\dot{\hat{x}} &= -(\kappa_{eff} - 2G_a\cos\theta)\,\delta\hat{x} + (\Delta + 2G_a\sin\theta)\,\delta\hat{y} + \sqrt{2\kappa}\delta\hat{x}_{in}, \\
\delta\dot{\hat{y}} &= G_0\delta\hat{q}_1 - (\Delta - 2G_a\sin\theta)\,\delta\hat{x} - (\kappa_{eff} + 2G_a\cos\theta)\,\delta\hat{y} + \sqrt{2\kappa}\delta\hat{y}_{in},
\end{aligned} \tag{3.50}
$$

Eq. (3.50) can be easily simplified into a more concise form

$$
\dot{\Pi}(t) = \aleph\Pi(t) + \mathbb{Q}(t), \tag{3.51}
$$

in which $\Pi(t) = (\delta\hat{q}_1, \delta\hat{p}_1, \delta\hat{q}_2, \delta\hat{p}_2, \delta\hat{x}, \delta\hat{y})^T$ and $\mathbb{Q}(t) = (0, \xi_1(t), 0, \xi_2(t), \sqrt{2\kappa}\delta\hat{x}_{in}, \sqrt{2\kappa}\delta\hat{y}_{in})^T$ represents the column vectors of fluctuation and input noise, respectively.

The drift matrix $\aleph$ can be defined as:

$$\aleph = \begin{pmatrix} 0 & \omega_1 & 0 & 0 & 0 & 0 \\ -\omega_1 & -\gamma_1 & -\eta & 0 & G_0 & 0 \\ 0 & 0 & 0 & \omega_2 & 0 & 0 \\ -\eta & 0 & -\omega_2 & -\gamma_2 & 0 & 0 \\ 0 & 0 & 0 & 0 & \Xi & \beta \\ G_0 & 0 & 0 & 0 & \varsigma & \varrho \end{pmatrix}, \tag{3.52}$$

where $\Xi = -\kappa_{eff} + 2G_a \cos\theta$, $\beta = \Delta + 2G_a \sin\theta$, $\varsigma = 2G_a \sin\theta - \Delta$, and $\varrho = -\kappa_{eff} - 2G_a \cos\theta$. Stability is an important component of optomechanical systems. A stable system ensures that all the eigenvalues of the drift matrix $\aleph$, have negative real parts. This stability condition can be efficiently analyzed using the Routh-Hurwitz criteria (DeJesus and Kaufman, 1987).

3.4.4 Stationary bipartite entanglement

We proceed to investigate the stationary bipartite entanglement between the mechanical modes. The system is in a CV Gaussian state and linearized dynamics. The steady state is fully represented by a covariance matrix 6×6, with components specified as (Mekonnen et al., 2024)

$$V_{ij} = \langle u_i(t)u_j(t') + u_j(t)u_i(t')\rangle/2. \tag{3.53}$$

In the end, the covariance matrix V fits the following Lyapunov equation

$$\aleph V + V\aleph^T = -D, \tag{3.54}$$

where, D represents a diagonal matrix known as a diffusion matrix. Using Eqs. (3.10) and (3.44), we can easily verify that

$$D = diag\ (0, \gamma_1(2\bar{n}+1), 0, \gamma_2(2\bar{n}+1), \kappa\tau/(1+\sqrt{\mu})^2, \kappa\tau/(1+\sqrt{\mu})^2). \tag{3.55}$$

Ultimately, the covariance matrix can be written as a block matrix

$$V = \begin{pmatrix} V_{m_1} & V_{m_1m_2} & V_{cm_1} \\ V_{m_1m_2}^T & V_{m_2} & V_{cm_2} \\ V_{cm_1}^T & V_{cm_2}^T & V_c \end{pmatrix}, \tag{3.56}$$

in which, every block signifies a 2×2 matrix. The diagonal blocks reflect the variance within each subsystem, namely the cavity and mechanical modes. The off-diagonal blocks show correlations between subsystems.

Next, we proceed to determine the bipartite entanglement between mechanical modes. Using Eq.(2.37), and replace ν_s by ξ^-, we easily quantify the bipartite entanglement. In which $\xi^- = \left[\frac{\Lambda - \sqrt{\Lambda^2 - 4det\sigma}}{2}\right]^{\frac{1}{2}}$ is the smallest symplectic eigenvalue of the partially transposed covariance matrix with $\Lambda = \det V_{m_1} + \det V_{m_2} - 2\det V_{m_1 m_2}$, and

$$\sigma = \begin{pmatrix} V_{m_1} & V_{m_1 m_2} \\ V_{m_1 m_2}^T & V_{m_2} \end{pmatrix}, \tag{3.57}$$

where V_{m_1}, V_{m_2} and $V_{m_1 m_2}$ are 2×2 block matrix. The two mechanical modes are said to be entangled if and only if the smallest symplectic eigenvalues satisfy conditions $\xi^- < 0.5$ or $E_N > 0$ (Abebe et al., 2020). As a result, we numerically describe the results of an analytical expression via the plots in Figures. (4.5-4.7), using experimentally feasible parameters.

3.5 Quantum coherence in electro-optomechanical system

In this section, we present a theoretical investigation of quantum coherence in a hybrid electro-optomechanical system that includes coherent feedback, an optical parametric amplifier, and an atomic ensemble. In particular, the hybrid system comprises a fixed mirror, a coherent feedback loop, two charged mechanical oscillators, an ensemble of two-level atoms, and an OPA placed inside the cavity. We first formulate the Hamiltonian of the system under consideration. Applying the resulting Hamiltonian of the system, we obtain the nonlinear quantum Langevin equations. Using numerical solutions of the Lyapunov equation and steady-state mean values, we quantify the Gaussian quantum coherence of single-mode, two-mode, and multimode hybrid systems.

3.5.1 Model and Hamiltonian of the system

We consider a hybrid electro-optomechanical system consisting of a stationary mirror and a mechanical oscillator (MR_1) that is interconnected with a second mechanical oscillator (MR_2) through the Coulomb force interaction (η) (Zhang et al., 2012), as illustrated in Fig. 3.3. Inside the cavity, there is a collection of two-level atoms and an OPA. The incident light field ($\hat{c}_{in}$) is directed via an asymmetric beam splitter (BS), while the transmitted portion of the input laser stimulates the cavity. The cavity mode is coupled to the mechanical oscillator (MR_1) via radiation pressure. The output field ($\hat{c}_{out}$) is entirely reflected by the mirror M, with a portion redirected back into the cavity through BS, creating a coherent feedback loop. The beam splitter is used to combine the light beams created by a laser source with those that exit the cavity via fixed mirrors. The unitary matrix of BS is defined in Eq.(3.34), where the amplitude transmission and reflection coefficients of the BS satisfy $t^2 + r^2 = 1$ (t and r are real and positive) (Mandel and Wolf, 1995). As a consequence, the transmitted part of the input laser has an amplitude of $t\Omega$, and the reflected part has an amplitude of $-r\Omega$. In actuality, $t = \sqrt{\tau}$ and $r = \sqrt{\mu}$ represent in terms of the transmittance τ and reflectance μ of the asymmetric beam splitter (Mekonnen et al., 2024). An OPA is pumped by a pump field with frequency $2\omega_l$, and its output frequency is ω_l (He et al., 2022). The total Hamiltonian of the hybrid system can be expressed as

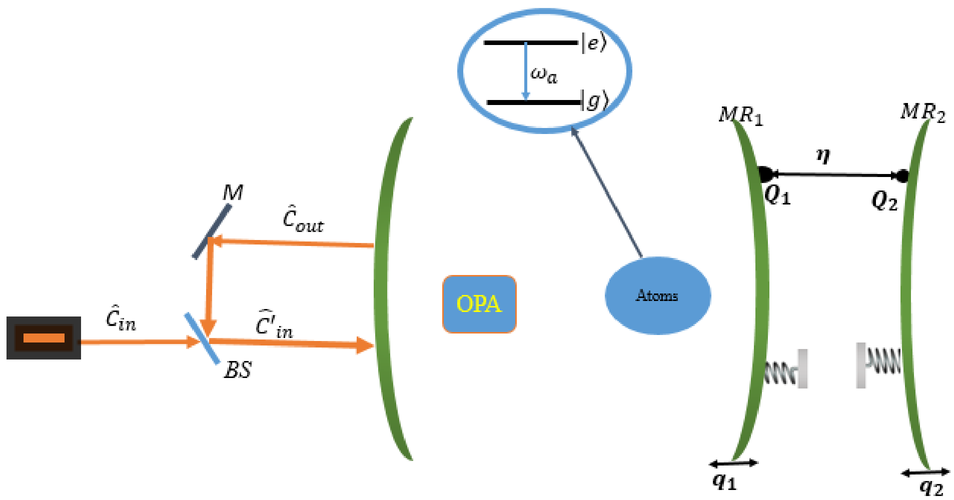

Figure 3.3: Schematic model of the hybrid optomechanical system with a coherent feedback loop. The cavity optomechanics system consists of a stationary mirror and a mechanical oscillator (MR_1) which is coupled to the other mechanical oscillator (MR_2) with Coulomb coupling strength η. Within the cavity, an ensemble of two-level atoms and an OPA are positioned. An input light field enters the cavity across an asymmetric beam splitter. The output field is reflected on the mirror M and a part of the output field is sent to the cavity via a beam splitter. The two-level atom has upper and lower energy eigen state denoted by $|e\rangle$ and $|g\rangle$, respectively. The electrodes on the two mechanical oscillators possess charges Q_1 and Q_2. q_1 and q_2 represent the small deviations of these oscillators from their equilibrium positions.

$$\begin{aligned}\hat{H} = &\hbar\omega_c \hat{c}^\dagger \hat{c} + \frac{1}{2}\hbar\omega_a \hat{s}_z + \sum_{j=1}^{2} \frac{\hbar\omega_j}{2}\left(\hat{p}_j^2 + \hat{q}_j^2\right) - \hbar g \hat{q}_1 \hat{c}^\dagger \hat{c} \\ &+ \hbar g_a \left(\hat{s}_+ \hat{c} + \hat{s}_- \hat{c}^\dagger\right) + i\hbar\Omega\sqrt{\tau}\left(\hat{c}^\dagger e^{-i\omega_l t} - \hat{c} e^{i\omega_l t}\right) \\ &+ i\hbar G_a \left(e^{i\theta}\hat{c}^{\dagger 2} e^{-2i\omega_l t} - e^{-i\theta}\hat{c}^2 e^{2i\omega_l t}\right) + \hat{H}_{coul},\end{aligned} \tag{3.58}$$

where the first term in the above equation describes the free energy of the cavity mode. The second term represents the free energy of the two-level atomic ensemble. This ensemble consists of N atoms characterized by individual intrinsic frequencies, denoted ω_a. The behavior of each atom within the ensemble is described by Pauli spin matrices, namely $\hat{\sigma}_z$, $\hat{\sigma}_+$, and $\hat{\sigma}_-$. The collective spin operator is defined as

$$\hat{s}_{+,-,z} = \sum_{k=1}^{N} \hat{\sigma}^k_{+,-,z}, \tag{3.59}$$

which $\hat{\sigma}_+ = |e\rangle\langle g|,\ \hat{\sigma}_- = |g\rangle\langle e|$, and $\hat{\sigma}_z = |e\rangle\langle e| - |g\rangle\langle g|$. The commutation relations are stated as Eqs. (2.5)-(2.6). The third term represents the free energy of the mechanical modes. The fourth term depict the interaction between the cavity field and the first charged mechanical oscillator, while g is the optomechanical coupling strength. The initial term in the second line implies the energy corresponding to the interaction between the cavity mode and the atomic ensemble, while g_a is the coupling strength between the single two-level atom and the cavity field. The second term in the second line indicates the cavity field driven by the transmitted portion of the input laser. The first term in the third line indicates the interaction of an OPA with the cavity field. Although G_a is the nonlinear gain of the OPA, and θ describes the phase of the optical field driving the OPA. The last term in the third line illustrates the Coulomb interaction potential, and the mathematical representation is similar in Eq.(3.2).

The collective spin operators are examined in the context of low atomic excitation, where all the atoms are in their ground state. The mean number of atoms in the excited state is predicted to be significantly less than the total number of atoms N. In this context $\langle \hat{a}^\dagger \hat{a}\rangle \ll N$ and using the Holstein-Primakof approximation, the collective spin operator of the atomic ensemble is given (Holstein and Primakoff, 1940)

$$\hat{s}_+ = \hat{a}^\dagger \sqrt{N - \hat{a}^\dagger \hat{a}} \simeq \sqrt{N}\hat{a}^\dagger, \tag{3.60}$$

$$\hat{s}_- = \hat{a}\sqrt{N - \hat{a}^\dagger \hat{a}} \simeq \sqrt{N}\hat{a}, \tag{3.61}$$

and

$$\hat{s}_z \simeq 2\hat{a}^\dagger \hat{a} - N. \tag{3.62}$$

The dynamics of atomic polarization can be characterized by the bosonic annihilation operator $\hat{a} = \frac{\hat{s}_-}{\sqrt{|\langle \hat{s}_z \rangle|}}$ and its Hermitian conjugate $\hat{a}^\dagger$, meets the commutation relation (Holstein and Primakoff, 1940)

$$[\hat{a}, \hat{a}^\dagger] = 1. \tag{3.63}$$

Utilizing Eqs.(3.60)-(3.62) into Eq.(3.58), we have found

$$\begin{aligned}\hat{H} &= \hbar\omega_c\hat{c}^\dagger\hat{c} + \hbar\omega_a\hat{a}^\dagger\hat{a} + \sum_{j=1}^{2}\frac{\hbar\omega_j}{2}\left(\hat{p}_j^2 + \hat{q}_j^2\right) - \hbar g q_1\hat{c}^\dagger\hat{c} + \hbar\lambda_a\left(\hat{a}^\dagger\hat{c} + \hat{a}\hat{c}^\dagger\right)\\ &+ i\hbar\Omega\sqrt{\tau}\left(\hat{c}^\dagger e^{-i\omega_l t} - \hat{c}e^{i\omega_l t}\right) + i\hbar G_a\left(e^{i\theta}\hat{c}^{\dagger 2}e^{-2i\omega_l t} - e^{-i\theta}\hat{c}^2 e^{2i\omega_l t}\right) + \hbar\eta q_1 q_2,\end{aligned} \tag{3.64}$$

where $\lambda_a = g_a\sqrt{N}$ corresponds to the atomic coupling strength with the cavity field. In a rotating frame with frequency ω_l, the hybrid systems Hamiltonian is expressed as

$$\begin{aligned}\hat{H} &= \hbar\Delta_o\hat{c}^\dagger\hat{c} + \hbar\Delta_a\hat{a}^\dagger\hat{a} + \sum_{j=1}^{2}\frac{\hbar\omega_j}{2}\left(\hat{p}_j^2 + \hat{q}_j^2\right) - \hbar g q_1\hat{c}^\dagger\hat{c} + \hbar\lambda_a\left(\hat{a}^\dagger\hat{c} + \hat{a}\hat{c}^\dagger\right)\\ &+ i\hbar\Omega\sqrt{\tau}\left(\hat{c}^\dagger - \hat{c}\right) + i\hbar G_a\left(e^{i\theta}\hat{c}^{\dagger 2} - e^{-i\theta}\hat{c}^2\right) + \hbar\eta q_1 q_2,\end{aligned} \tag{3.65}$$

where, Δ_o is the detuning of the cavity mode and Δ_a= $\omega_a - \omega_l$ represents detuning of the atomic mode.

3.5.2 Equations of the motion

The dynamics of the system can be well explained by the quantum Langevin equation. By substituting Eq.(3.65) into Eqs.(A.1)-(A.6) and applying Eq.(3.63) and Eqs.(A.7)-(A.10), we easily obtain the nonlinear quantum Langevin equations as follows:

$$\begin{aligned}\dot{\hat{q}}_1 &= \omega_1\hat{p}_1,\\ \dot{\hat{p}}_1 &= -\omega_1\hat{q}_1 - \gamma_1\hat{p}_1 - \eta\hat{q}_2 + g\hat{c}^\dagger\hat{c} + \xi_1(t),\\ \dot{\hat{q}}_2 &= \omega_2\hat{p}_2,\\ \dot{\hat{p}}_2 &= -\omega_2\hat{q}_2 - \gamma_2\hat{p}_2 - \eta\hat{q}_1 + \xi_2(t),\\ \dot{\hat{c}} &= -(\kappa_{eff} + i\Delta_o - ig\hat{q}_1)\hat{c} + 2G_a\hat{c}^\dagger e^{i\theta} - i\lambda_a\hat{a} + \Omega\sqrt{\tau} + \sqrt{2\kappa}\hat{c}_{fb}(t),\\ \dot{\hat{a}} &= -(\gamma_a + i\Delta_a)\hat{a} - i\lambda_a\hat{c} + \sqrt{2\gamma_a}\hat{a}_{in}(t),\end{aligned} \tag{3.66}$$

where γ_a is the decay rate of the atoms, and also $\hat{c}_{fb}$ is the effective input noise operator that is incident to the beam splitter, and $\hat{a}_{in}$ is the noise operator of the system that impacts the atomic field. The incident input field and the atomic fields are the initial vacuum reservoir. Following this, the expectation values of $\langle \hat{c}_{fb}(t) \rangle$ and $\langle \hat{c}_{fb}(t)\hat{c}^{\dagger}_{fb}(t') \rangle$ are given in Eq.(3.43) and Eq.(3.44), respectively. The expectation values of the noise operator of the system impact on the atomic field is given by (Mansouri et al., 2022)

$$\langle \hat{a}_{in}(t)\hat{a}^{\dagger}_{in}(t') \rangle = \delta(t - t'). \tag{3.67}$$

3.5.3 Steady state solutions of the equations of motion

The dynamics of a hybrid system can be easily linearized when the cavity is strongly driven by an input laser. Employing Eq.(2.36), we can rewrite each operator of Eq.(3.66) in terms of its steady-state value and fluctuation part. To determine the steady-state solution for each operator, begin by equating the time derivative of all components in Eq. (3.66) to zero and assuming that the mechanical damping factors, $\xi_1(t)$ and $\xi_2(t)$, do not have any influence on the steady-state system, allowing us to ignore minor terms. Consequently, the steady-state mean values of Eq. (3.66) can be formulated as follows:

$$\begin{aligned} p_1^s &= 0, \\ p_2^s &= 0, \\ q_1^s &= \frac{-\omega_2 g |c^s|^2}{\eta^2 - \omega_1\omega_2}, \\ q_2^s &= \frac{g|c^s|^2\eta}{\eta^2 - \omega_1\omega_2}, \end{aligned} \tag{3.68}$$

$$c^s = \frac{\sqrt{\tau}\Omega}{\kappa_{eff} + i\Delta - 2G_a e^{i\theta} + \frac{\lambda_a^2}{\gamma_a + i\Delta_a}}, \tag{3.69}$$

$$a^s = \frac{-i\lambda_a c^s}{\gamma_a + i\Delta_a}, \tag{3.70}$$

where $\Delta = \Delta_o - g q_1^s$ represents the effective cavity detuning from the input laser frequency in the existence of radiation pressure.

3.5.4 Quantum fluctuation and covariance matrix of the system

We now proceed to determine the quantum coherence of the various modes of the hybrid system. For this purpose, we establish the operators for the quadratures of the cavity field the same as in Eqs. (3.14),(3.48-3.49). Furthermore, to incorporate the atomic ensemble into the analysis, we introduce the quadratures corresponding to the atomic ensemble as follows:

$$\delta\hat{X} = (\delta\hat{a}^\dagger + \delta\hat{a})/\sqrt{2}, \tag{3.71}$$

$$\delta\hat{Y} = i(\delta\hat{a}^\dagger - \delta\hat{a})/\sqrt{2}, \tag{3.72}$$

and the corresponding Hermitian input noise operators are

$$\delta\hat{X}_{in} = (\delta\hat{a}_{in}^\dagger + \delta\hat{a}_{in})/\sqrt{2}, \tag{3.73}$$

$$\delta\hat{Y}_{in} = i(\delta\hat{a}_{in}^\dagger - \delta\hat{a}_{in})/\sqrt{2}. \tag{3.74}$$

Using the definition offered above and Eqs. (3.14),(3.48)-(3.49), we can formulate the linearized quantum Langevin equations as follows:

$$\begin{aligned}
\delta\dot{\hat{q}}_1 &= \omega_1\delta\hat{p}_1,\\
\delta\dot{\hat{p}}_1 &= -\omega_1\delta\hat{q}_1 - \gamma_1\delta\hat{p}_1 - \eta\delta\hat{q}_2 + G_0\delta\hat{x} + \xi_1(t),\\
\delta\dot{\hat{q}}_2 &= \omega_2\delta\hat{p}_2,\\
\delta\dot{\hat{p}}_2 &= -\omega_2\delta\hat{q}_2 - \gamma_2\delta\hat{p}_2 - \eta\delta\hat{q}_1 + \xi_2(t),\\
\delta\dot{\hat{x}} &= -(\kappa_{eff} - 2G_a\cos\theta)\delta\hat{x} + (\Delta + 2G_a\sin\theta)\delta\hat{y} + \lambda_a\delta Y + \sqrt{2\kappa}\delta\hat{x}_{in},\\
\delta\dot{\hat{y}} &= G_0\delta\hat{q}_1 - (\Delta - 2G_a\sin\theta)\delta\hat{x} - (\kappa_{eff} + 2G_a\cos\theta)\delta\hat{y} - \lambda_a\delta X + \sqrt{2\kappa}\delta\hat{y}_{in},\\
\delta\dot{\hat{X}} &= -\gamma_a\delta X + \Delta_a\delta Y + \lambda_a\delta y + \sqrt{2\gamma_a}\delta\hat{X}_{in},\\
\delta\dot{\hat{Y}} &= -\gamma_a\delta Y - \Delta_a\delta X - \lambda_a\delta x + \sqrt{2\gamma_a}\delta\hat{Y}_{in},
\end{aligned} \tag{3.75}$$

Eq. (3.75) can easily be expressed in a short manner

$$\dot{\Theta}(t) = \Re\Theta(t) + \zeta(t), \tag{3.76}$$

where $\Theta(t) = (\delta\hat{q}_1, \delta\hat{p}_1, \delta\hat{q}_2, \delta\hat{p}_2, \delta\hat{x}, \delta\hat{y}, \delta\hat{X}, \delta\hat{Y})^T$ and $\zeta(t) = (0, \xi_1(t), 0, \xi_2(t), \sqrt{2\kappa}\delta\hat{x}_{in}, \sqrt{2\kappa}\delta\hat{y}_{in}, \sqrt{2\gamma_a}\delta\hat{X}_{in}, \sqrt{2\gamma_a}\delta\hat{Y}_{in})^T$ are the column vector of the quadrature fluctuation and input noises, respectively. The drift matrix $\Re$ can be represented as:

$$\Re = \begin{pmatrix} 0 & \omega_1 & 0 & 0 & 0 & 0 & 0 & 0 \\ -\omega_1 & -\gamma_1 & -\eta & 0 & G_0 & 0 & 0 & 0 \\ 0 & 0 & 0 & \omega_2 & 0 & 0 & 0 & 0 \\ -\eta & 0 & -\omega_2 & -\gamma_2 & 0 & 0 & 0 & 0 \\ 0 & 0 & 0 & 0 & -\kappa_{eff} + 2G_a\cos\theta & \Delta + 2G_a\sin\theta & 0 & \lambda_a \\ G_0 & 0 & 0 & 0 & 2G_a\sin\theta - \Delta & \kappa_{eff} - 2G_a\cos\theta & -\lambda_a & 0 \\ 0 & 0 & 0 & 0 & 0 & \lambda_a & -\gamma_a & \Delta_a \\ 0 & 0 & 0 & 0 & -\lambda_a & 0 & -\Delta_a & -\gamma_a \end{pmatrix}. \tag{3.77}$$

The drift matrix in Eq. (3.77) provides all necessary information about the system. The system is regarded to have reached a stable steady-state condition only when all eigenvalues of the drift matrix are negative real parts. Using the Routh-Hurwitz criterion (DeJesus and Kaufman, 1987), the stability requirements can be achieved. The system under consideration here is described in terms of continuous variable Gaussian states and linearized dynamics. In this context, quantum fluctuations in the system are characterized by an 8×8 covariance matrix (CM), with the corresponding components defined as

$$V_{jk} = \langle u_j(t)u_k(t') + u_k(t)u_j(t')\rangle/2. \tag{3.78}$$

The steady-state covariance matrix can be described by Lyapunov equation

$$\Re V + V\Re^T + D = 0, \tag{3.79}$$

in which D is a diagonal matrix that is known as a diffusion matrix, that characterizes the noise correlations. Using Eqs.(3.10),(3.44),(3.67), one can easily verify that

$$D = diag(0, \gamma_1(2\bar{n}+1), 0, \gamma_2(2\bar{n}+1), \kappa\tau/(1+\sqrt{\mu})^2, \kappa\tau/(1+\sqrt{\mu})^2, \gamma_a, \gamma_a). \tag{3.80}$$

Furthermore, solving Eq.(3.79) analytically is complicated, therefore, we can utilize a numerical solution to analyze the Gaussian quantum coherence of the hybrid system. The numerical solution of Eq.(3.79) can be defined as

$$V=\begin{pmatrix} V_{m1} & V_{m1m2} & V_{m1o} & V_{m1a} \\ V_{m2m1} & V_{m2} & V_{m2o} & V_{m2a} \\ V_{om1} & V_{om2} & V_{o} & V_{oa} \\ V_{am1} & V_{am2} & V_{ao} & V_{a} \end{pmatrix}, \tag{3.81}$$

in which $V_j(j = m_1, m_2, o, a)$ represents the 2×2 block matrix of local properites of every mode, and $V_{j,k}(j, k = m_1, m_2, o, a)$ is the 2×2 block matrix of the correlations between the respective modes.

3.5.5 Quantification of Gaussian quantum coherence

We now seek to investigate the quantum coherence of a hybrid electro-optomechanical system using a coherent feedback loop composed of an optical parametric amplifier and two-level atomic ensembles. Employing Eq.(3.81), we can easily obtain the covariance matrix for each mode, such as mechanical oscillators, optical mode, and atomic mode. The covariance matrix for the first mechanical oscillator V_{m1}, the second mechanical oscillator V_{m2}, the optical mode V_o, and the atomic mode V_a are depicted below:

$$\begin{aligned} V_{m1} &= \begin{pmatrix} V_{11} & V_{12} \\ V_{21} & V_{22} \end{pmatrix}, V_{m2} = \begin{pmatrix} V_{33} & V_{34} \\ V_{43} & V_{44} \end{pmatrix}, \\ V_{o} &= \begin{pmatrix} V_{55} & V_{56} \\ V_{65} & V_{66} \end{pmatrix}, V_{a} = \begin{pmatrix} V_{77} & V_{78} \\ V_{87} & V_{88} \end{pmatrix}. \end{aligned} \tag{3.82}$$

In the following, the quantum coherence of any single-mode Gaussian state $\rho(V_j, \vec{d})$ is entirely captured by the first and second moments (covariance matrix(V)), the initial moment is described as $\vec{d} = (d_x, d_y)$, where d_x is the steady-state average values of any position mode and d_y is the steady-state mean momentum values of any mode. On accounts of Eq.(3.68), the first moments of the first mechanical mode are given by:

$$d_x = q_1^s = -\omega_2 g|c^s|^2/(\eta^2 - \omega_1\omega_2), \tag{3.83}$$

$$d_y = p_1^s = 0. \tag{3.84}$$

Similarly, the first moments of the second mechanical modes are

$$d_x = q_2^s = g|c^s|^2\eta/(\eta^2 - \omega_1\omega_2), \tag{3.85}$$

$$d_y = p_2^s = 0. \tag{3.86}$$

Using Eq.(3.69), we can efficiently derive the first moments of the optical mode such as:

$$d_x = (c^s + c^{*s})/\sqrt{2},\ d_y = i(c^{*s} - c^s)/\sqrt{2}. \tag{3.87}$$

Following a similar approach, Eq. (3.70) allows us to readily obtain the first moments of the atomic mode

$$d_x = (a^s + a^{*s})/\sqrt{2},\ d_y = i(a^{*s} - a^s)/\sqrt{2}. \tag{3.88}$$

Employing Eqs.(3.83-3.88) and Eq.(3.82) into Eq.(2.51), we can easily determine the quantum coherence of the one-mode Gaussian state $\rho(V_j, \vec{d})$. In addition, to quantify bipartite quantum coherence between subsystems, we can easily reduce the covariance matrix V from Eq.(3.81) into a 2×2 submatrix $V_{jk}(j, k = m_1, m_2, o, a)$. We easily calculate the bipartite quantum coherence $\rho(V_{jk}, \vec{d})$ using Eq.(2.52). Employing Eq.(2.53), we easily calculate the total quantum coherence of a CV system with four mode. As a result, we numerically describe the results of an analytical equation via the plots in Figs.(4.8)-(4.15), using experimentally parameters.

4

RESULTS AND DISCUSSION

This chapter presents the results and a discussion of the dissertation work in three sections. In the first section, we examined the impact of various parameters on the quantum correlation between mechanical modes. Specifically, we explored how the nonlinear gain of the OPA, the phase of the optical field driving the OPA, the Coulomb coupling strength, the environmental temperature, and the driven laser power influence the quantum correlation, as revealed through numerical simulations. The second section focuses on the steady-state entanglement between mechanical modes. Here, we evaluated the effects of Coulomb strength, the presence of the OPA, the phase of the OPA, the reflection coefficient, and the environmental temperature on the entanglement. In the last section, we examined how factors such as the OPA's nonlinear gain, reflection coefficient, atomic decay rate, atomic coupling, driving laser power, and ambient temperature influence quantum coherence using simulation numerical results.

Table 4.1: The experimental parameters for the plots in Figs. (4.1)-(4.7) have been chosen from the values provided in Refs.(Schliesser et al., 2008; Gigan et al., 2006) under standard conditions.

No	**Parameters**	**Values**
1	Mechanical frequency ($\omega_{m1} = \omega_{m2} = \omega_m$)	$200\pi\ MHz$
2	Mechanical damping rates ($\gamma_1 = \gamma_2 = \gamma_m$)	$20\pi\ Hz$
3	Cavity damping rates (κ)	$88.1\ MHz$
4	Mass of the mechanical oscillators ($m_1 = m_2 = m$)	$5\ ng$
5	Cavity length (L)	$1mm$
6	Wavelength of driving laser (λ)	$810nm$
7	Temperature (T)	$4mK$
8	Laser power (P)	$10mW$
9	Coulomb coupling strength (η)	$0.95\omega_m$

4.1 Quantification of quantum correlations

In this section, we investigate the quantum correlation through an optical parametric amplifier and a Coulomb-type interaction in the hybrid system. We used three quantum correlation quantifiers such as logarithmic negativity, steering, and discord. Further, to obtain the covariance matrix, we numerically solve Eq.(3.30) and compute the logarithmic negativity, which serves as a witness to quantum entanglement. Then, Gaussian quantum discord is calculated to quantify all non-classical correlations present in the system. In addition, we perform numerical calculations of quantum steering to determine the steerability between the mechanical modes. For the numerical simulations, we used the experimental parameters listed in Table (4.1).

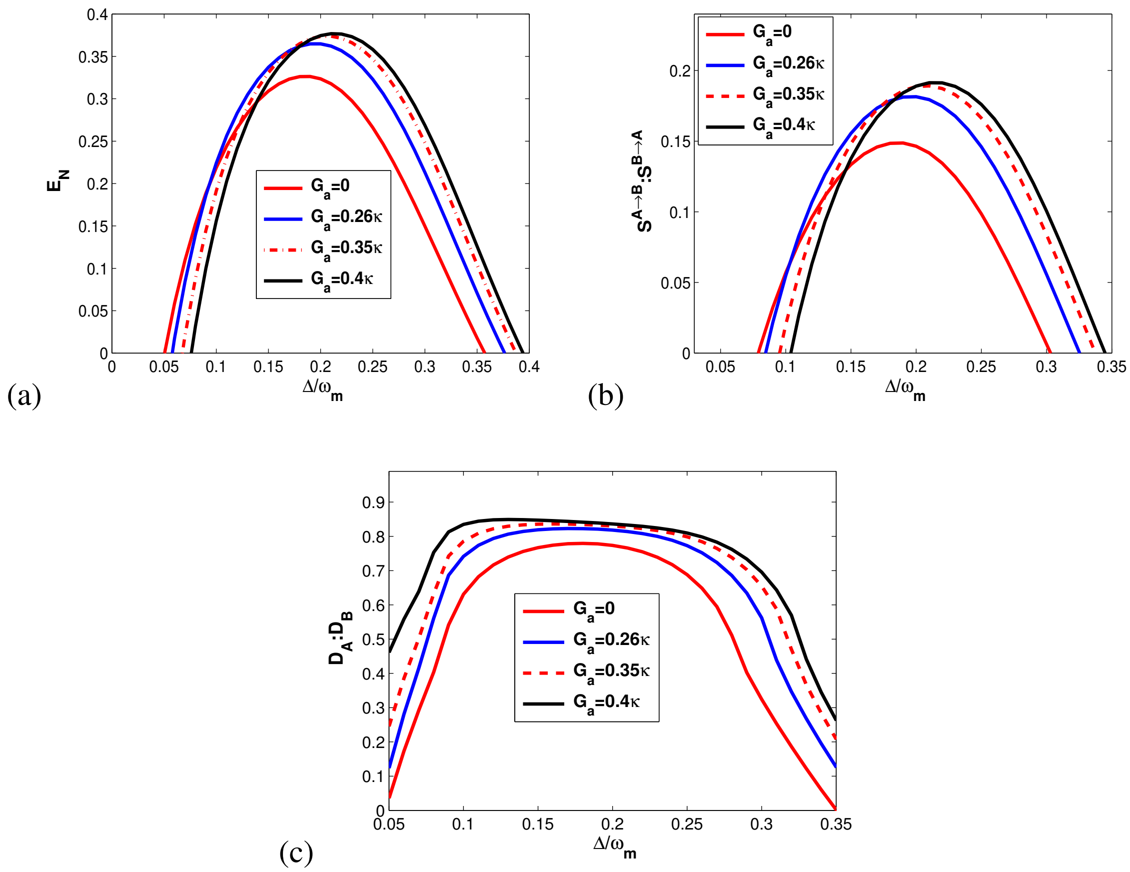

Figure 4.1: Plots of quantum correlations: (a) logarithmic negativity E_N, (b) quantum steering ($S^{A\to B} : S^{B\to A}$), and (c) quantum discord ($D_A : D_B$) as function of the normalized detuning Δ/ω_m for different values of the nonlinear gain of the OPA G_a with phase of the optical field driving the OPA ($\theta = 0$), temperature ($T = 4mK$), laser power ($P = 10mW$), and Coulomb coupling strength ($\eta = 0.95\omega_m$). Other parameters are listed in Table (4.1).

Figure (4.1), shows the measurement of quantum correlations between mechanical oscillators using logarithmic negativity E_N, quantum steering ($S^{A\to B} : S^{B\to A}$), and quantum discord ($D_A : D_B$) as a function of the normalized detuning Δ/ω_m for different values of nonlinear gain of the OPA. In Figure (4.1), we numerically display the effect of the nonlinear gain of the OPA on the quantum entanglement, quantum steering, and quantum discord between mechanical modes. Generate bipartite entanglement, quantum steering, and quantum discord between the mechanical modes as functions of normalized detuning for various nonlinear gain values of the OPA. Notably, we employed realistic parameters that enable significant quantum correlation between the mechanical modes. Specifically, one can observe that there is a correlation between the two oscillators, implying that there is a quantum correlation between them, even though they are separated. Additionally, Figs. (4.1)(a-c) show that when the nonlinear gain of the OPA coupling parameter grows, the quantum correlation between the oscillators intensifies. In Figs. (4.1) shows that increasing the nonlinear gain of the OPA enhances the quantum entanglement, quantum steering, and quantum discord between the mechanical modes compared to the absence of the OPA. This enhancement is attributed to the fact that increasing the nonlinear gain of the OPA corresponds to an increase in the photon number within the optical cavity. This elevated photon number leads to a stronger radiation pressure exerted on the mechanical oscillator (MR_1). Our findings are consistent with those reported in (Pan et al., 2023).

Next, we explore the crucial role of the Coulomb coupling strength η on the quantum correlations between the two mechanical oscillators separated in space. Figure (4.2), we plot quantum correlations using logarithmic negativity E_N, quantum steering ($S^{A\to B} : S^{B\to A}$), and quantum discord ($D_A : D_B$) as functions of normalized detuning Δ/ω_m for different values of the Coulomb coupling strength. Quantum correlation exists between the two mechanical oscillators, even when they are physically separated. As shown in Figure (4.2) (a-c), the presence of strong Coulomb coupling enhances the entanglement, quantum steering, and quantum discord between spatially separated mechanical oscillators. As depicted in Fig. (4.2), a larger Coulomb coupling strength leads to more strongly entangled mechanical oscillators. Moreover, in the absence of Coulomb coupling, entangling the two oscillators separately is impossible. Therefore, the Coulomb interaction between the two oscillators is the most crucial parameter for achieving state transfer between the subsystems. Therefore, our results are consistent with those reported in (Bai et al., 2017; Pan et al., 2023). Now, we consider the feasibility of choosing the numerical value of the coupling strength η in the experiment. If we apply the experimental parameters reported, that is, the gate voltage $V_1 = V_2 = 200V$, the capacitance of the gate $C_1 = C_2 = 2.4nF$ and the separation between mechanical oscillators without Coulomb and optomechanical interaction

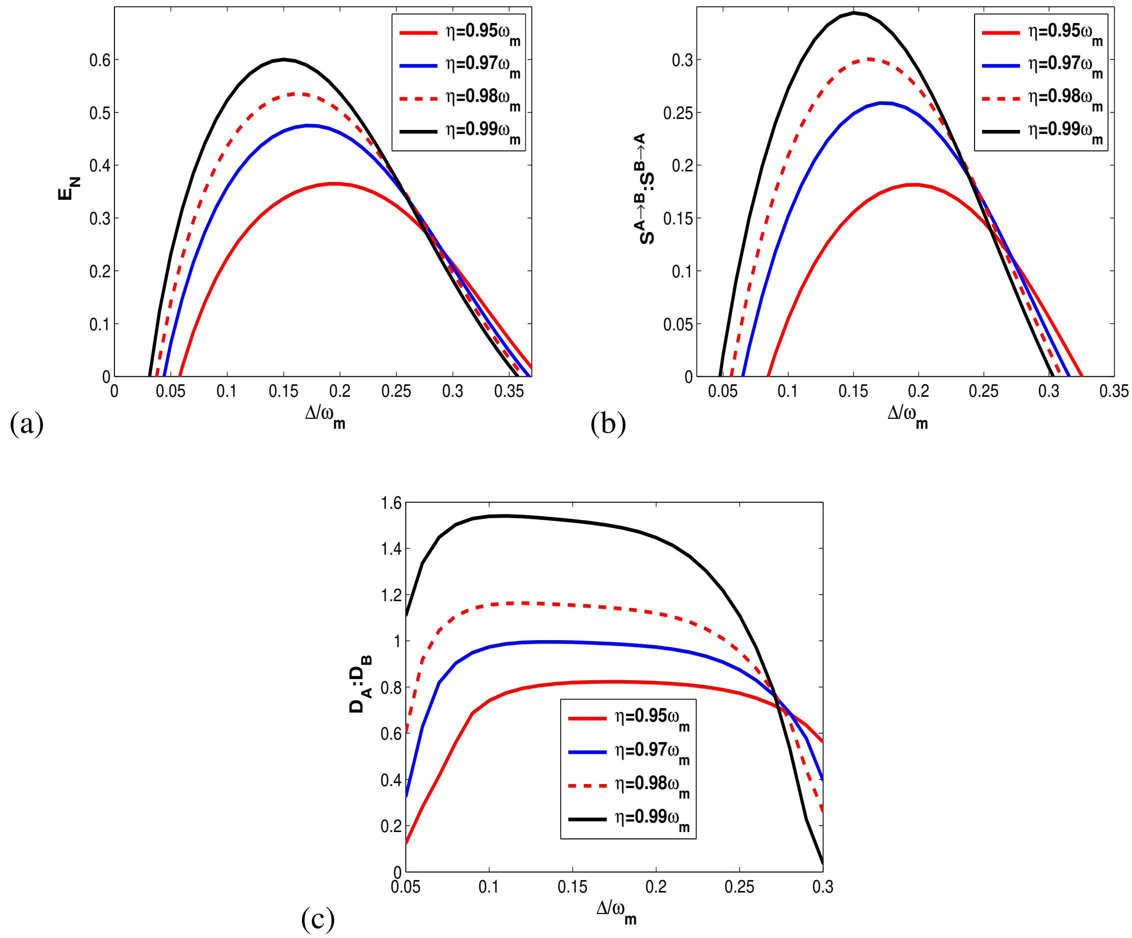

Figure 4.2: Plots of quantum correlations: (a) logarithmic negativity E_N, (b) quantum steering $(S^{A\to B} : S^{B\to A})$, and (c) quantum discord $(D_A : D_B)$ as a function of the normalized detuning Δ/ω_m for different value of Coulomb coupling strength η with the nonlinear gain of the OPA $(G_a = 0.26\kappa)$. Other parameters are the same as Fig. (4.1)

$r_0 = 160\mu m$ (Bai et al., 2017; Chen et al., 2015), in this situation $\eta \approx 0.33\omega_m$. If we compare the numerical values used in our coupled optomechanical system, it is obvious that our choice of the numerical value of coulomb coupling strength is easily executable in experiments. Thus, our hybrid optomechanical system can be realized by choosing the appropriate experimental parameters from (Schliesser et al., 2008; Gigan et al., 2006). The results show that the presence of strong Coulomb coupling enhances the quantum correlations between the mechanical oscillators, and Coulomb interactions are more prominent in quantum correlations.

We next examine the effect of the phase of the optical field driving the OPA on quantum correlations between the two separated mechanical oscillators in space. As shown in Fig. (4.3)

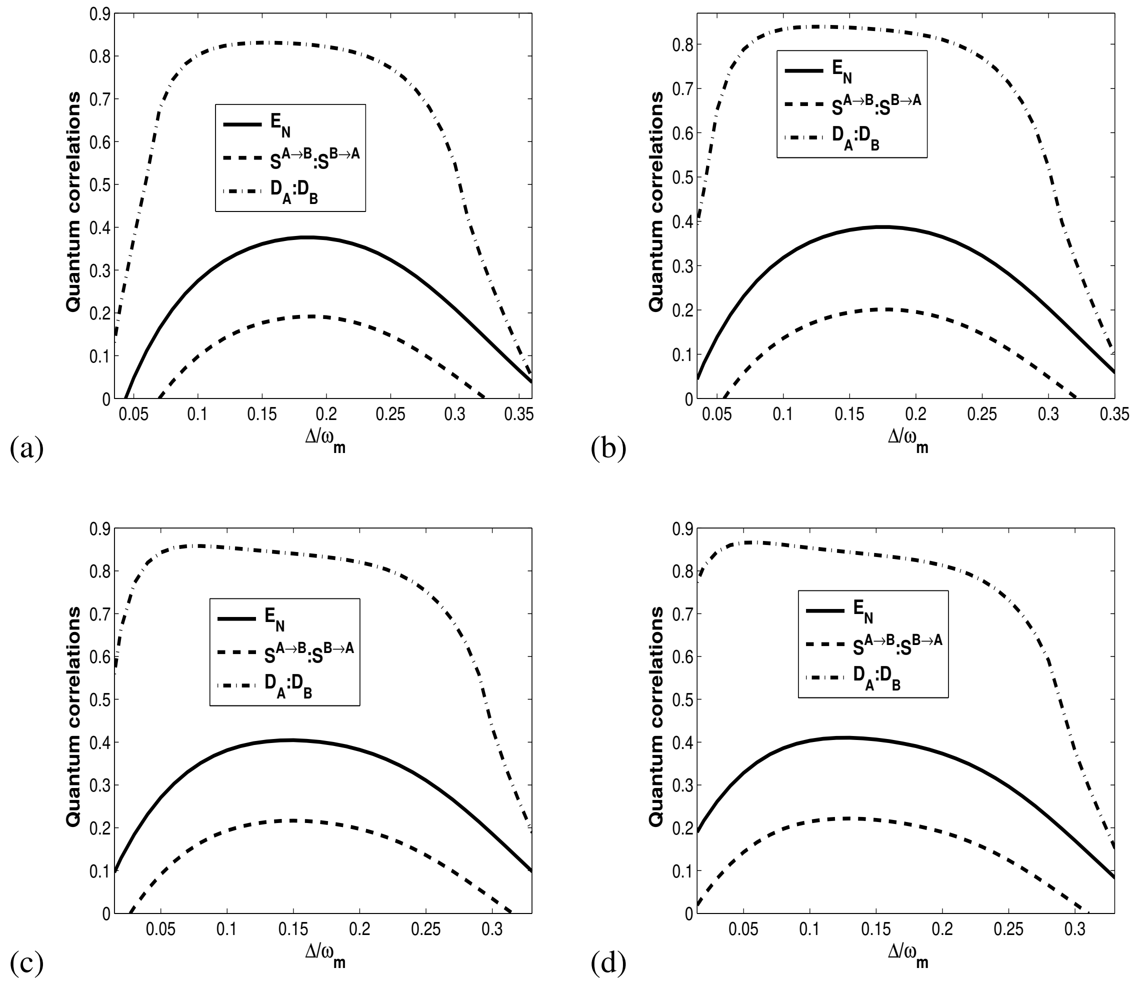

Figure 4.3: Plots of quantum correlations: logarithmic negativity E_N, quantum steering ($S^{A\rightarrow B}$: $S^{B\rightarrow A}$), and quantum discord ($D_A : D_B$) as a function of the normalized detuning Δ/ω_m for different values of the phase of the optical field driving the OPA, (a) $\theta = \pi/16$, (b) $\theta = \pi/8$, (c) $\theta = \pi/4$, and (d) $\theta = \pi/3$ with the nonlinear gain of the OPA ($G_a = 0.26\kappa$). Other parameters are the same as in Fig. (4.1)

(a)-(d), it can be seen that the quantum correlations increase with the phase θ increases with fixed values of the nonlinear gain of OPA (G_a) and the Coulomb coupling strength η. In addition, the optimum values of quantum steering and quantum discord occur in $\Delta/\omega_m = 0.13$, and $\Delta/\omega_m = 0.05$, respectively, for the case $\theta = \pi/3$. Thus, we deduced that the presence of phase fluctuation of the optical field driving the OPA affects the quantum correlations.

It is also significant to study the robustness of quantum correlations between the two mechanical oscillators against temperature. Figure (4.4) shows graphs of quantum correlations:

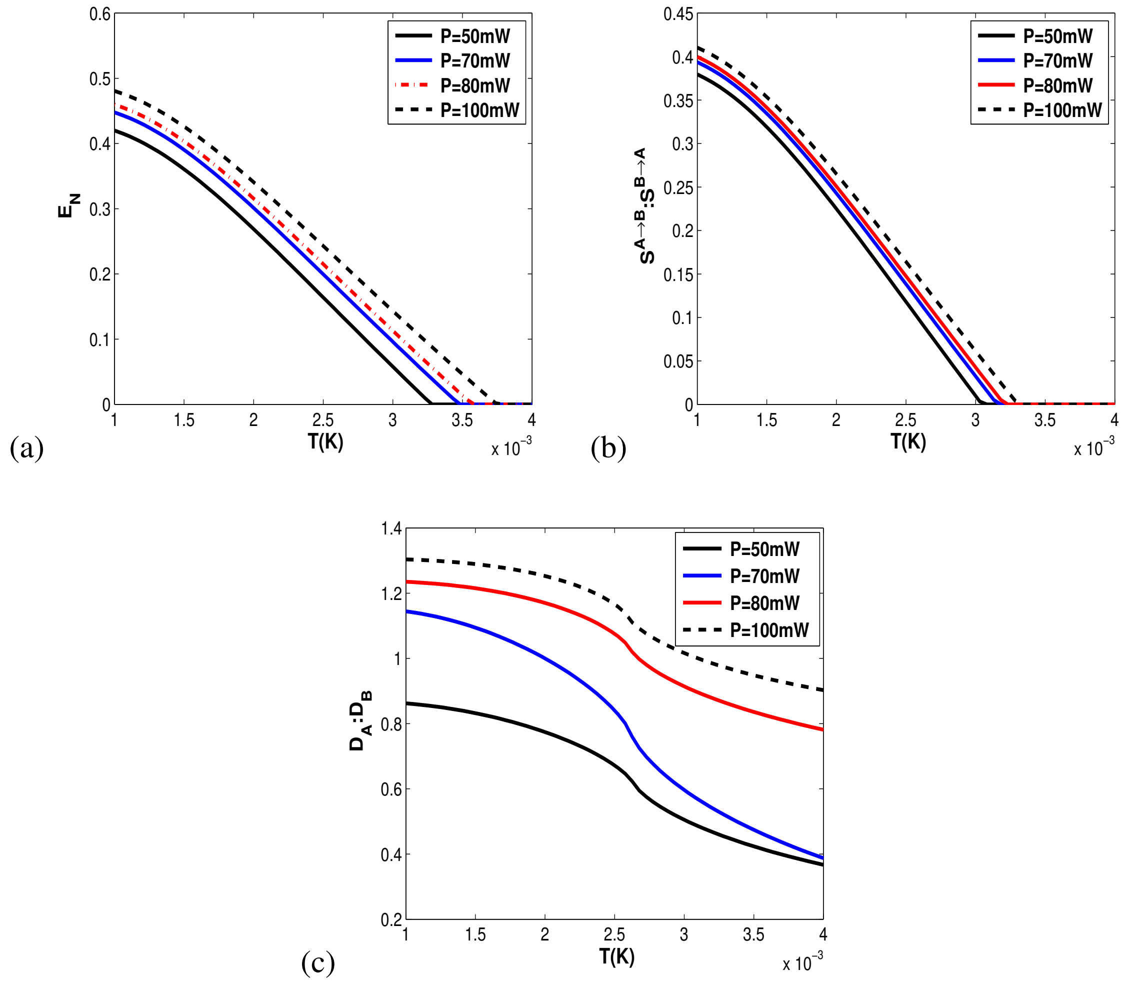

Figure 4.4: Plots of quantum correlations: (a) logarithmic negativity E_N, (b) quantum steering ($S^{A\rightarrow B}$: $S^{B\rightarrow A}$), and (c) quantum discord (D_A : D_B) as a function of the temperature for different values drive laser power with $\Delta = 0.6\omega_m$ with the nonlinear gain of the OPA ($G_a = 0.26\kappa$). The remaining set of parameters is the same as in Fig. (4.1)

(a) logarithmic negativity (E_N), (b) quantum steering ($S^{A\rightarrow B}$: $S^{B\rightarrow A}$), and (c) quantum discord (D_A : D_B) as a function of the temperature for the drive power of different values. As shown in Figure (4.4), quantum correlations such as entanglement, quantum steering, and quantum discord, become stronger as the laser power increases. The degree of the quantum correlations between the mechanical modes decreases as the temperature increases because thermal noise in the environment induces decoherence. The entanglement degrades to zero, this is the phenomenon of entanglement of sudden death (Al-Qasimi and James, 2008). According to these results, an increase in temperature leads to the transition from quantum to classical regimes, which is caused by thermal fluctuations. As a result, the hybrid system does not exhibit any entanglement in classical regimes, despite the presence of quite strong laser power. We deduced that the stronger the thermal noise, the higher the temperature of the environment. The entanglement between two separate oscillators is then submerged by strong thermal noise (Sohail et al., 2020). We note that the two-way steerable state vanishes with higher values of environmental temperature. In addition, we obtain better quantum discord at low temperatures, and even at higher temperature values, quantum discord is found to persist, although entanglement E_N vanishes completely, indicating that quantum discord extends beyond entanglement and confirms the robustness of this measure against fluctuations of the bath environment. Therefore, thermal fluctuations affect quantum correlation, while laser power enhances quantum correlation. We believe that these are appropriate measures to quantify quantum entanglement, quantum steering, and quantum discord and show that our proposed scheme enhances the quantum correlation and proves robust against fluctuations in the bath environment.

Furthermore, we can summarize the figures (4.1)-(4.4) showing that entanglement, quantum steering, and quantum discord all behave in the same way. As can be seen, quantum steering is bounded by quantum entanglement. We have $S^{A\to B} = S^{B\to A} > 0$ and logarithmic negativity $E_N > 0$ is the witness of two-way steering, while for $S^{A\to B} = S^{B\to A} = 0$ and $E_N > 0$, the two mechanical oscillators are not steerable (no-way steering). Thus, the quantum discord is more robust than entanglement as shown in figure (4.1)-(4.4), because when $0 \leq D_A \leq 1 : 0 \leq D_B \leq 1$ (the two mechanical oscillators are separable (if $E_N = 0$) or entangled (if $E_N > 0$). On the other hand, when $D_A > 1 : D_B > 1$ (i.e. the two mechanical oscillators must be entangled) and we have $E_N > 0$. Moreover, we can also see from figures (4.1)-(4.4), that the quantum discord is more dominant than the entanglement and is also a good quantifier of the quantum correlation. The presence of the OPA and strong Coulomb coupling enhances the quantum correlations between the two mechanical oscillators, and Coulomb interactions are more prominent in the electro-optomechanical system.

4.2 Measuring mechanical entanglement

In this section, we examine the enhancement of the steady-state entanglement of mechanical modes in the hybrid electro-optomechanical system via a coherent feedback loop. For simplicity, we assume that the parameters for both mechanical oscillators are identical as depicted in Table (4.1).

In Fig.(4.5), density plots of bipartite entanglement between the two mechanical modes as a function of the nonlinear gain of the OPA G_a and normalized detuning Δ/ω_m. Figure (4.5)

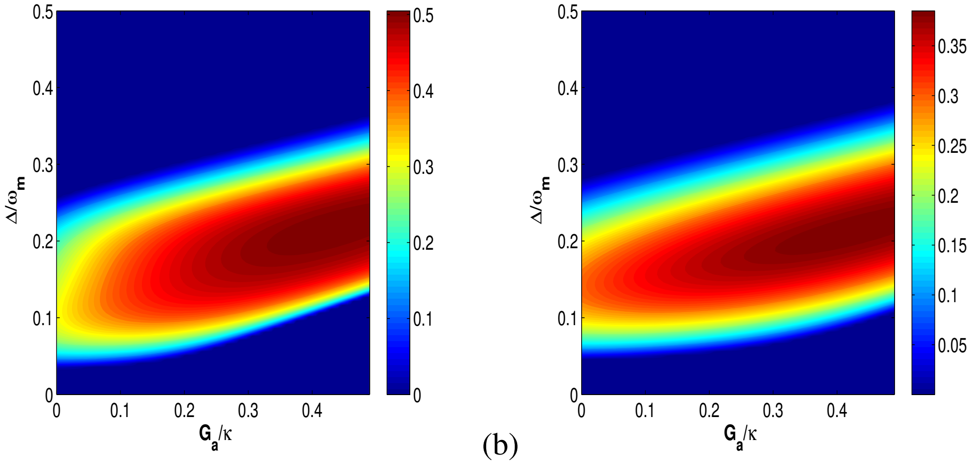

Figure 4.5: Density plot of the logarithmic negativity E_N between the two mechanical modes as a function of the nonlinear gain of the OPA G_a and normalized detuning Δ/ω_m, (a) the presence of coherent feedback ($r = 0.3$) and (b) absence of the coherent feedback ($r = 0$). The remaining parameters are listed in Table (4.1).

(a) presents a numerical analysis demonstrating the impact of the nonlinear gain of the OPA and the presence of a coherent feedback loop on the entanglement between the two mechanical oscillators. In Fig.(4.5) (a), the bipartite entanglement between the two mechanical modes strengthens as the gain of OPA G_a increases. Our findings align with those reported by (Pan et al., 2023). As shown in Fig. (4.5) (a) the bipartite entanglement between the two mechanical modes improved when coherent feedback effects are present. The presence of coherent feedback effects allows for the reinjection of photons into the cavity, which allows the enhancement of the entanglement generation. Our results agree with those of (Amazioug et al., 2020b). In this aspect, the combination of the nonlinear gain of the OPA and coherent feedback effects results in a large increase in bipartite entanglement between the mechanical modes. Therefore, the existence of the coherent feedback effect improves the entanglement compared to systems without the coherent feedback effect (Bai et al., 2017). Moreover, in Fig. (4.5) (b) we plot the bipartite entanglement versus normalized detuning Δ/ω_m and the nonlinear gain of the OPA in the absence of a coherent feedback loop. Fig. (4.5) (b) reveals that increasing the nonlinear gain G_a of the OPA yields enhanced levels of entanglement between the mechanical modes. This phenomenon arises due to the amplification of photon numbers within the cavity as a result of a higher nonlinear gain, consequently resulting in a more pronounced radiation pressure exerted on a mechanical oscillator.

Next, we proceed to examine the impact of the Coulomb coupling strength η and the environment temperature on the quantum entanglement. Fig. (4.6) (a) shows that the entanglement of

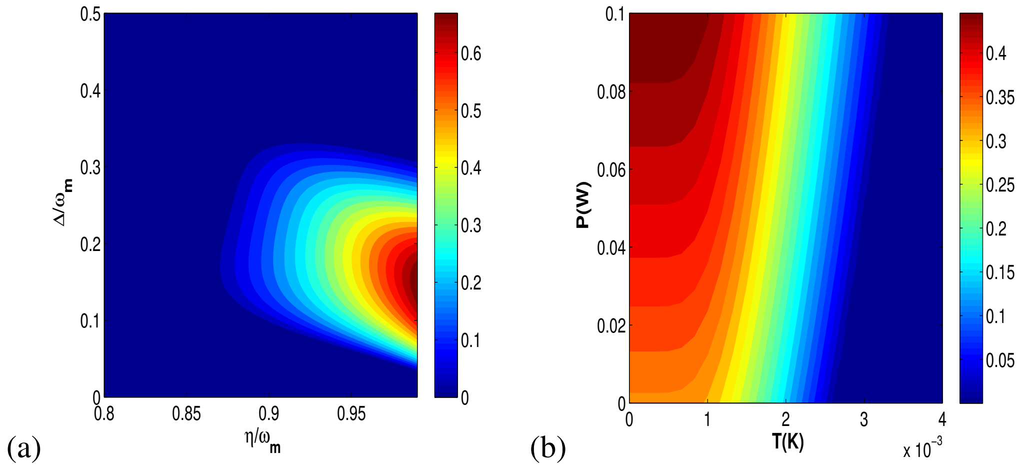

Figure 4.6: Density plot of the logarithmic negativity E_N between the two mechanical modes. (a) The plot of logarithmic negativity E_N versus Coulomb coupling strength η and normalized detuning Δ/ω_m, with fixed values of $G_a = 0.26\kappa$. (b) The plot logarithmic negativity E_N as the power and the environment temperature T, with $\Delta = 0.5\omega_m$, and $G_a = 0.26\kappa$. The remaining parameters are listed in Table 4.1.

spatially distant mechanical oscillators significantly enhances the existence of intense Coulomb coupling. The oscillators are entangled, indicating that there is a state transfer of the two charged mechanical oscillators, despite being spatially separated. Employing realistic parameters allows one to attain a substantial degree of quantum entanglement. Additionally, the absence of Coulomb coupling strength renders the entanglement of two separate oscillators impossible. It is worth noting that the Coulomb coupling strength is the crucial parameter for achieving state transfer between the two mechanical modes. Our results agree with (Pan et al., 2023). Fig. (4.6) (b) indicates that increasing the power of the drive laser enhances bipartite entanglement between the two mechanical modes, which may be attributed to the fact that increased power of the drive laser leads to stronger coupling between the mechanical modes. It is also obviously noted that the reservoir temperature induces decoherence in such an entanglement, and hence we observed the decay of the macroscopic entanglement as the temperature increases. Thermal noise in the surroundings provides random fluctuations that can disturb the entanglement between mechanical modes. Based on these findings, it has been observed that as the environmental temperature increases, a distinct shift occurs from the quantum realm to the classical regime. Therefore, our results are consistent with those reported in (Bai et al., 2017).

Finally, we investigate the influence of the phase of the optical parametric amplifier and the reflectivity coefficient on the entanglement between the two spatially separated mechanical oscillators. In Fig. (4.7) (a), we plot the steady-state entanglement versus the phase of the optical

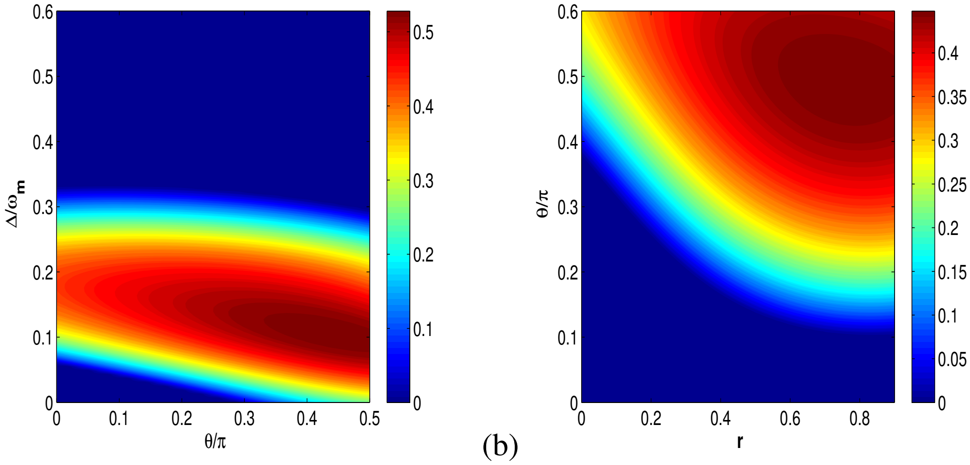

(a) (b)

Figure 4.7: Density plot of the logarithmic negativity E_N between the two mechanical modes. (a) The logarithmic negativity E_N versus the phase of the optical field driving the OPA and the normalized detuning Δ/ω_m, with fixed values of $G_a = 0.26\kappa$. (b) Plots of the logarithmic negativity E_N versus the phase of the optical field that drives the OPA and the presence of coherent feedback r, with $G_a = 0.26\kappa$ and $\Delta = 0.3\omega_m$. The remaining parameters are listed in Table 4.1.

field driving the OPA and the normalized detuning Δ/ω_m. As illustrated in Figure (4.7) (a), it is evident that the degree of entanglement between the two mechanical modes intensifies as the phase increases. Our results are consistent with those previously reported in (Bai et al., 2017). Fig.(4.7) (b), we plot the bipartite entanglement of the mechanical modes versus the reflectivity coefficient and the phase. Furthermore, Fig. (4.7) (b) illustrates that the degree of entanglement of mechanical modes improves as the phase of the OPA and the reflectivity coefficient increase. Furthermore, it should be noted that the coherent feedback effect facilitates the reinjection of photons into the cavity, thus enhancing the generation of entanglement (Mekonnen et al., 2024). The results show that the hybrid model, coupled through Coulomb interaction, exhibits a stronger degree of mechanical entanglement under the influence of the phase of the optical parametric amplifier and Coulomb coupling interaction. This indicates that a larger phase of the amplifier parameter leads to stronger mechanical entanglement. Furthermore, it can be seen that the presence of both the phase of the optical parametric amplifier and coherent feedback enhances the macroscopic entanglement between the two mechanical modes, compared to the scheme without the coherent feedback effect (Bai et al., 2017; Mekonnen et al., 2023). However, reducing the effective decay rate can enhance entanglement by preserving coherence and allowing for longer-lasting quantum correlations within the system. Our results align with those reported by (Amazioug et al., 2020b). Therefore, choosing the appropriate phase of OPA and incorporating a coherent feedback effect improve bipartite entanglement between the two mechanical modes.

4.3 Quantifying Gaussian quantum coherence

Following the theoretical investigation of the model considered, in this section, we address numerical results of the quantum coherence of systems of one mode, two modes, and a total mode. To assess the degree of quantum coherence, we use an analytical formula single mode, two-mode and total modes.To simplify the analysis, we take the parameters of each oscillator to be the same as shown in Table (4.2).

Table 4.2: The experimental parameters for the plots in Fig.(4.8-4.15) were taken from the values reported in Refs.(Schliesser et al., 2008; Gigan et al., 2006; Gröblacher et al., 2009) under standard conditions.

No	**Parameters**	**Values**
1	Mechanical frequency ($\omega_{m1} = \omega_{m2} = \omega_m$)	$200\pi\ MHz$
2	Mechanical damping rates ($\gamma_1 = \gamma_2 = \gamma_m$)	$20\pi\ Hz$
3	Cavity damping rates (κ)	88.1 MHz
4	Masses of the mechanical oscillators ($m_1 = m_2 = m$)	5 ng
5	Cavity length (L)	1 mm
6	Wavelength of driving laser (λ)	810 nm
7	Phase of the optical field (θ)	0
8	Temperature (T)	4 mK
9	Laser power (P)	50 mW
10	Coulomb coupling strength (η)	$0.95\omega_m$
11	Reflective coefficient (r)	0.3
12	Effective cavity detuning (Δ)	$0.2\omega_m$
13	Atomic decay rate (γ_a)	$0.5\omega_m$
14	Atomic coupling (λ_a)	$0.4\omega_m$
15	Atomic detuning (Δ_a)	$-\omega_m$

Fig. 4.8 reveals the impact of the non-linear gain of an OPA on quantum coherence employing different modes. As shown in Figs. 4.8(a)-(d), we observe that the single-mode quantum coherence of mechanical oscillators, C_{m1}: C_{m2}, the cavity mode, C_o, the atom mode, C_a, and the total coherence C_T improve with increasing nonlinear gain of the OPA. The nonlinear gain of the OPA effectively enhances the interaction strength within the system, which leads to stronger quantum coherence among the different modes. This enhancement occurs because the OPA introduces additional squeezed light into the system, which reduces noise and improves the coherence properties. It is evident that the quantum coherence of mechanical oscillators C_{m1}: C_{m2}, cavity mode C_o, atom mode C_a, and total coherence C_T decreases as the rate of atomic

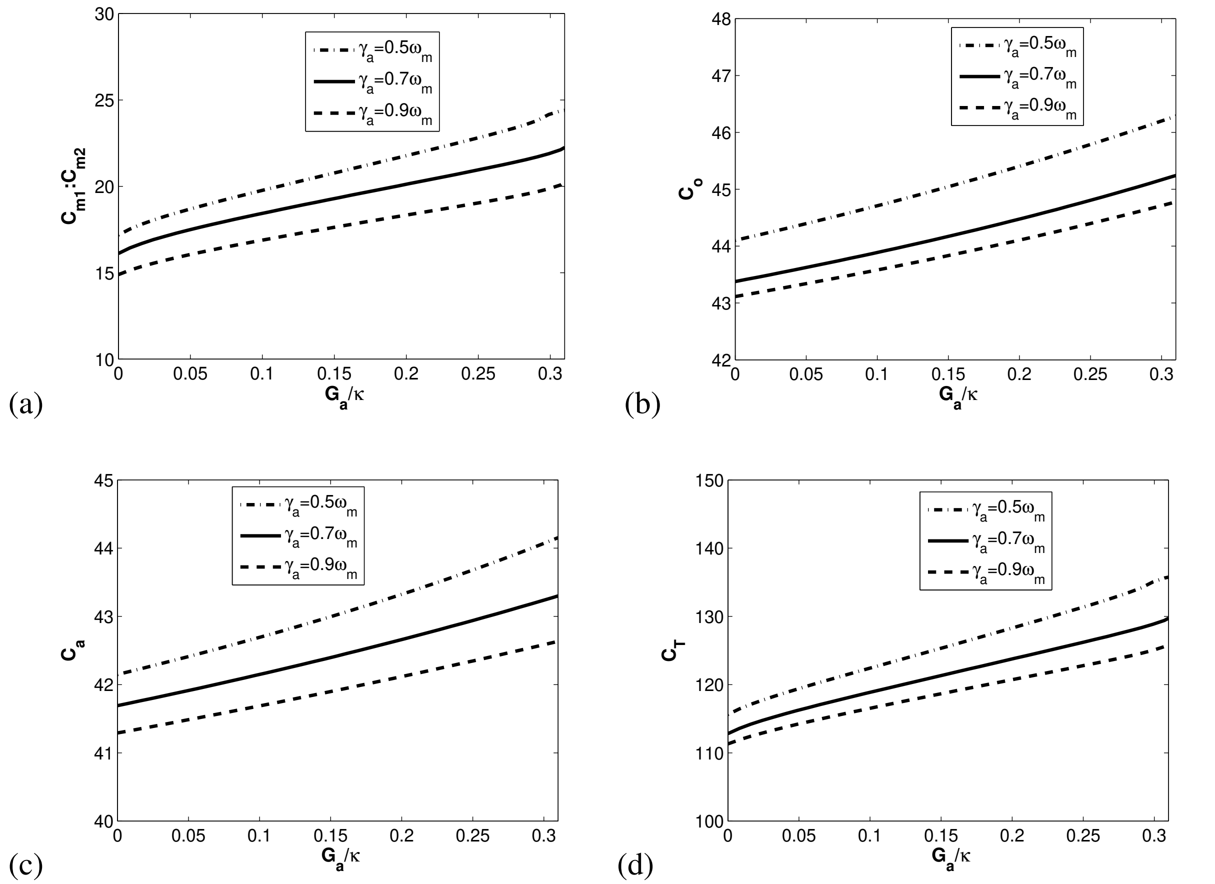

Figure 4.8: Plots of the quantum coherence (a) mechanical oscillators $C_{m1} : C_{m2}$, (b) cavity mode C_o, (c) the atom mode C_a and (d) the total coherence C_T as a function of the nonlinear gain of the OPA G_a for different values of the atomic decay rate γ_a. The remaining parameters are listed in Table 4.2.

decay increases. The rise in the rate of atomic decay increases the interactions between the atom and field, resulting in more frequent quantum state disruptions. These processes cause the atom to lose quantum information to the environment, thereby reducing the overall coherence of the system. Our results are consistent with those reported in (Singh et al., 2021). Furthermore, Fig. 4.8 shows that we attain the highest quantum coherence values when the nonlinear gain of the OPA is high and the atomic decay rate is low. This optimal scenario minimizes decoherence effects and maximizes the beneficial impact of the nonlinear gain of the OPA, allowing the system to maintain high levels of quantum coherence. The presence of a high non-linear gain OPA counteracts the decoherence introduced by atomic decay, maintaining stronger coherence among the system's components.

Next, we examine the effects of the reflective coefficient (r) and the nonlinear gain of the

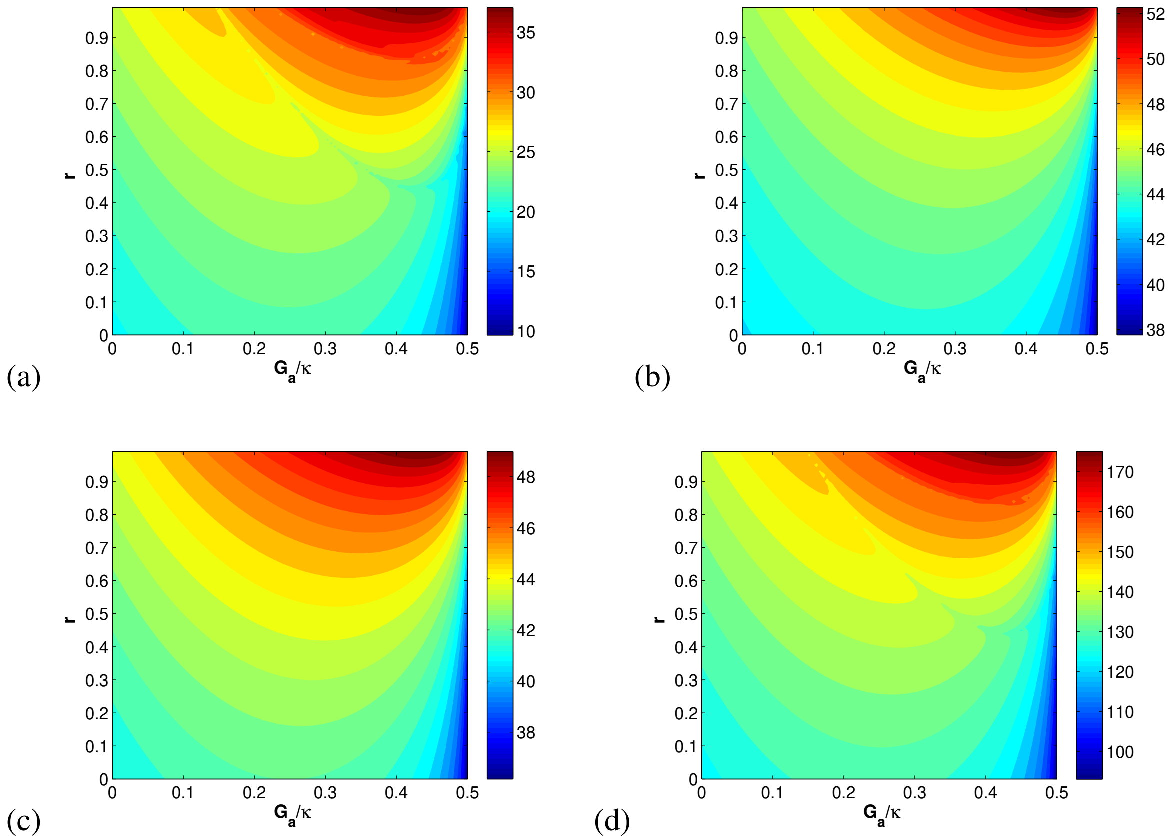

Figure 4.9: Density plots of the quantum coherence (a) mechanical oscillators $C_{m1} : C_{m2}$, (b) cavity mode C_o, (c) atom mode C_a, and (d) total coherence C_T as a function of the nonlinear gain of the OPA G_a and the reflective coefficient (r). The remaining parameters are listed in Table. 4.2.

OPA G_a on quantum coherence, such as mechanical oscillators $C_{m1} : C_{m2}$, cavity mode C_o, atom mode C_a, and total coherence C_T. Figure. (4.9) (a)-(d) demonstrates that boosting the nonlinear gain of the OPA and the reflectivity coefficient boosts the quantum coherence. When the nonlinear gain grows, the number of photons in the cavity increases, resulting in a higher level of quantum coherence inside the system. Furthermore, higher reflectivity coefficients r promote quantum coherence and allow more sustained quantum correlations in the system. When r approaches 1, the entire output field is reflected back into the system, effectively closing the feedback loop. This implies that almost no light (very minimal) is lost to the environment and the decay rate of the cavity mode is minimized. Besides, as r approaches 1, there is a corresponding decrease in effective decay rates (κ_{eff}), which leads to an enhancement of quantum coherence. The reduced dissipation and minimal interaction with the environment help preserve coherence. As a result, the existence of nonlinear gain OPA, and coherent feedback effect increases quantum coherence when compared to their absence.

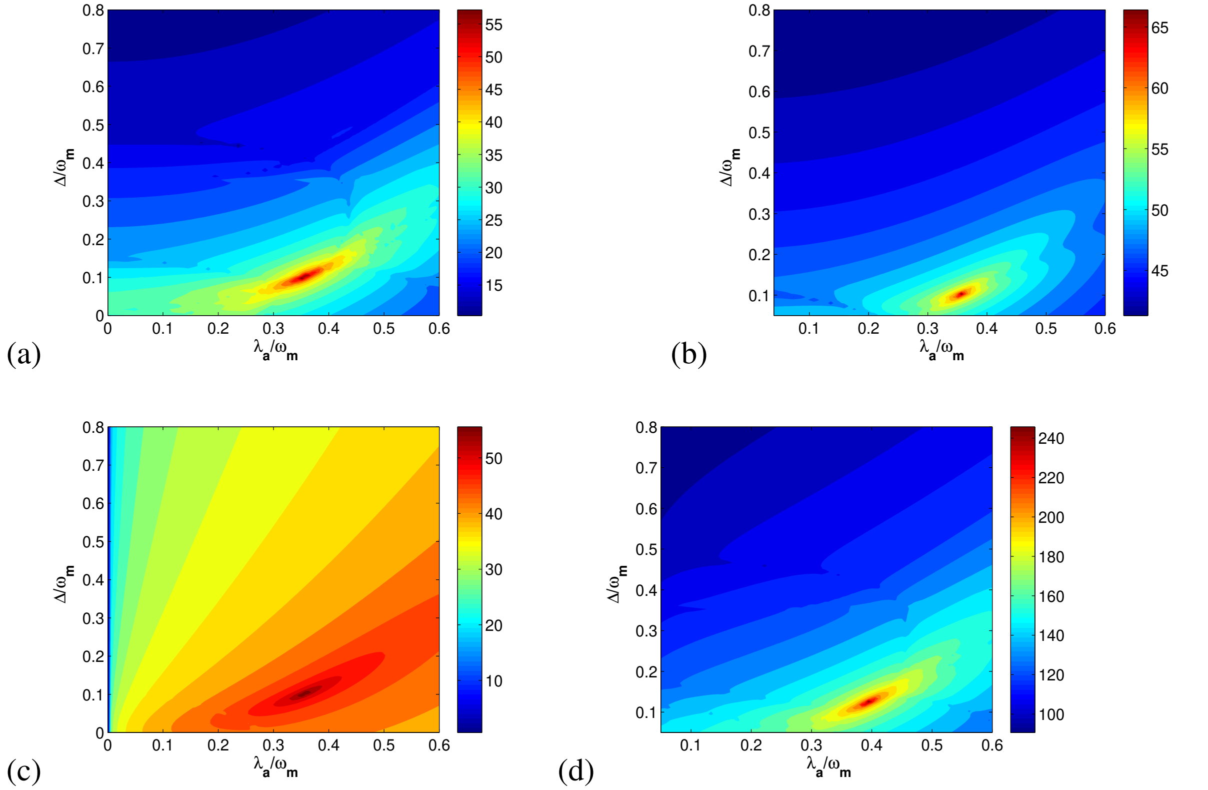

Figure 4.10: Density plots of the quantum coherence (a) mechanical oscillators $C_{m1} : C_{m2}$, (b) the cavity mode C_o, (c) the atom C_a and (d) the total coherence C_T as a function of the atomic coupling λ_a and normalized detuning Δ/ω_m. The remaining parameters are listed in Table 4.2.

Next, we examine the crucial role of atomic coupling (λ_a) in quantum coherence. Figs. (4.10) (a)-(d) show that the quantum coherence for different modes improves as the atomic coupling λ_a increases to certain values, but decreases after reaching a threshold value of λ_a. We found that optimal values of quantum coherence occur within the range of atomic coupling $\lambda_a = 0.3\omega_m - 0.4\omega_m$. This is so because at these values the coupling strength effectively balances the enhancement of coherent interactions between the atomic ensemble and the optical field while minimizing decoherence effects. In this range, the interactions are strong enough to sustain stable superpositions and promote entangled states without overwhelming the system with excessive noise or instability. Furthermore, quantum coherence is strengthened when the normalized detuning Δ/ω_m increases to specific values, but then drops. We also see that smaller values of normalized detuning Δ/ω_m result in the highest quantum coherence values. Furthermore, atomic coupling enhances quantum coherence compared to the lack of atomic coupling. Atomic coupling allows for the interchange of quantum information between the atom and other modes, promoting correlation and coherence.

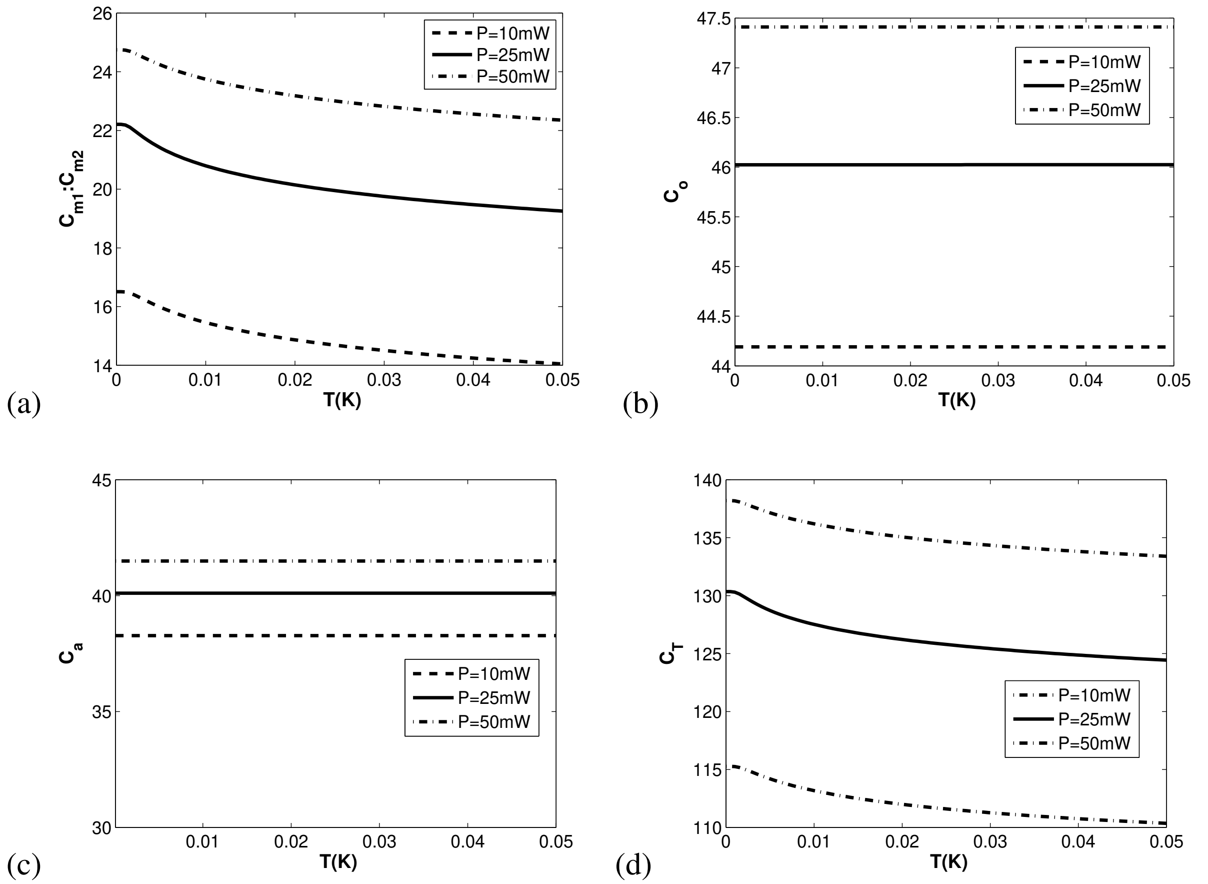

Figure 4.11: Plots of the quantum coherence (a) mechanical oscillators C_{m1} : C_{m2},(b) the cavity mode C_o, (c) the atom C_a, and (d) the total coherence C_T as a function of the temperature for different of values drive laser power. The remaining parameters are listed in Table 4.2.

To investigate the effect of temperature on single-mode quantum coherence in the system, we plot in Fig. (4.11), the quantum coherence of (a) mechanical oscillators C_{m1}: C_{m2}, (b) cavity mode C_o, (c) atom mode C_a, and (d) total coherence C_T versus temperature for different values of driving laser power. The results show that when laser power increases, the quantum coherence of a single mode and overall coherence strengthen. Increased laser power strengthens the system's interaction, resulting in improved coherence across all modes. Figs. (4.11)(a) and (d) show that the quantum coherence C_{m1}: C_{m2}, and C_T decrease with increasing ambient temperature. Mechanical oscillators are very sensitive to variations in ambient temperature, which cause decoherence effects. This sensitivity originates from the fact that higher temperatures increase phonon interactions inside mechanical oscillators, resulting in increased thermal noise and a loss of coherence. In contrast, Figs. (4.11)(b) and (c) show that C_o and C_a remain relatively constant when the ambient temperature increases. Temperature variations have less of a direct impact on these modes, resulting in greater stability. The cavity mode, which primarily involves photons, and the atom mode, which involves internal atomic states, are more separated from thermal phonons, resulting in less direct thermal disruption as compared to mechanical oscillators. Our results are consistent with those reported in (Zhai and Guo, 2022).

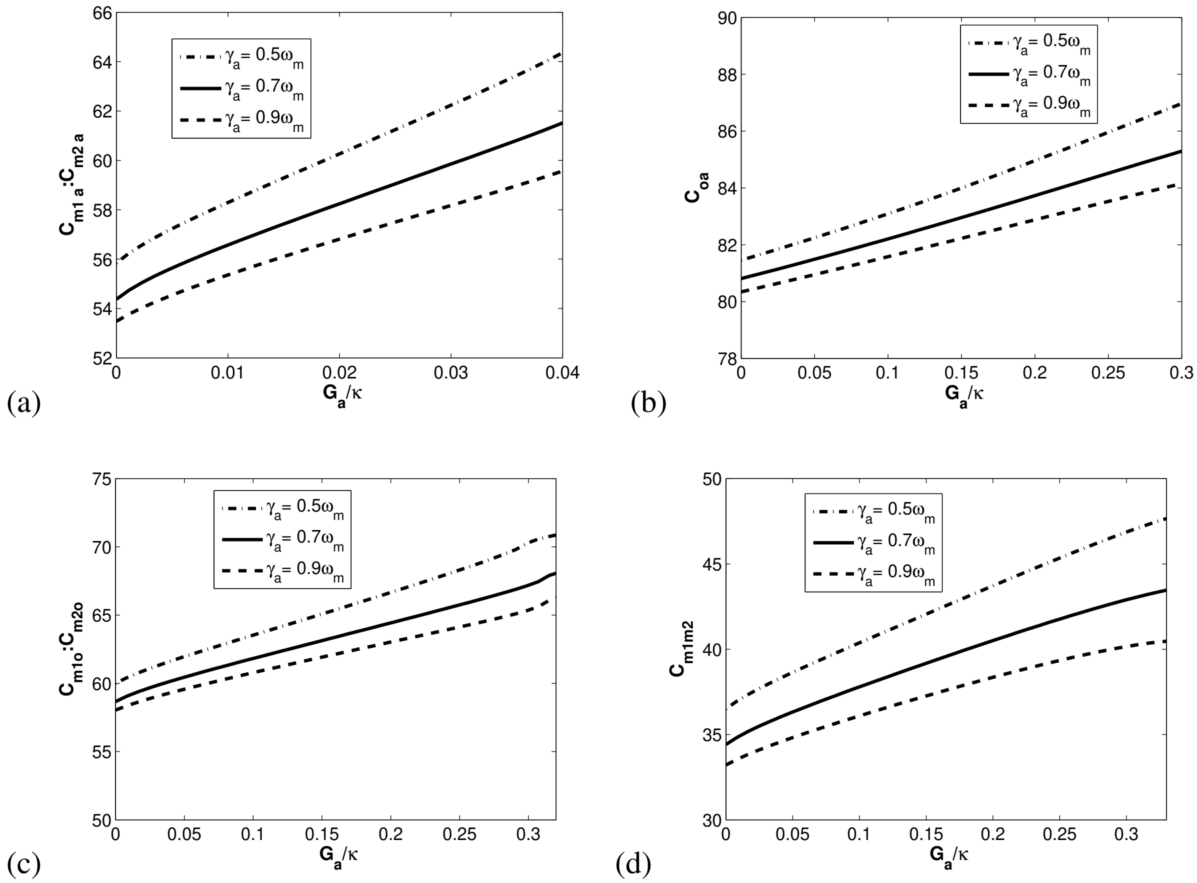

Figure 4.12: Plots of the bipartite quantum coherence between (a) the mechanical and atom mode $C_{m1a} : C_{m2a}$, (b) the cavity and atom mode C_{oa}, (c) the mechanical and cavity mode $C_{m1o} : C_{m2o}$, and the mechanical and mechanical mode C_{m1m2} as a function of the nonlinear gain of the OPA G_a for different values of the atomic decay rate. The remaining parameters are listed in Table 4.2.

Next, our analysis focuses on examining the results of bipartite quantum coherence between the mechanical and atom modes (C_{m1a}, C_{m2a}), the cavity and atom modes (C_{oa}), the mechanical and cavity modes (C_{m1o}: C_{m2o}), and the mechanical and mechanical modes (C_{m1m2}). For this, we present in Fig.(4.12) the four bipartite quantum coherences as a function of the nonlinear gain of the OPA (G_a) for different values of the atomic decay rate. As can be seen in Fig.(4.12), improving the values of the nonlinear gain of the OPA (G_a) boosts bipartite quantum coherence. The nonlinear gain enhances the amplification of quantum information in the system. This amplification process maintains and enhances coherence between subsystems, resulting in greater bipartite quantum coherence. Specifically, the OPA introduces additional squeezed light, which improves correlations and minimizes noise, boosting coherence between distinct pairings of modes. Furthermore, when the rate of atomic decay increases, bipartite quantum coherence diminishes. Our findings agree with (Singh et al., 2021). These results correspond exactly with those shown in Fig. (4.12) for the single mode.

In Fig. (4.13), we plot the four bipartite quantum coherence as a function of the normalized detuning (Δ/ω_m) for different values of the atomic ensemble coupling strength (λ_a). As shown in Fig.(4.13) the bipartite quantum coherence between the subsystems monotonically decreases as Δ/ω_m increases. We also noticed that increasing the coupling strength of the atomic ensemble λ_a enhances the quantum coherence between subsystems. In particular, we obtain better results in bipartite quantum coherence between the cavity and atom modes compared to the others. As the atomic ensemble coupling strength increases, the atoms exhibit stronger correlations and collective behavior. This collective mode of operation enables the atoms to share and exchange coherence more efficiently with the cavity mode.

Following, we examine how the non-linear gain of the OPA and the reflective coefficient impact bipartite quantum coherence. For this, we plot the four bipartite quantum coherence as a function of the nonlinear gain of the OPA and reflective coefficient values. Figs. (4.14) (a)-(d) show that increasing the nonlinear gain values of the OPA and the reflective coefficient improves the bipartite quantum coherence. Increasing values of the nonlinear gain of the OPA G_a raises the number of photons in the optical cavity, leading to better quantum coherence. Furthermore, higher reflective coefficients result in stronger quantum coherence, which increases total quantum coherence in the system. Reducing the effective decay rate (κ_{eff}) improves quantum coherence and allows for longer quantum correlations in the system. We can observe that $C_{oa} > C_{m1o}, C_{m2o} > C_{m1a}$, $C_{m2a} > C_{m1m2}$. As a result, the presence of nonlinear gain OPA and coherent feedback effects improves the bipartite quantum coherence between the two subsystems.

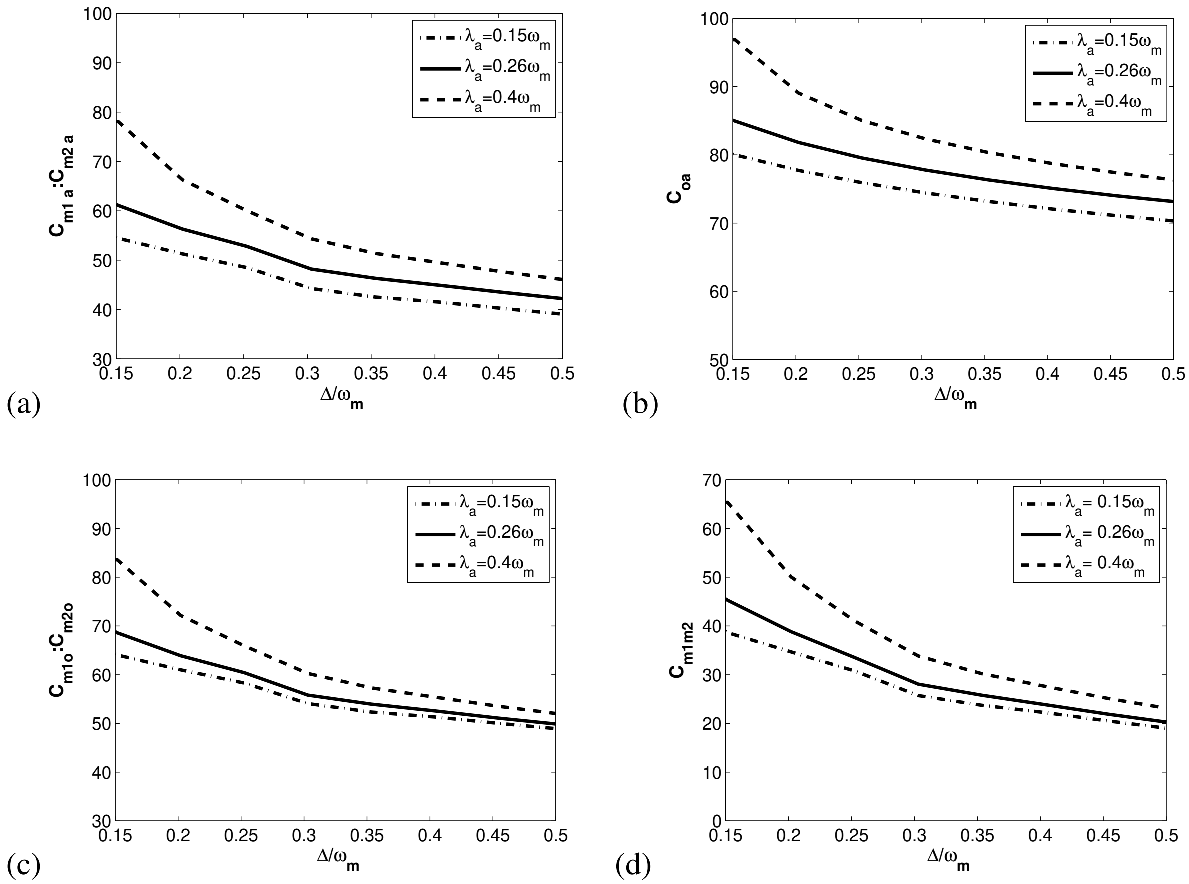

Figure 4.13: Plots of bipartite quantum coherence between (a) the mechanical and atom mode $C_{m1a} : C_{m2a}$, (b) the cavity and atom mode C_{oa}, (c) the mechanical and cavity mode $C_{m1o} : C_{m2o}$, and the mechanical and mechanical mode C_{m1m2} as a function of the normalized detuning Δ/ω_m for different values of the atomic ensemble coupling strength λ_a. The remaining parameters are listed in Table 4.2.

In Fig. (4.15), we present plots of bipartite quantum coherence between (a) the mechanical and atom modes $C_{m1a} : C_{m2a}$, (b) the cavity and atom modes C_{oa}, (c) the mechanical and cavity modes $C_{m1o} : C_{m2o}$, and the mechanical and mechanical modes C_{m1m2} versus the temperature for various laser power values. Figs. (4.15) (a-d) shows that quantum coherence improves with increasing driving power. Our results are in line with (Singh et al., 2021). Furthermore, as illustrated in Figs. (4.15) (a), (c), and (d), the bipartite quantum coherence decreases as the ambient temperature increases, due to the greater impact of thermal noise on mechanical oscillators. Fig. (4.15)(b) depicts that temperature fluctuations do not affect bipartite quantum coherence between the cavity and atom modes. The cavity and atom modes do not interact directly with the environmental temperature. Our findings are in line with (Zhai and Guo, 2022).

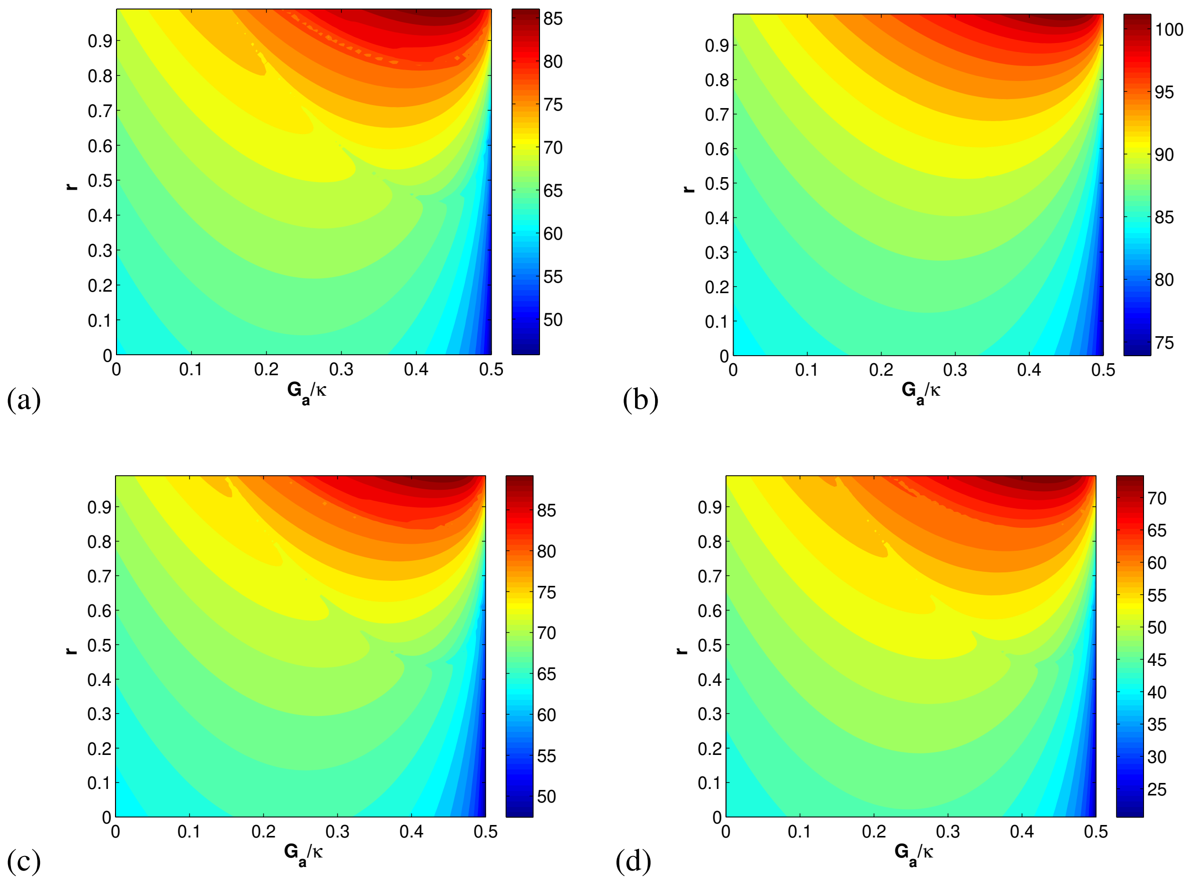

Figure 4.14: Plots of the bipartite quantum coherence between (a) the mechanical and atom mode $C_{m1a} : C_{m2a}$, (b) the cavity and atom mode C_{oa}, (c) the mechanical and cavity mode $C_{m1o} : C_{m2o}$, and (d) the mechanical and mechanical mode C_{m1m2} as a function of the nonlinear gain of the OPA G_a for different values of the reflective coefficient (r). The remaining parameters are listed in Table 4.2.

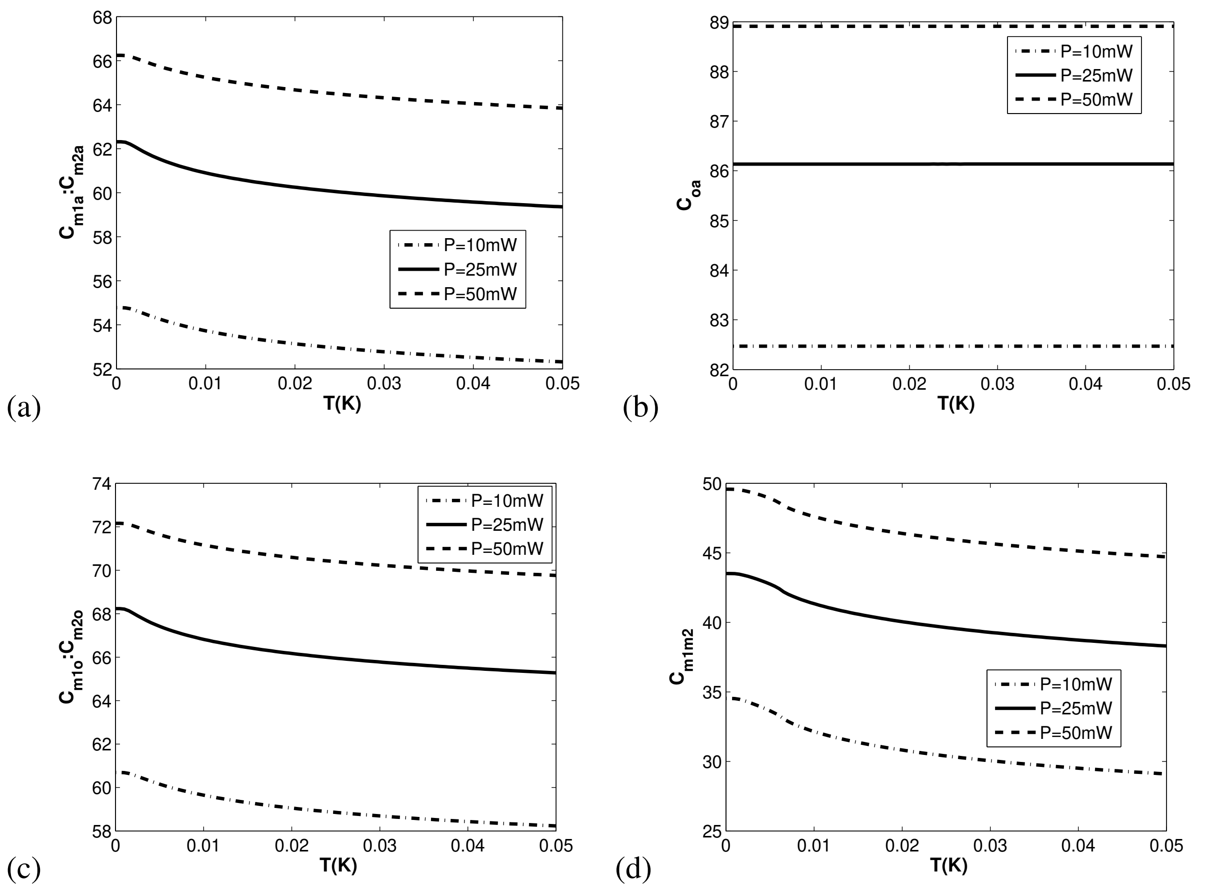

Figure 4.15: Plots of the bipartite quantum coherence between (a) the mechanical and atom mode $C_{m1a} : C_{m2a}$, (b) the cavity and atom mode C_{oa}, (c) the mechanical and cavity mode $C_{m1o} : C_{m2o}$, and (d) the mechanical and mechanical mode C_{m1m2} versus the temperature for various values laser power, with $G_a = 0.45\kappa$. The remaining parameters are listed in Table 4.2.

5

CONCLUSIONS AND RECOMMENDATIONS

5.1 Conclusions

In this dissertation, we have investigated the quantum features in an electro-optomechanical system, which includes an optical parametric amplifier, coherent feedback, and an ensemble of two-level atoms. In this research, we have studied three cases. In the first part of this work, we investigated quantum correlation in an electro-optomechanical system enhanced by an optical parametric amplifier and Coulomb-type interaction. We used logarithmic negativity, quantum discord, and steerability to measure the quantum correlation between mechanical oscillators. Our result shows that the presence of OPA, strong Coulomb coupling, and an appropriate phase choice of the optical field driving the OPA enhance the quantum correlations between mechanical oscillators. However, quantum correlations such as entanglement, steering,and quantum discord decrease rapidly with increasing temperature as a result of decoherence. The results show that as the temperature increases, the quantum entanglement decays to zero, a phenomenon known as the sudden death of quantum entanglement. Although the two-way steerable state disappears at higher environmental temperatures, quantum discord remains persistent, even as quantum entanglement vanishes. In the second part of this work, we have studied the entanglement between mechanical modes. We analyze the bipartite entanglement between the two mechanical modes using logarithmic negativity. Our findings show that the existence of the OPA increases the bipartite entanglement between the two mechanical modes. In addition, the presence of strong Coulomb coupling and coherent feedback mechanisms significantly boost the entanglement between the two mechanical modes. Moreover, reducing the effective decay rate can enhance entanglement by preserving coherence and allowing for longer-lasting quantum correlations within the system. We also found that choosing the proper phase for the optical field driving the OPA enhances the degree of entanglement. Furthermore, the bipartite entanglement between mechanical modes increases with drive laser power and decreases with environmental temperature increases because of thermal noise causing decoherence. Finally, we have explored the enhancement of quantum coherence in a hybrid electro-optomechanical system. By solving numerical Lyapunov equations and analyzing steady-state mean values, we quantified the Gaussian quantum coherence of the proposed system. The findings show that quantum coherence is enhanced by the nonlinear gain of the OPA and the coherent feedback effect, which increases photon numbers in the cavity. Higher reflective coefficients or lower effective decay rates further maximize quantum coherence. Additionally, strong driving laser intensity and the presence of two-level atoms also contribute to improved quantum coherence, while higher atomic decay rates can lead to a reduction in quantum coherence. Some quantum coherence modes decreased with increasing temperature, though the cavity and atomic modes remain temperature insensitive. Overall, our scheme improves the quantum coherence and robustness to environmental temperature variations, providing a strong foundation for continuous-variable quantum information processing.

5.2 Recommendations

The main finding of this research is the enhancement of quantum features within a hybrid electro-optomechanical system. Future investigations could broaden the scope of optomechanics to encompass a wider range of parameters and quantum resources. I recommended that future research be expanded to explore quantum effects such as fidelity, quantum monogamy, bistability of mechanical modes, ground state cooling, mechanical squeezing, and transparency phenomena through theoretical approaches. Furthermore, to enhance quantum communication, sensing, and metrology, researchers can integrate nonlinear devices like Kerr mediums, cascade three-level lasers, and squeezed vacuum reservoirs into the electro-optomechanical system.

Appendix

A Derivation of quantum Langevin equations

We employ quantum Langevin equations to examine the dynamics of a system, which includes all the damping and noise effects. The quantum Langevin equation is developed by phenomenologically including the noise and dissipation processes into the Heisenberg operator equation. Employing Eq.(2.33), the nonlinear quantum Langevin equations for the system can be written as follows:

$$\dot{\hat{q}}_1 = -i[\hat{q}_1, \hat{H}], \tag{A.1}$$

$$\dot{\hat{p}}_1 = -i[\hat{p}_1, \hat{H}] - \gamma_1 \hat{p}_1 + \xi_1(t), \tag{A.2}$$

$$\dot{\hat{q}}_2 = -i[\hat{q}_2, \hat{H}], \tag{A.3}$$

$$\dot{\hat{p}}_2 = -i[\hat{p}_2, \hat{H}] - \gamma_2 \hat{p}_2 + \xi_2(t), \tag{A.4}$$

$$\dot{\hat{c}} = -i[\hat{c}, \hat{H}] - \kappa \hat{c} + \sqrt{2\kappa}\hat{c}_{in}, \tag{A.5}$$

and

$$\dot{\hat{a}} = -i[\hat{a}, \hat{H}] - \gamma_a \hat{a} + \sqrt{2\gamma_a}\hat{a}_{in}, \tag{A.6}$$

The commutation relation of the following operators can be written in the following form.

$$[\hat{p}_i, \hat{a}] = [\hat{q}_i, \hat{a}] = [\hat{p}_i, \hat{p}_i] = [\hat{q}_i, \hat{q}_i] = [\hat{a}, \hat{a}] = [\hat{c}, \hat{c}] = [\hat{p}_i, \hat{c}] = [\hat{q}_i, \hat{c}] = 0. \tag{A.7}$$

$$[\hat{p}_i, \hat{q}_j^2] = -2i\hbar \hat{q}_j \delta_{ij}. \tag{A.8}$$

$$[\hat{q}_i, \hat{p}_j^2] = 2i\hbar \hat{p}_j \delta_{ij}. \tag{A.9}$$

$$[\hat{q}_i, \hat{p}_j] = i\hbar \delta_{ij}. \tag{A.10}$$

and

$$[\hat{c}, \hat{c}^\dagger] = 1. \tag{A.11}$$

B Derivation of a steady state solution and quantum Langevin equation for the fluctuations

In the semi-classical approach, a quantum operator is linearized by expressing it as the sum of the average value and quantum fluctuation which is defined as Eq.(2.36). To achieve a steady-state solution, we set the fluctuations to mean-zero values and apply the derivatives to zero. In this context, the steady-state solution of the equation can be written as

$$\dot{q_j} = \omega_j p_j^s = 0, j = 1, 2. \tag{B.1}$$

from Eq.(B.1), we easily obtain the steady-state solution as follows:

$$p_1^s = p_2^s = 0. \tag{B.2}$$

Next we seek to determine the values of q_1^s and q_2^s using Eq.(2.36), we have

$$\dot{p_1} = -\omega_1 q_1^s - \eta q_2^s + g|c^s|^2 = 0, \tag{B.3}$$

and

$$\dot{p_2} = -\omega_2 q_2^s - \eta q_1^s = 0. \tag{B.4}$$

Finally, Eq.B.3 and Eq.B.4 solved simultaneously, we obtain easily

$$q_1^s = \frac{-\omega_2 g|c^s|^2}{\eta^2 - \omega_1\omega_2}, \tag{B.5}$$

$$q_2^s = \frac{g|c^s|^2\eta}{\eta^2 - \omega_1\omega_2}. \tag{B.6}$$

Following the same manner, one can easily verify that

$$c_s = \frac{\kappa - i\Delta + 2G_a e^{i\theta}}{\kappa^2 + \Delta^2 - 4G_a^2}\Omega, \tag{B.7}$$

where $\Delta = \Delta_o - gq_1^s$ is the effective cavity detuning.

Following the same method, one can straightforwardly verify that in the steady state of the atomic operator

$$a^s = \frac{-i\lambda_a c^s}{\gamma_a + i\Delta_a}, \tag{B.8}$$

On account of Eqs.(B.5-B.7), the linear quantum Langevin equations for the fluctuations can be written as

$$\delta\dot{\hat{q}}_1 = \omega_1 \delta\hat{p}_1, \tag{B.9}$$

$$\delta\dot{\hat{p}}_1 = -\omega_1 \delta\hat{q}_1 - \gamma_1 \delta\hat{p}_1 - \eta\delta\hat{q}_2 + gc^s(\delta\hat{c} + \delta\hat{c}^\dagger) + \xi_1(t), \tag{B.10}$$

$$\delta\dot{\hat{q}}_2 = \omega_2 \delta\hat{p}_2, \tag{B.11}$$

$$\delta\dot{\hat{p}}_2 = -\omega_2 \delta\hat{q}_2 - \gamma_2 \delta\hat{p}_2 - \eta\delta\hat{q}_1 + \xi_2(t), \tag{B.12}$$

$$\delta\dot{\hat{c}} = -(\kappa + i\Delta)\delta\hat{c} + igc^s\delta\hat{q}_1 + 2G_a\delta\hat{c}^\dagger e^{i\theta} + \sqrt{2\kappa}\delta\hat{c}_{in}, \tag{B.13}$$

and

$$\delta\dot{\hat{c}}^\dagger = -(\kappa - i\Delta)\delta\hat{c}^\dagger - igc^s\delta\hat{q}_1 + 2G_a\delta\hat{c}e^{-i\theta} + \sqrt{2\kappa}\delta\hat{c}_{in}^\dagger. \tag{B.14}$$

List of Publications

1. Mekonnen, H. D., Tesfahannes, T. G., Darge, T. Y., and Kumela, A. G. (2023). Quantum correlation in a nanoelectro-optomechanical system enhanced by an optical parametric amplifier and coulomb-type interaction. Scientific Reports, 13(1):13800.

2. Mekonnen, H. D., Tesfahannes, T. G., Darge, T. Y., and Eshete, S. (2024). Boosting macroscopic entanglement in a charged-cavity optomechanical system through coherent feedback loop. Journal of Optics, pages 1–9.

3. Mekonnen, H. D., Tesfahannes, T. G., Darge, T. Y., Kumela, A. G., Hidki, A., and Tadess, M. (2024). Enhancing Quantum Coherence in Hybrid Optomechanical Systems with Coherent Feedback, Atomic Ensembles, and Optical Parametric Amplifier. Journal of Physica Scripta.

List of Publications as Co-Author

1. Kumela, A. G., Gemta, A. B., Hordofa, A.K., Desta, T.A., Mulubirhan, D., Mekonnen, H.D. (2023). Optoplasmonic biosensor for lung cancer telediagnosis: Design and simulation analysis. Sensors International, Elsevier.

2. Kibret, A. A., Beisie, E. A., Mekonnen, H.D., Darge, T.Y., Tesfahannes, T.G. (2024). Generation of quantum correlations through optical parametric amplification in a hybrid optomechanical system. European Physical Journal Plus, 139(8)705.

3. Tesfahannes, T. G., Abie, B. G., Mekonnen, H. D., Mazaheri,M. (2024). Transfer of quantum correlations through strong coupling in a three-mode optomechanical system. Journal of Optics, pages 1–11.

4. Kumela, A.G., Gemta, A.B., Hordofa, A.K., Desta, T.A., Dangish, M., Mekonnen, H. D.(2023).The quantum features of correlated photons with the effect of phase fluctuation. Ukrainian journal of physics, 68(2) 81.

5. Kumela, A.G., Gemta, A.B., Hordofa, A.K., Birhanu, R., Mekonnen, H. D., Sherefedin, U., Woldegiorges, K.(2023). Review of hybridization of plasmonic and photonic crystal biosensors for effective cancer cell diagnosis. Nanoscale Advances, Royal Society of Chemistry.

6. Kumela, A.G., Gemta, A.B., Hordofa, A.K., Birhanu, R., Mekonnen, H. D., Sherefedin, U., Tadesse, M.(2023). Quantum machine learning-assisted lung cancer telemedicine. AIP Advances, 13(7).

List of Conference Participation

I have been participating national conferences.

1. The 18th National Conference of the Ethiopian Physical Society was held at Addis Ababa University in February 2024.

Award and special Recognition

1. Ethiopian Physical Society in North America (EPSNA) 2024G.C award regards recognition of the highest scholastic achievement and service to the community.

Bibliography

Abebe, T., Gemechu, N., Shogile, K., Hailemariam, S., Gashu, C., and Adisu, S. (2020). Entanglement quantification using various inseparability criteria for correlated photons. *Romanian Journal of Physics*, 65(3-4):107.

Adesso, G., Bromley, T. R., and Cianciaruso, M. (2016). Measures and applications of quantum correlations. *Journal of Physics A: Mathematical and Theoretical*, 49(47):473001.

Adesso, G. and Datta, A. (2010). Quantum versus classical correlations in gaussian states. *Physical Review Letters*, 105(3):030501.

Adesso, G., Serafini, A., and Illuminati, F. (2006). Multipartite entanglement in three-mode gaussian states of continuous-variable systems: Quantification, sharing structure, and decoherence. *Physical Review A—Atomic, Molecular, and Optical Physics*, 73(3):032345.

Agarwal, G. and Huang, S. (2016). Strong mechanical squeezing and its detection. *Physical Review A*, 93(4):043844.

Al-Qasimi, A. and James, D. F. (2008). Sudden death of entanglement at finite temperature. *Physical Review A*, 77(1):012117.

Amazioug, M., Daoud, M., Singh, S., and Asjad, M. (2022). Strong photon antibunching effect in a double cavity optomechanical system with squeezed driving. *arXiv preprint arXiv:2209.07401*.

Amazioug, M., Maroufi, B., and Daoud, M. (2020a). Creating mirror–mirror quantum correlations in optomechanics. *The European Physical Journal D*, 74:1–9.

Amazioug, M., Maroufi, B., and Daoud, M. (2020b). Using coherent feedback loop for high quantum state transfer in optomechanics. *Physics Letters A*, 384(27):126705.

Amazioug, M., Nassik, M., and Habiballah, N. (2018a). Entanglement, epr steering and gaussian geometric discord in a double cavity optomechanical systems. *The European Physical Journal D*, 72:1–9.

Amazioug, M., Nassik, M., and Habiballah, N. (2018b). Measure of general quantum correlations in optomechanics. *International Journal of Quantum Information*, 16(05):1850043.

Amazioug, M., Teklu, B., and Asjad, M. (2023). Enhancement of magnon–photon–phonon entanglement in a cavity magnomechanics with coherent feedback loop. *Scientific Reports*, 13(1):3833.

Aolita, L., De Melo, F., and Davidovich, L. (2015). Open-system dynamics of entanglement: a key issues review. *Reports on Progress in Physics*, 78(4):042001.

Aoune, D. and Habiballah, N. (2022). Quantifying of quantum correlations in an optomechanical system with cross-kerr interaction. *Journal of Russian Laser Research*, 43(4):406–415.

Arcizet, O., Cohadon, P.-F., Briant, T., Pinard, M., and Heidmann, A. (2006). Radiation-pressure cooling and optomechanical instability of a micromirror. *Nature*, 444(7115):71–74.

Ari, A. B. (2021). *Nanomechanical Resonators at Extreme Dissipation: Measurement of the Brownian Force in a Highly Viscous Liquid and Optomechanical Resonators for Quantum-Limited Transduction*. PhD thesis, Boston University.

Asjad, M., Tombesi, P., and Vitali, D. (2016). Feedback control of two-mode output entanglement and steering in cavity optomechanics. *Physical Review A*, 94(5):052312.

Aspelmeyer, M., Gröblacher, S., Hammerer, K., and Kiesel, N. (2010). Quantum optomechanics—throwing a glance. *JOSA B*, 27(6):A189–A197.

Aspelmeyer, M., Kippenberg, T. J., and Marquardt, F. (2014). Cavity optomechanics. *Reviews of Modern Physics*, 86(4):1391.

Baek, K., Sohbi, A., Lee, J., Kim, J., and Nha, H. (2020). Quantifying coherence of quantum measurements. *New Journal of Physics*, 22(9):093019.

Bai, C.-H., Wang, D.-Y., Wang, H.-F., Zhu, A.-D., and Zhang, S. (2017). Classical-to-quantum transition behavior between two oscillators separated in space under the action of optomechanical interaction. *Scientific Reports*, 7(1):1–12.

Bai, C.-H., Wang, D.-Y., Zhang, S., Liu, S., and Wang, H.-F. (2021). Generation of strong mechanical–mechanical entanglement by pump modulation. *Advanced Quantum Technologies*, 4(5):2000149.

Barzanjeh, S., Xuereb, A., Gröblacher, S., Paternostro, M., Regal, C. A., and Weig, E. M. (2022). Optomechanics for quantum technologies. *Nature Physics*, 18(1):15–24.

Baumgratz, T., Cramer, M., and Plenio, M. B. (2014). Quantifying coherence. *Physical review letters*, 113(14):140401.

Bennett, C. H., Brassard, G., Crépeau, C., Jozsa, R., Peres, A., and Wootters, W. K. (1993). Teleporting an unknown quantum state via dual classical and einstein-podolsky-rosen channels. *Physical review letters*, 70(13):1895.

Bennett, C. H., Grudka, A., Horodecki, M., Horodecki, P., and Horodecki, R. (2011). Postulates for measures of genuine multipartite correlations. *Physical Review A Atomic, Molecular, and Optical Physics*, 83(1):012312.

Beth, R. A. (1936). Mechanical detection and measurement of the angular momentum of light. *Physical Review*, 50(2):115.

Bougouffa, S., Al-Hmoud, M., and Hakami, J. W. (2022). Probing quantum correlations in a hybrid optomechanical system. *International Journal of Theoretical Physics*, 61(7):190.

Braginskiĭ, V., Manukin, A. B., and Tikhonov, M. Y. (1970). Investigation of dissipative ponderomotive effects of electromagnetic radiation. *Soviet Journal of Experimental and Theoretical Physics*, 31:829.

Braginsky, V. (1967). Zhetf 52, 986 (1967); vb braginsky, ab manukin. *Sov. Phys. JETP*, 26:653.

Braginsky, V., Manukin, A., and Hamilton, W. O. (1978). Measurement of weak forces in physics experiments.

Braginsky, V. and Vyatchanin, S. (2002). Low quantum noise tranquilizer for fabry–perot interferometer. *Physics Letters A*, 293(5-6):228–234.

Braginsky, V. B., Caves, C. M., and Thorne, K. S. (1977). Laboratory experiments to test relativistic gravity. *Physical Review D*, 15(8):2047.

Breuer, H.-P. and Petruccione, F. (2002). *The theory of open quantum systems*. Oxford University Press, USA.

Briegel, H.-J., Dür, W., Cirac, J. I., and Zoller, P. (1998). Quantum repeaters: the role of imperfect local operations in quantum communication. *Physical Review Letters*, 81(26):5932.

Brunner, N., Cavalcanti, D., Pironio, S., Scarani, V., and Wehner, S. (2014). Publisher's note: Bell nonlocality [rev. mod. phys. 86, 419 (2014)]. *Reviews of Modern Physics*, 86(2):839–840.

Burgwal, R., del Pino, J., and Verhagen, E. (2020). Comparing nonlinear optomechanical coupling in membrane-in-the-middle and single-cavity systems. *New Journal of Physics*, 22(11):113006.

Çakir, Ö., Klyachko, A. A., and Shumovsky, A. S. (2005). Steady-state entanglement of two atoms created by classical driving field. *Physical Review A*, 71(3):034303.

Cavalcanti, D. and Skrzypczyk, P. (2016). Quantum steering: a review with focus on semidefinite programming. *Reports on Progress in Physics*, 80(2):024001.

Caves, C. M. (1980). Quantum-mechanical radiation-pressure fluctuations in an interferometer. *Physical Review Letters*, 45(2):75.

Chan, J., Alegre, T. M., Safavi-Naeini, A. H., Hill, J. T., Krause, A., Gröblacher, S., Aspelmeyer, M., and Painter, O. (2011). Laser cooling of a nanomechanical oscillator into its quantum ground state. *Nature*, 478(7367):89–92.

Chen, R.-X., Shen, L.-T., and Zheng, S.-B. (2015). Dissipation-induced optomechanical entanglement with the assistance of coulomb interaction. *Physical Review A*, 91(2):022326.

Cimini, V., Gianani, I., Sbroscia, M., Sperling, J., and Barbieri, M. (2019). Measuring coherence of quantum measurements. *Physical Review Research*, 1(3):033020.

Cohadon, P.-F., Heidmann, A., and Pinard, M. (1999). Cooling of a mirror by radiation pressure. *Physical Review Letters*, 83(16):3174.

Cohen, C. and Tannoudji, J. (1992). Dupont-roc, g. grynberg, atom-photoninteractions.

Collini, E., Wong, C. Y., Wilk, K. E., Curmi, P. M., Brumer, P., and Scholes, G. D. (2010). Coherently wired light-harvesting in photosynthetic marine algae at ambient temperature. *Nature*, 463(7281):644–647.

Cory, D. G. and Havel, T. F. (2004). Ion entanglement in quantum information processing. *Science*, 304(5676):1456–1457.

Daley, A. J. (2014). Quantum trajectories and open many-body quantum systems. *Advances in Physics*, 63(2):77–149.

Dantan, A., Genes, C., Vitali, D., and Pinard, M. (2008). Self-cooling of a movable mirror to the ground state using radiation pressure. *Physical Review A—Atomic, Molecular, and Optical Physics*, 77(1):011804.

De Chiara, G. and Sanpera, A. (2018). Genuine quantum correlations in quantum many-body systems: a review of recent progress. *Reports on Progress in Physics*, 81(7):074002.

De Vega, I. and Alonso, D. (2017). Dynamics of non-markovian open quantum systems. *Reviews of Modern Physics*, 89(1):015001.

DeJesus, E. X. and Kaufman, C. (1987). Routh-hurwitz criterion in the examination of eigenvalues of a system of nonlinear ordinary differential equations. *Physical Review A*, 35(12):5288.

Demkowicz-Dobrzański, R. and Maccone, L. (2014). Using entanglement against noise in quantum metrology. *Physical review letters*, 113(25):250801.

DiVincenzo, D. P. (2000). The physical implementation of quantum computation. *Fortschritte der Physik: Progress of Physics*, 48(9-11):771–783.

Duan, L.-M., Giedke, G., Cirac, J. I., and Zoller, P. (2000). Inseparability criterion for continuous variable systems. *Physical review letters*, 84(12):2722.

Eckstein, A., Christ, A., Mosley, P. J., and Silberhorn, C. (2011). Highly efficient single-pass source of pulsed single-mode twin beams of light. *Physical Review Letters*, 106(1):013603.

Einstein, A. (1909). On the development of our understanding of the nature and composition of radiation. *Physikalische Zeitschrift*, 10(22):817–826.

Einstein, A., Podolsky, B., and Rosen, N. (1935). Einsteinpodolskyrosen. *Phys. Rev.*, 47:777.

Eshete, S. (2022). Quantum correlations in optomechanical system in the presence of optical feedback. *Physics Open*, 11:100100.

Fedorov, M., Efremov, M., Kazakov, A., Chan, K., Law, C., and Eberly, J. (2005). Spontaneous emission of a photon: Wave-packet structures and atom-photon entanglement. *Physical Review A*, 72(3):032110.

Frisch, R. (1933). Experimental demonstration of einstein's radiation recoil. *Zeitschrift für Phys*, 86:42–45.

Galve, F., Giorgi, G. L., and Zambrini, R. (2011). Maximally discordant mixed states of two qubits. *Physical Review A*, 83(1):012102.

Ge, W., Al-Amri, M., Nha, H., and Zubairy, M. S. (2013). Entanglement of movable mirrors in a correlated emission laser via cascade-driven coherence. *Physical Review A*, 88(5):052301.

Gebremariam, T., Zeng, Y., and Li, C. (2017). Dynamics of quantum correlations for two mode entangled coherent fields. *Results in physics*, 7:3773–3777.

Genes, C., Mari, A., Tombesi, P., and Vitali, D. (2008a). Robust entanglement of a micromechanical resonator with output optical fields. *Physical Review A*, 78(3):032316.

Genes, C., Vitali, D., and Tombesi, P. (2008b). Emergence of atom-light-mirror entanglement inside an optical cavity. *Physical Review A*, 77(5):050307.

Gerry, C. C. and Knight, P. L. (2023). *Introductory quantum optics*. Cambridge university press.

Ghobadi, R., Kumar, S., Pepper, B., Bouwmeester, D., Lvovsky, A., and Simon, C. (2014). Optomechanical micro-macro entanglement. *Physical Review Letters*, 112(8):080503.

Gigan, S., Böhm, H., Paternostro, M., Blaser, F., Langer, G., Hertzberg, J., Schwab, K. C., Bäuerle, D., Aspelmeyer, M., and Zeilinger, A. (2006). Self-cooling of a micromirror by radiation pressure. *Nature*, 444(7115):67–70.

Giorda, P. and Paris, M. G. (2010). Gaussian quantum discord. *Physical Review Letters*, 105(2):020503.

Giovannetti, V., Lloyd, S., and Maccone, L. (2011). Advances in quantum metrology. nat. photon. 5, 222 (2011).

Giovannetti, V., Mancini, S., and Tombesi, P. (2001). Radiation pressure induced einstein-podolsky-rosen paradox. *Europhysics Letters*, 54(5):559.

Girolami, D. (2014). Observable measure of quantum coherence in finite dimensional systems. *Physical review letters*, 113(17):170401.

Gisin, N., Ribordy, G., Tittel, W., and Zbinden, H. (2002). Quantum cryptography. *Reviews of modern physics*, 74(1):145.

Gough, J. E. and Wildfeuer, S. (2009). Enhancement of field squeezing using coherent feedback. *Physical Review A Atomic, Molecular, and Optical Physics*, 80(4):042107.

Gröblacher, S., Hammerer, K., Vanner, M. R., and Aspelmeyer, M. (2009). Observation of strong coupling between a micromechanical resonator and an optical cavity field. *Nature*, 460(7256):724–727.

Händchen, V., Eberle, T., Steinlechner, S., Samblowski, A., Franz, T., Werner, R. F., and Schnabel, R. (2012). Observation of one-way einstein–podolsky–rosen steering. *Nature Photonics*, 6(9):596–599.

Hansryd, J., Andrekson, P. A., Westlund, M., Li, J., and Hedekvist, P.-O. (2002). Fiber-based optical parametric amplifiers and their applications. *IEEE Journal of Selected Topics in Quantum Electronics*, 8(3):506–520.

Harwood, A., Brunelli, M., and Serafini, A. (2021). Cavity optomechanics assisted by optical coherent feedback. *Physical Review A*, 103(2):023509.

He, Q., Badshah, F., Song, Y., Wang, L., Liang, E., and Su, S.-L. (2022). Force sensing and cooling for the mechanical membrane in a hybrid optomechanical system. *Physical Review A*, 105(1):013503.

He, W.-p. and Li, F.-l. (2007). Generation of broadband entangled light through cascading nondegenerate optical parametric amplifiers. *Physical Review A*, 76(1):012328.

Head-Marsden, K., Flick, J., Ciccarino, C. J., and Narang, P. (2020). Quantum information and algorithms for correlated quantum matter. *Chemical Reviews*, 121(5):3061–3120.

Henderson, L. and Vedral, V. (2001). Classical, quantum and total correlations. *Journal of physics A: mathematical and general*, 34(35):6899.

Hilico, L., Courty, J., Fabre, C., Giacobino, E., Abram, I., and Oudar, J. (1992). Squeezing with χ (3) materials. *Applied Physics B*, 55:202–209.

Hirose, M. and Cappellaro, P. (2016). Coherent feedback control of a single qubit in diamond. *Nature*, 532(7597):77–80.

Hirvensalo, M. (2013). *Quantum computing*. Springer Science & Business Media.

Holstein, T. and Primakoff, H. (1940). Field dependence of the intrinsic domain magnetization of a ferromagnet. *Physical Review*, 58(12):1098.

Horodecki, R., Horodecki, P., Horodecki, M., and Horodecki, K. (2009). Quantum entanglement. *Reviews of Modern Physics*, 81(2):865.

Hou, J.-X., Liu, S.-Y., Wang, X.-H., and Yang, W.-L. (2017). Role of coherence during classical and quantum decoherence. *Physical Review A*, 96(4):042324.

Hu, C.-S., Yang, Z.-B., Wu, H., Li, Y., and Zheng, S.-B. (2018). Twofold mechanical squeezing in a cavity optomechanical system. *Physical Review A*, 98(2):023807.

Huang, S. and Agarwal, G. (2009). Enhancement of cavity cooling of a micromechanical mirror using parametric interactions. *Physical Review A*, 79(1):013821.

Huang, S. and Chen, A. (2018). Improving the cooling of a mechanical oscillator in a dissipative optomechanical system with an optical parametric amplifier. *Physical Review A*, 98(6):063818.

Huang, S. and Chen, A. (2019). Cooling of a mechanical oscillator and normal mode splitting in optomechanical systems with coherent feedback. *Applied Sciences*, 9(16):3402.

Jacobs, K., Tombesi, P., Collett, M., and Walls, D. (1994). Quantum-nondemolition measurement of photon number using radiation pressure. *Physical Review A*, 49(3):1961.

Jacobs, K., Wang, X., and Wiseman, H. M. (2014). Coherent feedback that beats all measurement-based feedback protocols. *New Journal of Physics*, 16(7):073036.

Jennewein, T., Simon, C., Weihs, G., Weinfurter, H., and Zeilinger, A. (2000). Quantum cryptography with entangled photons. *Physical review letters*, 84(20):4729.

Jin, L., Peng, J.-X., Yuan, Q.-Z., and Feng, X.-L. (2021). Macroscopic quantum coherence in a spinning optomechanical system. *Optics Express*, 29(25):41191–41205.

Jones, S. J., Wiseman, H. M., and Doherty, A. C. (2007). Entanglement, einstein-podolsky-rosen correlations, bell nonlocality, and steering. *Physical Review A*, 76(5):052116.

Joshi, C., Larson, J., Jonson, M., Andersson, E., and Öhberg, P. (2012). Entanglement of distant optomechanical systems. *Physical Review A*, 85(3):033805.

Karuza, M., Biancofiore, C., Bawaj, M., Molinelli, C., Galassi, M., Natali, R., Tombesi, P., Di Giuseppe, G., and Vitali, D. (2013). Optomechanically induced transparency in a membrane-in-the-middle setup at room temperature. *Physical Review A*, 88(1):013804.

Kassahun, F. (2014). Refined quantum analysis of light. *Create Space Independent Publishing Platform*.

Kepler, J. (1963). De cometis libelli tres.

Kerckhoff, J., Andrews, R. W., Ku, H., Kindel, W. F., Cicak, K., Simmonds, R. W., and Lehnert, K. (2013). Tunable coupling to a mechanical oscillator circuit using a coherent feedback network. *Physical Review X*, 3(2):021013.

Kerckhoff, J., Nurdin, H. I., Pavlichin, D. S., and Mabuchi, H. (2010). Designing quantum memories with embedded control: photonic circuits for autonomous quantum error correction. *Physical Review Letters*, 105(4):040502.

Kippenberg, T., Rokhsari, H., Carmon, T., Scherer, A., and Vahala, K. (2005). Analysis of radiation-pressure induced mechanical oscillation of an optical microcavity. *Physical Review Letters*, 95(3):033901.

Kippenberg, T. J. and Vahala, K. J. (2007). Cavity opto-mechanics. *Optics express*, 15(25):17172–17205.

Kippenberg, T. J. and Vahala, K. J. (2008). Cavity optomechanics: back-action at the mesoscale. *science*, 321(5893):1172–1176.

Kogias, I. and Adesso, G. (2015). Einstein–podolsky–rosen steering measure for two-mode continuous variable states. *JOSA B*, 32(4):A27–A33.

Kogias, I., Lee, A. R., Ragy, S., and Adesso, G. (2015). Quantification of gaussian quantum steering. *Physical Review Letters*, 114(6):060403.

Krenn, M., Malik, M., Scheidl, T., Ursin, R., and Zeilinger, A. (2016). Quantum communication with photons. *Optics in our Time*, 18:455.

Kundu, A., Jin, C., and Peng, J.-X. (2021). Study of the optical response and coherence of a quadratically coupled optomechanical system. *Physica Scripta*, 96(6):065102.

Law, Y. Z., Bancal, J.-D., Scarani, V., et al. (2014). Quantum randomness extraction for various levels of characterization of the devices. *Journal of Physics A: Mathematical and Theoretical*, 47(42):424028.

Lebedev, P. (1901). Investigations into the pressure forces of light. *Annals of Physics*, 311(11):433–458.

Leggett, A. J., Chakravarty, S., Dorsey, A. T., Fisher, M. P., Garg, A., and Zwerger, W. (1987). Dynamics of the dissipative two-state system. *Reviews of Modern Physics*, 59(1):1.

Li, G., Nie, W., Li, X., Li, M., Chen, A., and Lan, Y. (2019). Quantum coherence transfer between an optical cavity and mechanical resonators. *Science China Physics, Mechanics & Astronomy*, 62:1–12.

Li, J., Li, G., Zippilli, S., Vitali, D., and Zhang, T. (2017). Enhanced entanglement of two different mechanical resonators via coherent feedback. *Physical Review A*, 95(4):043819.

Li, W.-A. and Huang, G.-Y. (2019). Enhancement of optomechanically induced sum sidebands using parametric interactions. *Physical Review A*, 100(2):023838.

Li, Y., Wang, Y., Sun, H., Liu, K., and Gao, J. (2023). Normal-mode splitting in an optomechanical system enhanced by an optical parametric amplifier and coherent feedback. *Journal of Optics*, 25(7):075201.

Liao, J.-Q. and Tian, L. (2016). Macroscopic quantum superposition in cavity optomechanics. *Physical review letters*, 116(16):163602.

Liu, C., Dutton, Z., Behroozi, C. H., and Hau, L. V. (2001). Observation of coherent optical information storage in an atomic medium using halted light pulses. *Nature*, 409(6819):490–493.

Liu, N., Chang, R., Zhang, S., and Liang, J. Q. (2022). Ground-state cooling of the mechanical resonator in an optomechanical cavity with two-level atomic ensemble. *International Journal of Theoretical Physics*, 61(4):120.

Lloyd, S. (2000). Coherent quantum feedback. *Physical Review A*, 62(2):022108.

Lostaglio, M., Jennings, D., and Rudolph, T. (2015). Description of quantum coherence in thermodynamic processes requires constraints beyond free energy. *Nature communications*, 6(1):6383.

Lü, L., Wei, Q., and Jia, H. (2022). Entanglement response in modulation optomechanical system controlled by the feedback optical field. *International Journal of Theoretical Physics*, 61(5):152.

Ma, J., Yadin, B., Girolami, D., Vedral, V., and Gu, M. (2016). Converting coherence to quantum correlations. *Physical review letters*, 116(16):160407.

Ma, P.-C., Zhang, J.-Q., Xiao, Y., Feng, M., and Zhang, Z.-M. (2014). Tunable double optomechanically induced transparency in an optomechanical system. *Physical Review A*, 90(4):043825.

Ma, Y., Liu, W., Liu, X., Wang, N., and Zhang, H. (2024). Review of sensing and actuation technologies–from optical mems and nanophotonics to photonic nanosystems. *International Journal of Optomechatronics*, 18(1):2342279.

Ma, Y.-H. and Zhou, L. (2012). Enhanced entanglement between a movable mirror and a cavity field assisted by two-level atoms. *Journal of Applied Physics*, 111(10).

Mabuchi, H. (2008). Coherent-feedback quantum control with a dynamic compensator. *Physical Review A*, 78(3):032323.

Mancini, S. and Tombesi, P. (1994). Quantum noise reduction by radiation pressure. *Physical Review A*, 49(5):4055.

Mancini, S., Vitali, D., and Tombesi, P. (1998). Optomechanical cooling of a macroscopic oscillator by homodyne feedback. *Physical Review Letters*, 80(4):688.

Mandel, L. and Wolf, E. (1995). Effect of an attenuator or beam splitter on the quantum field. *Optical Coherence and Quantum Optics; Cambridge University Press: Cambridge, UK*, pages 639–640.

Mansouri, D., Rezaie, B., Ranjbar N, A., Daeichian, A., et al. (2022). Coherent feedback ground-state cooling for a mechanical resonator assisted by an atomic ensemble. *The European Physical Journal Plus*, 137(9):1–10.

Manzoni, C. and Cerullo, G. (2016). Design criteria for ultrafast optical parametric amplifiers. *Journal of Optics*, 18(10):103501.

Maquedano, L. and Costa, A. C. (2024). Analysis of quantum steering measures. *Entropy*, 26(3):257.

Marhic, M. E., Andrekson, P. A., Petropoulos, P., Radic, S., Peucheret, C., and Jazayerifar, M. (2015). Fiber optical parametric amplifiers in optical communication systems. *Laser & photonics reviews*, 9(1):50–74.

Marquardt, F. and Girvin, S. M. (2009). Optomechanics (a brief review). *arXiv preprint arXiv:0905.0566*.

Marshall, W., Simon, C., Penrose, R., and Bouwmeester, D. (2003). Towards quantum superpositions of a mirror. *Physical Review Letters*, 91(13):130401.

Mathew, J. P., Pino, J. d., and Verhagen, E. (2020). Synthetic gauge fields for phonon transport in a nano-optomechanical system. *Nature nanotechnology*, 15(3):198–202.

Mattle, K., Weinfurter, H., Kwiat, P. G., and Zeilinger, A. (1996). Dense coding in experimental quantum communication. *Physical review letters*, 76(25):4656.

Mekonnen, H. D., Tesfahannes, T. G., Darge, T. Y., and Eshete, S. (2024). Boosting macroscopic entanglement in charged cavity optomechanical system through coherent feedback loop. *Journal of Optics*, pages 1–9.

Mekonnen, H. D., Tesfahannes, T. G., Darge, T. Y., and Kumela, A. G. (2023). Quantum correlation in a nano-electro-optomechanical system enhanced by an optical parametric amplifier and coulomb-type interaction. *Scientific Reports*, 13(1):13800.

Meystre, P. (2013). A short walk through quantum optomechanics. *Annalen der Physik*, 525(3):215–233.

Midolo, L., Schliesser, A., and Fiore, A. (2018). Nano-opto-electro-mechanical systems. *Nature nanotechnology*, 13(1):11–18.

Morsch, O. and Oberthaler, M. (2006). Dynamics of bose-einstein condensates in optical lattices. *Reviews of modern physics*, 78(1):179.

Napoli, C., Bromley, T. R., Cianciaruso, M., Piani, M., Johnston, N., and Adesso, G. (2016). Robustness of coherence: an operational and observable measure of quantum coherence. *Physical review letters*, 116(15):150502.

Nelson, R. J., Weinstein, Y., Cory, D., and Lloyd, S. (2000). Experimental demonstration of fully coherent quantum feedback. *Physical Review Letters*, 85(14):3045.

Nichols, E. F. and Hull, G. F. (1901). A preliminary communication on the pressure of heat and light radiation. *Physical Review (Series I)*, 13(5):307.

Nielsen, M. A. and Chuang, I. L. (2001). Quantum computation and quantum information. *Phys. Today*, 54(2):60.

Nielsen, M. A. and Chuang, I. L. (2010). *Quantum computation and quantum information*. Cambridge university press.

O'brien, J. L., Furusawa, A., and Vučković, J. (2009). Photonic quantum technologies. *Nature Photonics*, 3(12):687–695.

Ollivier, H. and Zurek, W. H. (2001). Quantum discord: a measure of the quantumness of correlations. *Physical review letters*, 88(1):017901.

O'Connell, A. D., Hofheinz, M., Ansmann, M., Bialczak, R. C., Lenander, M., Lucero, E., Neeley, M., Sank, D., Wang, H., Weides, M., et al. (2010). Quantum ground state and single-phonon control of a mechanical resonator. *Nature*, 464(7289):697–703.

Pan, G., Xiao, R., and Zhai, C. (2022). Entanglement and output squeezing in a distant nano-electro-optomechanical system generated by optical parametric amplifiers. *Laser Physics Letters*, 19(5):055203.

Pan, G., Xiao, R., and Zhai, C. (2023). Enhanced entanglement and output squeezing in electro-optomechanical system with an optical parametric amplifier. *The European Physical Journal D*, 77(2):25.

Peano, V., Schwefel, H., Marquardt, C., and Marquardt, F. (2015). Intracavity squeezing can enhance quantum-limited optomechanical position detection through deamplification. *Physical Review Letters*, 115(24):243603.

Pellizzari, T., Gardiner, S. A., Cirac, J. I., and Zoller, P. (1995). Decoherence, continuous observation, and quantum computing: A cavity qed model. *Physical Review Letters*, 75(21):3788.

Piani, M. and Watrous, J. (2015). Necessary and sufficient quantum information characterization of einstein-podolsky-rosen steering. *Physical review letters*, 114(6):060404.

Pinard, M., Dantan, A., Vitali, D., Arcizet, O., Briant, T., and Heidmann, A. (2005). Entangling movable mirrors in a double-cavity system. *EuroPhysics Letters*, 72(5):747.

Poderini, D., Polino, E., Rodari, G., Suprano, A., Chaves, R., and Sciarrino, F. (2022). Ab initio experimental violation of bell inequalities. *Physical Review Research*, 4(1):013159.

Priyesh, K. and Ramesh, B. T. (2014). *Studies on the interaction of two level atoms with quantized electromagnetic field*. PhD thesis, Citeseer.

Reed, A., Mayer, K., Teufel, J., Burkhart, L., Pfaff, W., Reagor, M., Sletten, L., Ma, X., Schoelkopf, R., Knill, E., et al. (2017). Faithful conversion of propagating quantum information to mechanical motion. *Nature Physics*, 13(12):1163–1167.

Reid, M. (2013). Signifying quantum benchmarks for qubit teleportation and secure quantum communication using einstein-podolsky-rosen steering inequalities. *Physical Review A*, 88(6):062338.

Reid, M. D., Drummond, P., Bowen, W., Cavalcanti, E. G., Lam, P. K., Bachor, H., Andersen, U. L., and Leuchs, G. (2009). Colloquium: the einstein-podolsky-rosen paradox: from concepts to applications. *Reviews of Modern Physics*, 81(4):1727–1751.

Rohde, H., Gulde, S., Roos, C., Barton, P., Leibfried, D., Eschner, J., Schmidt-Kaler, F., and Blatt, R. (2001). Sympathetic ground-state cooling and coherent manipulation with two-ion crystals. *Journal of Optics B: Quantum and Semiclassical Optics*, 3(1):S34.

Sato, Y., Tanaka, Y., Upham, J., Takahashi, Y., Asano, T., and Noda, S. (2012). Strong coupling between distant photonic nanocavities and its dynamic control. *Nature Photonics*, 6(1):56–61.

Sazonova, V., Yaish, Y., Üstünel, H., Roundy, D., Arias, T. A., and McEuen, P. L. (2004). A tunable carbon nanotube electromechanical oscillator. *Nature*, 431(7006):284–287.

Schleich, W. P., Ranade, K. S., Anton, C., Arndt, M., Aspelmeyer, M., Bayer, M., Berg, G., Calarco, T., Fuchs, H., Giacobino, E., et al. (2016). Quantum technology: from research to application. *Applied Physics B*, 122:1–31.

Schliesser, A., Rivière, R., Anetsberger, G., Arcizet, O., and Kippenberg, T. J. (2008). Resolved-sideband cooling of a micromechanical oscillator. *Nature Physics*, 4(5):415–419.

Schmid, G. L., Ngai, C. T., Ernzer, M., Aguilera, M. B., Karg, T. M., and Treutlein, P. (2022). Coherent feedback cooling of a nanomechanical membrane with atomic spins. *Physical Review X*, 12(1):011020.

Schrödinger, E. (1935). Discussion of probability relations between separated systems. In *Mathematical Proceedings of the Cambridge Philosophical Society*, volume 31, pages 555–563. Cambridge University Press.

Scully, M. O. and Zubairy, M. S. (1997). *Quantum optics*. Cambridge university press.

Serafini, A. (2012). Feedback control in quantum optics: An overview of experimental breakthroughs and areas of application. *International Scholarly Research Notices*, 2012(1):275016.

Simon, R. (2000). Peres-horodecki separability criterion for continuous variable systems. *Physical Review Letters*, 84(12):2726.

Singh, S. and Ooi, C. R. (2014). Quantum correlations of quadratic optomechanical oscillator. *JOSA B*, 31(10):2390–2398.

Singh, S., Peng, J.-X., Asjad, M., and Mazaheri, M. (2021). Entanglement and coherence in a hybrid laguerre–gaussian rotating cavity optomechanical system with two-level atoms. *Journal of Physics B: Atomic, Molecular and Optical Physics*, 54(21):215502.

Slussarenko, S. and Pryde, G. J. (2019). Photonic quantum information processing: A concise review. *Applied Physics Reviews*, 6(4).

Sohail, A., Rana, M., Ikram, S., Munir, T., Hussain, T., Ahmed, R., and Yu, C.-s. (2020). Enhancement of mechanical entanglement in hybrid optomechanical system. *Quantum Information Processing*, 19:1–18.

Stute, A., Casabone, B., Schindler, P., Monz, T., Schmidt, P., Brandstätter, B., Northup, T., and Blatt, R. (2012). Tunable ion–photon entanglement in an optical cavity. *Nature*, 485(7399):482–485.

Teklu, B., Byrnes, T., and Khan, F. S. (2018). Cavity-induced mirror-mirror entanglement in a single-atom raman laser. *Physical Review A*, 97(2):023829.

Tesfa, S. (2021). *Quantum Optical Processes: From Basics to Applications*, volume 976. Springer Nature.

Tesfahannes, T. G. (2020). Generation of the bipartite entanglement and correlations in an optomechanical array. *JOSA B*, 37(11):A245–A252.

Tesfahannes, T. G. (2021). Enhanced optomechanically induced transparency via atomic ensemble in optomechanical system. *Quantum Information Processing*, 20(3):116.

Tesfahannes, T. G., Abie, B. G., Mekonnen, H. D., and Mazaheri, M. (2024). Transfer of quantum correlations through strong coupling in a three-mode optomechanical system. *Journal of Optics*, pages 1–11.

Tesfahannes, T. G. and Getahune, M. D. (2020). Steady-state quantum correlation measurement in hybrid optomechanical systems. *International Journal of Quantum Information*, 18(07):2050046.

Uola, R., Costa, A. C., Nguyen, H. C., and Gühne, O. (2020). Quantum steering. *Reviews of Modern Physics*, 92(1):015001.

Vaidman, L. (1994). Teleportation of quantum states. *Physical Review A*, 49(2):1473.

Vidal, G. and Werner, R. F. (2002). Computable measure of entanglement. *Physical Review A*, 65(3):032314.

Vitali, D., Gigan, S., Ferreira, A., Böhm, H., Tombesi, P., Guerreiro, A., Vedral, V., Zeilinger, A., and Aspelmeyer, M. (2007a). Optomechanical entanglement between a movable mirror and a cavity field. *Physical Review Letters*, 98(3):030405.

Vitali, D., Mancini, S., and Tombesi, P. (2007b). Stationary entanglement between two movable mirrors in a classically driven fabry–perot cavity. *Journal of Physics A: Mathematical and Theoretical*, 40(28):8055.

Walls, D., Milburn, G., Walls, D., and Milburn, G. (1994). Atomic optics. *Quantum Optics*, pages 315–340.

Wang, D., Xia, C., Wang, Q., Wu, Y., Liu, F., Zhang, Y., and Xiao, M. (2015a). Feedback-optimized extraordinary optical transmission of continuous-variable entangled states. *Physical Review B*, 91(12):121406.

Wang, J., Tian, X.-D., Liu, Y.-M., Cui, C.-L., and Wu, J.-H. (2018). Entanglement manipulation via coulomb interaction in an optomechanical cavity assisted by two-level cold atoms. *Laser Physics*, 28(6):065202.

Wang, X., Qiu, L., Li, S., Zhang, C., and Ye, B. (2015b). Relating quantum discord with the quantum dense coding capacity. *Journal of Experimental and Theoretical Physics*, 120:9–14.

Wang, Z. and Safavi-Naeini, A. H. (2017). Enhancing a slow and weak optomechanical nonlinearity with delayed quantum feedback. *Nature communications*, 8(1):15886.

Weis, S., Rivière, R., Deléglise, S., Gavartin, E., Arcizet, O., Schliesser, A., and Kippenberg, T. J. (2010). Optomechanically induced transparency. *Science*, 330(6010):1520–1523.

Werner, R. F. (1989). Quantum states with einstein-podolsky-rosen correlations admitting a hidden-variable model. *Physical Review A*, 40(8):4277.

Wiseman, H. and Milburn, G. (1994a). Squeezing via feedback. *Physical Review A*, 49(2):1350.

Wiseman, H. M. and Milburn, G. J. (1994b). All-optical versus electro-optical quantum-limited feedback. *Physical Review A*, 49(5):4110.

Wittmann, B., Ramelow, S., Steinlechner, F., Langford, N. K., Brunner, N., Wiseman, H. M., Ursin, R., and Zeilinger, A. (2012). Loophole-free einstein–podolsky–rosen experiment via quantum steering. *New Journal of Physics*, 14(5):053030.

Wu, L.-A., Kimble, H., Hall, J., and Wu, H. (1986). Generation of squeezed states by parametric down conversion. *Physical Review Letters*, 57(20):2520.

Xi, Z., Li, Y., and Fan, H. (2015). Quantum coherence and correlations in quantum system. *Scientific reports*, 5(1):10922.

Xiong, H., Si, L.-G., and Wu, Y. (2017). Precision measurement of electrical charges in an optomechanical system beyond linearized dynamics. *Applied Physics Letters*, 110(17).

Xu, N., Cheng, Z.-D., Tang, J.-D., Lv, X.-M., Li, T., Guo, M.-L., Wang, Y., Song, H.-Z., Zhou, Q., and Deng, G.-W. (2021). Recent advances in nano-opto-electro-mechanical systems. *Nanophotonics*, 10(9):2265–2281.

Yang, X., Ling, Y., Shao, X., and Xiao, M. (2017). Generation of robust tripartite entanglement with a single-cavity optomechanical system. *Physical Review A*, 95(5):052303.

Yu, D.-h., Zhang, L.-q., and Yu, C.-s. (2020). Quantifying coherence in terms of the pure-state coherence. *Physical Review A*, 101(6):062114.

Zhai, L. and Guo, J.-L. (2022). Quantum coherence in a coupled optomechanical system with atomic ensemble. *Physica A: Statistical Mechanics and its Applications*, 587:126523.

Zhai, L.-l., Du, H.-J., and Guo, J.-L. (2023). Mechanical squeezing and entanglement in coupled optomechanical system with modulated optical parametric amplifier. *Quantum Information Processing*, 22(5):211.

Zhang, C.-y., Li, H., Pan, G.-x., and Sheng, Z.-q. (2016). Entanglement of movable mirror and cavity field enhanced by an optical parametric amplifier. *Chinese Physics B*, 25(7):074202.

Zhang, J., Liu, Y.-x., Wu, R.-B., Jacobs, K., and Nori, F. (2017). Quantum feedback: theory, experiments, and applications. *Physics Reports*, 679:1–60.

Zhang, J., Peng, K., and Braunstein, S. L. (2003). Quantum-state transfer from light to macroscopic oscillators. *Physical Review A*, 68(1):013808.

Zhang, J.-Q., Li, Y., Feng, M., and Xu, Y. (2012). Precision measurement of electrical charge with optomechanically induced transparency. *Physical Review A*, 86(5):053806.

Zheng, Q., Xu, J., Yao, Y., and Li, Y. (2016). Detecting macroscopic quantum coherence with a cavity optomechanical system. *Physical Review A*, 94(5):052314.

Zhou, L., Han, Y., Jing, J., and Zhang, W. (2011). Entanglement of nanomechanical oscillators and two-mode fields induced by atomic coherence. *Physical Review A*, 83(5):052117.

Zhou, Y., Jia, X., Li, F., Yu, J., Xie, C., and Peng, K. (2015). Quantum coherent feedback control for generation system of optical entangled state. *Scientific Reports*, 5(1):11132.

Zhu, J., Wang, C., Tao, C., Fu, Z., Liu, H., Bo, F., Yang, L., Zhang, G., and Xu, J. (2023). Local chirality at exceptional points in optical whispering-gallery microcavities. *Physical Review A*, 108(4):L041501.